TUDelft

Delft University of Technology

Macroscopic Characteristics of Bicycle Traffic Flow

A bird's-eye view of cycling

Wierbos, M.J.

Publication date
2021

Document Version
Final published version

Citation (APA)
Wierbos, M. J. (2021). *Macroscopic Characteristics of Bicycle Traffic Flow: A bird's-eye view of cycling.* [Dissertation (TU Delft), Delft University of Technology]. TRAIL Research School.

Important note
To cite this publication, please use the final published version (if applicable).
Please check the document version above.

Macroscopic Characteristics of Bicycle Traffic Flow

A bird's-eye view of cycling

M.J. Wierbos

Delft University of Technology, 2021

.

Macroscopic Characteristics of Bicycle Traffic Flow

A bird's-eye view of cycling

Dit proefschrift is goedgekeurd door de promotoren:
Prof.dr.ir. S.P. Hoogendoorn
Dr. V.L. Knoop

Samenstelling van de promotiecommissie:

Rector Magnificus	voorzitter
Prof. dr. ir. S.P. Hoogendoorn	Technische Universiteit Delft, promotor
Dr. V.L. Knoop	Technische Universiteit Delft, promotor

Onafhankelijke leden:

Prof. dr. R.L. Bertini	Oregon State University, Verenigde Staten
Prof. dr. H.S. Mahmassani	Northwestern University, Verenigde Staten
Prof. dr. M. Menendez	New York University Abu Dhabi, Verenigde Arabische Emiraten
Prof. dr. A. Schadschneider	Universität zu Köln, Duitsland
Prof. dr. G.P. van Wee	Technische Universiteit Delft
Prof. dr. L. Leclercq	Technische Universiteit Delft (reservelid)

Printed in The Netherlands

"You are braver than you believe,
stronger than you seem,
and smarter than you think."

A.A. Milne
(Winnie the Pooh)

Preface

This dissertation concludes my PhD journey. It was a period full of life-changing experiences to which I look back with joy and pride. I have learned so much by the many events that have occurred. Professionally, I have grown as a researcher by attending courses, presenting at conferences, talking to peers, organizing cycling experiments and publishing articles. On a personal level, I have grown by going through the process of buying and renovating a house, by having to cope with a worldwide pandemic, and most importantly by becoming a parent twice. Throughout these transitions, I felt supported by many people who I would like to thank.

First of all my supervisors. Serge, thank you for the many pleasant meetings, understanding words and positive feedback along the way. Despite your busy agenda, I felt continuously supported. Also, thanks for facilitating the friendly and open atmosphere within the department. The informal moments at the coffee machine, the allegro outings, and the Popcorn pictures have often improved my work spirit. Victor, I have appreciated your involvement and enthusiasm for my project. Even though I struggled with it at the start, thank you for the freedom you gave me in choosing my research direction. Furthermore, thanks for the emotional support, the helping hand in coding Matlab and for being readily available for questions. Bernat and Flurin, thank you for the positive coaching and elaborated feedback in the first years of my project.

Special thanks to my committee members who have taken the time to read and assess this dissertation and who have provided me with valuable feedback. Robert Bertini, thank you for organizing the summer school in 2019, for participating in the cycling experiment, and the feedback on the scientific paper. Working with you was a pleasure. Hani Mahmassani and Monica Menendez, you might not remember it but our informal talks at TRB 2018 and 2019 made a great impression on me. Your genuine interest and kindness have boosted my confidence as a scientist. Bert van Wee, thank you for the pleasant informal talks during the many TRAIL events. Ludovic Leclercq, my memories to TRB and hEART in Athens would not have been so great without you, thanks! Andreas Schadschneider, thank you for prioritizing the assessment of my dissertation while you had so many things on your mind after the flood in Köln.

My research output would not have been so high without the help of certain people within the department. Edwin and Peter, thanks for all your help in preparing and executing the experiments, for fixing numerous technical problems, and for providing me with good quality

coffee. Winnie and Alexandra, thank you for the collaboration in the Ahoy experiment. It was a great experience to organize it and I am forever proud that we pulled it off together. I hope the data set will be used for further awesome research in the future. Dorine, thank you for sharing the code that enabled us to automatically extract the bicycle trajectories. Also, your efforts to bring cohesion to the Active Mode Lab are dearly appreciated. The organized meetings and activities made me feel like a true member of the team. Finally, many thanks to the management assistants Moreen, Dehlaila, Priscilla, and Rajshree for scheduling meetings, organizing outings and arranging all things that keep the department running.

My fellow allegri, thank you for your infectiously enthusiastic view on active mode traffic. Tim, Lara, Alexandra, Vincent, Danique, Florian, Alphonse, Giulia, Ilse, Xiaocheng, Yan, Bernat, Flurin, Yufei, Dorine, Victor, Oded, Winnie and Serge, I have enjoyed being part of the research team and to learn about the different aspects of active mode research that I did not realize existed. Thank you for introducing me to the world of wayfinding, activity scheduling, route choice behavior, and many more interesting topics. It was a pleasure to work with you and learn from you. Also, the team spirit and willingness to help was overwhelming. Thank you for your assistance during the many experiments that were conducted, the great fun that I had during our outings, and the positive memories that I have of working together in Delft and at the AMS institute on Fridays.

This research project would not have been finished without the social support that I received from my colleagues. The many gatherings, the lunch breaks, and coffee moments gave me joy and motivation in my daily work. In particular, I would like to thank Xavi, Paul and Boudewijn, the best roommates a newby could wish for. I will not forget the warm welcome and the support that you gave me during the difficult first months of my project. Paul, thank you also for the great time I had while traveling together to Washington DC and New York City. Tim, you made my day whenever we discussed the latest developments in Boer Zoekt Vrouw or Heel Holland Bakt. My roommates in 4.40, Danique, Lara, Vincent, Florian, and Alexandra, thanks for the chit-chat, for showing interest in me as a person, and for sharing your thoughts whenever you saw something interesting on my computer screen. My peers in room 4.36, Giulia, Alphonse and Tim, thanks for entertaining me with the wide variety of sounds that could be heard through the wall, and for always being up for a coffee break. Lucia, Nejc, Martijn, and Yan, thanks for the virtual lunch meetings during Corona time. And thank you Pablo, Bahman, Yihong, Reanne, Maria, Konstanze, Niharika, Malvika, Panchamy, Ding, Tin, Peter, Maryna, Roy, Na, Paul vG, and all other awesome T&P people who were up for a chat whenever I needed it.

I had a lot of help during the last stretch of the PhD journey. Conchita, thanks for checking my work on layout issues and getting me in contact with the publisher. Manja, thank you for taking my portrait photo, and all those lovely pictures of Stef and Daan. Tim and Giulia, thank you for being my paranymphs. And Pablo, thank you for agreeing to take pictures on the day of the defense.

A big thanks also goes to my friends with whom I have shared many moments of joy outside of office hours. Mijn oud-studiegenoten Hilke, Eva en Daniël, Utrecht-en-omstreken-

Contents

Chapter 1

Introduction

Cycling is healthy, environmentally friendly, sustainable, flexible, space-saving and more. Therefore, city dwellers are widely encouraged to use the bicycle as their mode of transport. But at the same time, the infrastructure of many urban areas is struggling to cope with the growing volume of bicyclists, leading to delays, reduced comfort, and parking problems. Handling the enhanced bicycle demand requires adjustments to ensure a positive cycling experience, for example to road infrastructure, traffic signals, and parking facilities. However, the scientific knowledge on this matter is limited and few generic design guidelines exist, leading to a different approach in each municipality. Apart from being costly, these city-specific adaptations result in different looks of the urban infrastructure, which potentially leads to confusing and unsafe situations for travelers.

This dissertation provides insight into the dynamics of bicycle flow by examining cycling movements in crowded conditions. Patterns in the bicycle behavior are discovered by looking at the motion from a bird's-eye perspective, and properties of bicycle flow are identified by aggregating individual characteristics. These patterns and properties are useful pieces of information that help to pinpoint effective measures to better manage the urban traffic. For example, knowing the preferred distance to others while cycling or at standstill, can lead to guidelines on how wide bike paths should be or what the required size is of waiting areas at intersections. Furthermore, unraveling patterns in cycling movements can identify factors that improve the efficiency of bicycle streams and with it, enhance the flow of total urban traffic.

This introduction continues by elaborating on the need for understanding bicycle traffic in Section 1.1 and identifies the scientific relevance of this thesis, and specifies the research focus. Then, Section 1.2 addresses the main objective and research questions, Section 1.3 describes the research approach, Section 1.4 presents the context of the study, and Section 1.5 briefly explains the principles of traffic flow theory that are used in this dissertation. An overview of the research contributions are listed in Section 1.6 and finally, the outline the thesis structure is given in Section 1.7.

1.1   Need for understanding bicycle flow dynamics

In some places around the world, cyclists are a rarity, while in others they are everywhere you look. The latter is the case in the Netherlands, where 28% of all trips are made by bicycle. For trips within a city, the modal share is even higher, reaching up to 50% in some places (De Haas and Hamersma, 2020). This high demand leads to congestion and delays, which is best noticeable at intersections. The highest perceived crowdedness however, is experienced while cycling on busy bike paths (CROW, 2017b), and is related to the wide variety of bicycle types. Hindrance occurs, for example, due to the spatial impact of cargo bikes or the speed difference between conventional and electric bikes. Recent research has shown that some people become reluctant to cycle because they feel unsafe in crowded situations (De Winter, 2020). To prevent the pro-cycling culture from being negatively affected by its own success, it is important to find ways to better manage the bicycle flow. Doing so, requires a deeper understanding of bicycle flows and the underlying behavior.

The current level of understanding of bicycle flow dynamics is limited, despite the growing scientific interest it has received in recent decades. The earlier papers already addressed the cycling movements at intersections (Opiela et al., 1980), and on one-way paths (Botma and Papendrecht, 1991; Navin, 1994), leading to valuable insights regarding speed, volume, passing maneuvers, etc. However, the findings were focused on free-flow situations, which means that cyclists move at their desired speed and congestion is absent. Over time, more case studies were conducted to also include busy traffic conditions, leading to interesting findings on for instance, intersection capacity (e.g., Raksuntorn and Khan (2003), Wang et al. (2011), Hoogendoorn and Daamen (2016)). However, the underlying data is location specific and thus differs in terms of path segregation, path width, bicycle type, and more. Also, the focus of each study differs, leading to scattered insights into cycling behavior. To gain general insights and theories, more data is required that enables the comparison between sites.

Another way to build up knowledge on an unknown subject like bicycle flow is by comparing it to a similar topic that has been well studied. To this end, experiments have been conducted to find similarities between bicycle, pedestrian and motorized traffic. In these experiments, the participants moved along circular or oval shaped tracks while maintaining their order, indicating that overtaking was not allowed. By varying the number of people on the track, the density, average speed and flow could be studied from free-flow to congested conditions, as well as the relation between these flow characteristics. Results showed great resemblance between the different modalities, indicating equivalent behavioral mechanisms (Zhang et al., 2014; Zhao and Zhang, 2017). As a consequence, existing modeling concepts for car traffic could be used to simulate bicycle traffic also. Based on this knowledge, other single-file experiments have been conducted to compare the results with the outcomes of the first bicycle models (e.g., Andresen et al. (2014), Jiang et al. (2016)). However, these models concerns following movements only. It is unknown whether this comparison to car traffic holds when cyclists can cycle more freely and are allowed to overtake each other.

Developing traffic flow models is important because they are helpful tools to predict and understand traffic patterns. By simulating different scenarios regarding demand or fleet

composition, infrastructural changes can be developed without spending money on the implementation. However, a model is as accurate as its foundation, meaning that the outcomes depend heavily on the underlying assumptions. To date, cyclists have been included in traffic models but their behavior has been simplified, for example cars with different speed characteristics (e.g., Jia et al. (2007), Jin et al. (2015)) or greater freedom of movement (e.g., Andresen et al. (2014)). Although these models contribute to the understanding of bicycle traffic, they are unable to capture the true nature of bicycle flow. This includes complex movements in congested conditions such as multi-channel flow and anticipation behavior, which have not yet been comprehensively described. To simulate bicycle flow in a more realistic manner, it is important to examine and describe the dynamics of bicycle flow in crowded situations.

In this quest, choices can be made regarding the level of detail in which the movements are described. The microscopic perspective describes the movements of every cyclist individually. This means that the level of detail is high and that describing the combined bicycle flow results in a large set of complex equations. A less detailed approach is the macroscopic one, which represents the cycling movements as a collective and on an aggregated scale. Describing bicycle flow on this level requires less variables and analytical expressions than the microscopic one. As a result, the macroscopic model is easier to implement in applications such as traffic control. However, this level is also associated with high traffic volumes and is therefore not often considered as a suitable option for modeling bicycle flow. The bicycle volumes in the Netherlands are adequate to also examine this, yet unexplored, modeling approach for describing bicycle traffic flow.

Macroscopic flow models describe traffic flow in aggregated terms and do not specify the individual travelers. They are build on the principle of mass conservation, which means that, for example, a change in speed must coincide with an opposite change in density. A key element of this model type is the fundamental diagram, which describes the equilibrium relation between density, speed and flow. For car traffic, multiple shapes of this fundamental relation have been proposed, like the parabolic (Greenshields, 1935) and triangular shape (Daganzo, 1994). For following-only bicycle movements, a scaled version of these shapes can be used because of the aforementioned resemblance in behavioral mechanisms between cars and cyclists (Zhang et al., 2014). However, due to the lack of empirical data, no fundamental diagram has been proposed so far that applies to the situation where cyclists are allowed to overtake. To determine such relation, a deeper understanding of bicycle flow dynamics in congested conditions is required.

Summarizing, there is a need for information to better manage bicycle traffic and design (network) infrastructure such that crowdedness on bike paths and congestion at intersections can be reduced. The development of bicycle traffic flow models can help in this manner, but this requires better understanding bicycle flow, especially in the situation where cyclists are allowed to overtake. To arrive at general insights about this matter, there is a need for empirical data both on bike paths and at intersections. Furthermore, the characteristics of bicycle flow need to be identified in such a way that bicycle flow can be described on the macroscopic level.

1.1.1   Scientific focus

The need for better understanding bicycle flow dynamics has been established. However, there are many choices to be made about what to focus on to deepen this knowledge. Four aspects are now addressed to specify the research focus.

Congested flow conditions
The traffic flow conditions are classified as either free-flow or congested. In free flow, cyclists can move at their desired speed, while they are being constrained by others in congested conditions. Previous research has focused on the unconstrained movement, thereby diving into typical values for speed, overtaking maneuvers, and path positioning in low demand situations. How these variables change under congested conditions is yet unclear, while this is an important aspect of the dynamics of bicycle traffic flow. As mentioned earlier, the congested flow situation has been studied for single-file movement, but not yet for the situation where cyclists are allowed to overtake. Therefore, this dissertation focuses on analyzing bicycle flow in busy traffic situations where cyclists can follow, move alongside, and overtake each other.

Simple infrastructure setting
Busy traffic situations occur both at urban streets as well as at intersections. Furthermore, bicycle infrastructure comes in many types and shapes. For example, the facilities differ in their level of segregation, such as shared streets, on-street bike lanes, and off-street bike paths. Other differences occur in, for example, path width, slope, directionality (i.e., uni-, bi-directional), shared use (e.g., with pedestrians or mopeds), intersection type (i.e., controlled vs uncontrolled) and priority regulation favoring cars, cyclists, or another mode. The cycling behavior is expected to vary per situation, especially in the degree of interaction with other traffic modes. Given the limited understanding of bicycle flow dynamics in itself, the scope of this research is narrowed down to capture primarily bicycle movements that are least influenced by interactions with infrastructure or other traffic modes. The focus is therefore on uni-directional flow to exclude influences by oncoming traffic, and on simple infrastructural setting, such as separated bike lanes and controlled intersections, without height differences and where the interaction with other traffic is limited.

Macroscopic traffic variables
Understanding the overall dynamics of bicycle flow is done best by taking a macroscopic approach. Although individual data contains more information and thus potentially leads to a better understanding, it may also create an information overload. By looking at the aggregated properties only, the fluctuations of individual cycling preferences are filtered, which enables the identification of cycling patterns and relations. For this reason, the focus in this dissertation lies on analyzing the macroscopic quantities density, speed and flow of bicycle traffic.

Interaction with other modes and bicycle types
On many cycle paths, cyclists share the infrastructure with mopeds, cargo bikes, racing bikes and more. The composition of the bicycle stream influences the flow dynamics due to differences in, for instance, speed, dimension, and maneuverability. To better understand

bicycle traffic flow, it is key to also analyze the impact of stream composition by comparing a homogeneous situation with a heterogeneous one. In practice however, bicycle traffic is always of a heterogeneous composition. Therefore, it is also important to apply the knowledge on bicycle flow to mixed traffic situations. For this reason, the focus of this dissertation is not solely on uniform bicycle flow, but also on applying it to mixed traffic situations.

1.2   Aim and research questions

This dissertation's objective is to better understand the dynamics of bicycle traffic flow in high demand situations, where cyclists can use the full width of the available path and are allowed to overtake. The obtained knowledge should shed light on the relation between flow variables in bicycle traffic, and describe typical cycling behavior on a macroscopic level such that cyclists can be included in traffic flow models. This aim is reflected by the following research question:

How do the macroscopic quantities density, speed and flow of bicycle traffic relate to each other, and how can cycling behavior be integrated in a macroscopic flow model?

This overarching research question is split up into three parts with associated subquestions. The focus is first on gathering and analyzing empirical data, where a distinction is being made between straight paths and intersections. After that, a switch is being made to modeling bicycle flows. The associated subquestions are listed below, as well as the chapter number in which each question will be addressed. Each chapter contains a background section in which the scientific need for this question is addressed.

Part I: Empirical research into bicycle flow on single paths

- How to design a cycling experiment that can capture the key flow characteristics of bicycle traffic? (Chapter 2)

- How do density, speed and flow relate to each other for uni–directional bicycle flow, and how are these affected by path width and anticipation behavior? (Chapter 3)

- How does path width influence the maximum flow on a uni-directional bike path? (Chapter 4)

Part II: Empirical research into bicycle flow at controlled intersections

- What is the influence of jam density and merging cyclists on the queue discharge rate at a controlled intersection? (Chapter 5)

- Can the jam density of bicycle queues be influenced by managing the queue build-up and if so, does the relation between jam density and discharge rate hold for higher jam density values? (Chapter 6)

Part III: Modeling bicycle flow

- How can we describe and model bicycle flow in a mixed traffic situation? (Chapter 7)

1.3   Research approach

Empirical data is key to unravel the dynamics of bicycle flow. Therefore, the primary approach to answer the research questions in part I and II is to observe and analyze bicycle movements. The data is collected in a real-life setting and via multiple controlled experiments.

A controlled experiment facilitates that person-specific information is available, for instance via questionnaires. This environment also allows for investigating the effect of specific influencing factors, such as jam density or path width, by performing different scenarios with identical group of participants. This type of experiment is therefore a useful way to gather data on specific parts of bicycle traffic flow, and is used three times in this dissertation, in Chapter 2, 4 and 6.

The real-life environment captures the natural cycling behavior since the cyclists are, apart from an information sign, hardly aware of being observed. An advantage of this intrusive sensing approach is that influencing factors such as time pressure, cycling experience and familiarity with the infrastructure are unaffected. The downside is that information regarding these and other factors is missing, which complicates the comparison to other samples. The unobtrusive observation is used in Chapter 5.

Part III of this thesis focuses solely on modeling bicycle flow. Here, general observations of typical cycling behavior are used to first, develop a way to include typical bicycle behavior in a macroscopic model and second, to face-validate the modeling outcome for different scenarios.

1.4   Research context

This doctoral research was part of the ALLEGRO project, which is short for unrAvelLing sLow modE travelinG and tRaffic: with innOvative data to a new transportation and traffic theory for pedestrians and bicycles. Although the project description mentions slow modes, the combined term for cyclists and pedestrians was adapted to active modes instead. The project was financed by the European Research Counsel under grant number 667792, and provided eight PhD and three Postdoc positions, which were all based at Delft University of Technology. The overall objective of ALLEGRO was:

"To develop and empirically underpin comprehensive behavioral theories, conceptual and mathematical models to explain and predict the dynamics of pedestrians, cyclists, as well as mixed flows at all relevant behavioral levels, including acquiring spatial knowledge, activity scheduling, route choice and operations, within an urban context, with a special focus on the role of ICT on learning, and choice behaviour." – Hoogendoorn (2014).

Within ALLEGRO, three pillars were identified, being: Active Mode Urban Mobility Laboratory, Transportation and Traffic Flow Theory for Active Modes in an Urban Context, and Theory and Laboratory Applications. This research fits in the second theme and concerns

the macroscopic theory and modeling of cycle flows. Four other topics fitted in this theme of which one was the microscopic theory and modeling of cycling behavior, which was studied by Alexandra Gavriilidou. Since the topics are closely related, the issue of data scarcity was tackled as a collaboration, resulting in the organization of a large-scale cycling experiment, which is described in Chapter 2.

1.5   Theory of traffic flow

This section describes in short the principles of traffic flow theory that are used in this dissertation. As mentioned earlier, traffic can be described with different level of detail. On the microscopic level, the movements are described using individual speed v, spacing s, headway h, where $v = \frac{dx}{dt}$, while the macroscopic level describes the motion as a whole in terms of density k, average speed u and flow q. The two approaches describe the same traffic situation and are thus intertwined.

The density is the number of cyclists on a road stretch at a certain time. In the one-dimensional situation, where cyclists are only following each other, equals density the inverse of the spacing, $k = 1/s$ and is expressed in cyclists per meter. Since cyclists also move alongside and overtake each other, the density in usually expressed in two dimensions. In this case, the density equals the inverse of the individual area A_i, $k = 1/A_i$, and is expressed in cyc/m^2. This concept of individual area, or voronoi area, is further explained in Chapter 3.

The flow is the number of cyclists that pass a certain location per unit of time (cyc/s of cyc/h). This definition of flow is used to describe traffic in the uninterrupted flow situation. In this dissertation, the term flow is used also in combination with the cumulative cyclist number and queue discharge rate. The cumulative flow is the total number of cyclists that has passed a certain point at a moment in time. The term is further explained in Chapter 4. The queue discharge rate is used to describe the maximum flow after a stop moment, so in the interrupted flow situation. Chapter 5 and 6 analyzes the queue discharge flow at intersections and connects it to the jam density. The latter is the density at a standstill, which covers a large range due to the varying distances that cyclists maintain to each other when stopping in a queue.

The macroscopic quantities density, speed, and flow are related to each other in uninterrupted flow conditions via the equation $q = ku$. This means that one of the variables can be computed if the other two are known. Also, it means that the flow is zero when either the density or speed is zero. The equilibrium relation between density and speed is determined empirically and is known as the fundamental diagram, as posed first by Greenshields (1935). Several different shapes of the relation are proposed for motorized and pedestrian traffic but none yet for non-lane-based bicycle traffic. This is mainly due to the lack of empirical data which is addressed in Chapter 2.

The fundamental diagram is an important input for a macroscopic flow model. To this end, Chapter 7 uses an adjusted form of the diagram that is proposed in Daganzo (1994). This diagram has a triangular shape where flow increases with increasing density in the free-flow

branch, and flow decreases with increasing density in the congested branch. The two sides
are separated at the critical density and capacity flow. Travelers move at their desired speed
in the free-flow state, while they reduce speed in congested conditions due to crowdedness
on the road. This simplified relation was established for car traffic, but holds also for single
file bicycle flow (Zhang et al., 2014) as long as a scaling correction is applied based on the
typical speed of cyclists and dimension of their bikes. Chapter 3 addresses the shape of the
density–flow relation for the non-lane-based flow, where cyclists are free to move alongside
and overtake each other.

Apart from the speed–density relation, a key ingredient for a macroscopic model is the con-
tinuity equation. This equation follows from the conservation of mass, i.e. cyclists, and
prescribes that a change in density over time must coincide with an opposite change in flow
over space. In other words, traffic participants should not appear of disappear from the
road. Chapter 7 uses the Lagrangian representation of traffic, which shows the traffic evo-
lution with time, visualized by trajectories of platoon heads. This differs from the Eulerian
representation which visualizes the number of travelers that has passed a certain location
at a moment in time. The advantage of using the Lagrangian method lies in the accuracy
of the numerical solution of the model. More details on the model, numerical scheme and
proposed fundamental diagram can be found in Chapter 7.

1.6   Contributions

The research in this dissertation leads to multiple insights on the dynamics of bicycle flow
and the underlying behavior, thereby contributing to the overall understanding of bicycle
flow on the aggregated level. This section highlights the main contributions of this thesis,
both to science and to society.

1.6.1   Scientific contributions

The most important contributions to science are listed below.

- **Collection of novel empirical data sets**
  Multiple experiments are described in this dissertation, leading to the extension of
  empirical data on, primarily non-following, bicycle flow. On request, this data can be
  made available for future research projects. The most important contribution is the
  data set resulting from the large-scale cycling experiment (Chapter 2), which consists
  of trajectory data of cyclists moving in different infrastructural settings. Other data
  sets varies from cyclist counts at a bottleneck situation (Chapter 3) and counts at
  intersections (Chapter 5, 6).

- **Identifying macroscopic characteristics of bicycle flow in relation to path width**
  This thesis examines the density, speed and flow in bicycle streams and quantifies
  their relation to path width (Chapter 3, 4). Furthermore, capacity estimates are pro-
  vided for different path widths. To date, a large variation in characteristic values for
  density, speed and flow has been reported, which is presumably due to differences
  in infrastructural setting or fleet composition. This thesis specifies the variables for

a series of path widths, based on the same group of cyclists. Controlling for the cyclist flow composition leads to a better understanding of the impact of path width and enables the comparison to findings at other sites.

- **Establishing bicycle fundamental relations**
  The research in this thesis sheds light on the characteristics of bicycle streams along a wide density range. More specifically, the relation between density and speed, and density and flow is addressed, covering both the free-flow and congested conditions (Chapter 3). The shape of the density–flow relation differs for the following and the, newly-explored, non-following situation, especially in the congested branch. Instead of a decrease in flow with density, the relation shows a stagnation in flow with increasing density, indicating that cyclists can maintain in motion while cycling in close proximity to others. This process is highly influenced by anticipation, indicating that it is necessary to include the downstream conditions when modeling bicycle flows.

- **Understanding of behavioral patterns in bicycle streams**
  This dissertation observes and analysis cycling movements in different settings, leading to three main insights regarding aggregated behavior and movement patterns. First one is the capacity drop phenomenon (Chapter 4), which is a well-known event in motorized traffic but has not been observed before in bicycle traffic. It concerns the systematic difference in capacity before and after the onset of congestion. Second one is the tendency of cyclists moving in crowded conditions to cycle in different formations depending on path width (Chapter 3, 4). This configuration is linked to the number of sublanes, which can partially overlap. The spacial headway increases when the active sublanes have more overlap. As a result, the sequence in formations going from a 2.00-meter to a 0.50-meter path shows analogy to a merging process. Third insight is that cyclists anticipate upon downstream conditions on two different ways (Chapter 3). Some cyclists stop pedaling when they see congestion ahead, thereby cycling at lower speed than what is expected based on the direct density conditions. Other cyclists accelerate to fill gaps that appear by the premature slowing down of cyclists who stopped pedaling. Furthermore, cyclists are observed to temporarily accept moving at high speed in a high density conditions when they have visual confirmation that the conditions downstream are favorable.

- **Insight into the discharge process of bicycle queues**
  The queue discharge process at a controlled bicycle intersection is studied, looking specifically at the discharge rate, jam density, queue configuration, and merging cyclists (Chapter 5, 6). The efficiency of the discharge process is captured by the discharge rate, which in turn depends on the jam density. Higher jam density leads to higher discharge rates, which leaves the question how the density at standstill can be influenced. Multiple configurations are tested, resulting in a jam density double that of the value observed in real-life, showing the potential of managing the queue build-up process for optimizing the throughput for all traffic modes. Furthermore, a novel bicycle equivalent unit is introduced to correct the discharge rate for the impact of cyclists joining in from different directions during the queue discharge process.

- **Macroscopic modeling of bicycle traffic flow** This thesis describes the first macroscopic flow model for mixed traffic that includes bicycle traffic (Chapter 7). The movements of (groups of) cars and cyclists are simulated by specifying a unique speed function for each mode of transport that takes into account the proximity of all modes. This class-specific approach enables the modeling of typical cycling behavior such as maneuvering along a queue of cars in congested conditions. Furthermore, anticipation behavior is included in the model by only taking into account the downstream conditions.

1.6.2   Societal contributions

This research into bicycle traffic flow serves a societal purpose. The findings are most relevant to urban areas with already a high share of cyclists in place, while some are interesting for cities with low cyclist demand. The main societal contributions are now discussed, ordered in its applicability to urban environments ranging from high to low cyclist demand.

Cities with high cyclist demand
The research in this paper is highly relevant for urban environments with a large share of cyclists, where problems such as congestion at intersections and overcrowded bike paths are occurring at a daily basis. The findings regarding intersection efficiency provide a hands-on solution to improve the throughflow by managing the queue build-up process. Solely implementing measures to increase the jam density will already reduce the delay for cyclists, while also adapting the signal timing will improve the throughflow for other traffic modes as well. On one-ways paths, the obtained insights will not directly lead to a decrease in (perceived) crowdedness. However, a high flow and thus small delay can be ensured by adapting the infrastructure such that cyclists have a clear visual range and that the peak demand matches the path capacity. The obtained knowledge on the density–flow and density–speed relations, as well as the development of a macroscopic flow model for cyclists is most relevant for this high demand situation. Although they are not directly applicable in practice, they do provide key information to further develop modeling tools to simulate bicycle traffic. These tools can, in time, be used to identify (future) bottlenecks in the urban infrastructure, and to develop plans to address or mitigate the resulting delay.

Cities with medium cyclist demand
Depending on the maturity and bikeability of the existing infrastructure, a medium cyclist demand may or may not lead to problems. In either case, the cycling infrastructure can be designed or adapted using the reported capacity values for different path widths. Similar to the high demand case, the insights regarding jam density and discharge rate can be applied in practice to not only decrease the delay for cyclists, but to also improve the throughflow for other traffic modes.

Cities with low cyclist demand
This research findings can also be applied to enhance the bikeability in areas with only a small share of cyclists. Here, bike users will be moving in free-flow conditions, meaning that they have the freedom to cycle at their desired speed. Most relevant findings in this case are those on capacity and intersection efficiency. Depending on the municipalities' ambitions

of promoting the bicycle, the urban infrastructure can be designed such that the capacity of bike paths fit the current or envisioned demand. Also, measures to increase jam density and thus optimize the intersection capacity can be implemented. This will most likely lead to results quickly, because fewer cyclists have to adapt their behavior and queuing grids are better visible on the path.

1.7   Thesis outline

The visual outline of this dissertation is presented in Figure 1.1. It shows the structure and the topics of the individual chapters, which are based on five published articles and one submitted manuscript that is under review. The book consists of three parts, which can be read consecutively as well as independently.

Part I addresses the uninterrupted and uni-directional flow situation, meaning that the flow on single paths is being studied where cyclists do not have to stop due to external factors such as a traffic signal or having to give priority. Cyclists may need to change their speed and stop because of internal factors, such as changes in density or speed within the stream of cyclists. This internal connection between density, speed and flow has been studied in ring-road experiments before with the restriction that cyclists were not allowed to overtake. However, little data is available on cycling situations that enable overtaking and anticipation behavior. To overcome this hurdle, a large-scale cycling experiment has been organized in which cyclists were allowed to use the full width of the path. The set-up and execution of this experiment is described in **Chapter 2**.
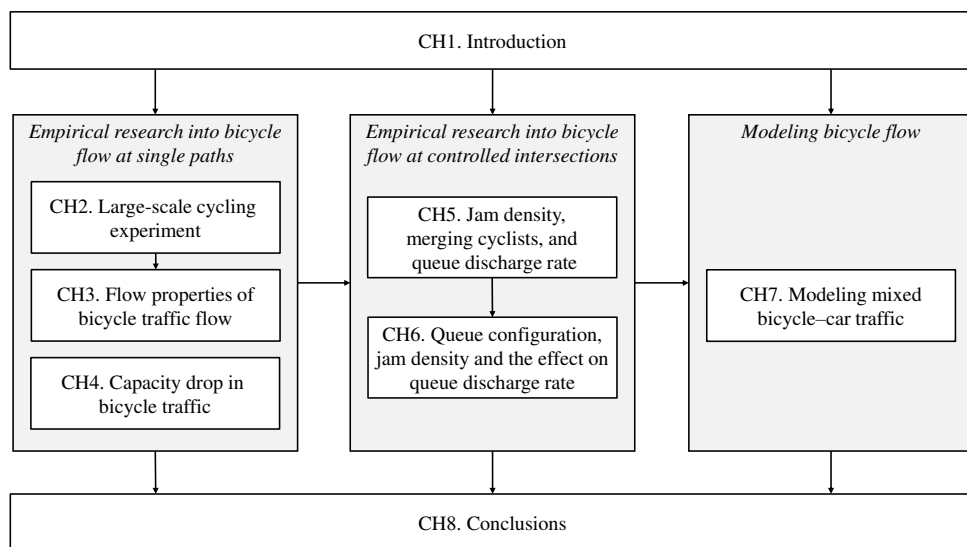
Figure 1.1: Visual outline of the thesis, arrows indicate the reading order.

Based on the empirical data from the large-scale experiment, the aggregated variables density, speed and flow are analyzed in **Chapter 3**, as well as cycling patterns for different variations in path narrowing situations. The main interest is whether the relaxation of the single-file movement leads to different insights into bicycle traffic flow compared to earlier research. And whether anticipation behavior can be identified and quantified. A second, smaller, experiment is set up to examine the influence of path width to the maximum flow in **Chapter 4**. Here, the macroscopic quantity flow is analyzed quantitatively for different path widths. An qualitative analysis shows patterns in bicyclist configuration on the path.

The interrupted flow situation is studied in **Part II** of the dissertation, being intersections. It thereby focuses on the influencing factors of the queue discharge rate, which is a crucial element for the efficiency of an intersection. The higher the queue discharge rate, the more cyclists can pass the intersection during the green signal. First, the discharge rate is studied in a real-life setting in **Chapter 5**. Here, the focus is on the influence of jam density, which is higher when cyclists queue up closer together, and the influence of cyclists that merge into the queue during discharge phase.

It is found that the jam density has a positive influence on the queue discharge rate, thereby implying that the efficiency of the queue discharge process is higher when cyclists maintain a small distance to each other in the queue. To test if this relation between jam density and discharge rates holds for higher density values as well, the queue discharge process is observed in the setting of a controlled experiment in **Chapter 6**. Here, the process of queue formation is influenced with the aim to increase the jam density and to study the effect in the discharge rate.

In the final part of the dissertation, **Part III**, the focus shifts to representing bicycle traffic in a mixed traffic model. **Chapter 7** aims is to represent bicycle traffic in a mixed bicycle–car traffic situation. More specifically, it describes the typical cyclist behavior of overtaking car traffic in congested situations. The chapter describes how an existing first-order flow model for motorized traffic is expanded to also include cyclists. This modeling approach is a first step to include bicycle behavior in macroscopic traffic models.

Finally, **Chapter 8** combines all findings and presents the conclusions of the dissertation. Furthermore, it addresses the implications for practice and lists the scientific contributions and open questions.

Part I

Empirical research into bicycle flow on single paths

Chapter 2

Large-scale bicycle flow experiment: set-up and implementation

Empirical data is key in developing new insights and theories about bicycle traffic flow, but little such data is available. To overcome this data shortage, we designed and executed a large-scale experiment in which cyclists moved along a continuous track. The experiment allows us to observe cycling behavior in different infrastructural settings, such as a merging, crossing, narrowing, curved and straight stretch. This chapter describes the setup and implementation of the experiment, thereby answering the following research question: *How can we design a cycling experiment that can capture the key flow characteristics of bicycle traffic?*

Along with the preparation, design, and execution of the experiment, this chapter also presents descriptive statistics for the participants and the bicycles involved. The resulting dataset is the input for the analysis in Chapter 3.

The large-scale experiment was prepared, designed and executed in close collaboration with Alexandra Gavriilidou and her supervisors. Alexandra took the lead the writing process and is therefore the first author of this chapter.

Abstract

Cycling research at the operational behavioral level is limited, mainly because of the lack of empirical data. To overcome this data shortage, we performed a controlled, large-scale cycling experiment in the Netherlands. In this paper we describe the methodology for setting up and implementing such an experiment, from the motivation of its design using a conceptual model describing cyclist behavior to adjustments that were required during the experiment. The main contribution of this paper is, therefore, to be used as a guide in future experimental data collections. Moreover, we present the characteristics of the participants and their bicycles, and provide a qualitative description of phenomena observed during the experiment. Finally, we elaborate on the potential that the collected dataset holds for future research into understanding and modeling operational cycling behavior.

2.1   Introduction

Cycling as a main mode of transportation has in recent years been promoted by many governments worldwide due to its health and environmental benefits. The focus is mostly on finding ways to attract more people to the bicycle, while at the same time it is important to ensure a safe and comfortable infrastructure that can accommodate high cyclist volumes. This requires understanding of bicycle traffic characteristics, as well as insights into behavior of cyclists while cycling on the road and making decisions to interact with other traffic participants and with the infrastructure. Research in this field is, however, limited and that is to a large extent due to the lack of empirical data.

To overcome this shortage of data, we performed a controlled large-scale cycling experiment. This paper describes the methodology for setting up and implementing such an experiment. These steps may be used as a guide in future experimental data collections and as a reference for future analyses using the data. We describe the collected dataset and elaborate on its potential uses. The contribution of this paper is, therefore, threefold: (i) delineating the process to set up a large-scale cycling experiment; (ii) describing the performance of the experiment, and; (iii) presenting a large database of cyclist trajectories.

This paper is structured as follows. In section 2.2 we provide a background of existing literature on operational cycling behavior and identify the research gaps. Based on these, we formulate our research objectives in section 2.3 and discuss the findings of a stated preference survey that we conducted as a first step to meet the objectives (section 2.4). Section 2.5 describes the development of the data collection plan, while section 2.6 discusses its implementation. In section 2.7 the dataset is presented, followed by an outlook of future research.

2.2   Background on operational cycling behavior

This section provides an overview of existing research on the operational cycling behavior on an individual and on an aggregated level and identifies research gaps in each level.

2.2.1 Individual cycling behavior

Operational cycling behavior on an individual level can be represented by decisions regarding the use of the provided infrastructure while cycling and the interaction with other traffic participants.

In unconstrained situations, interaction decisions depend on the individual's choice for speed and positioning on the cycle path. A number of studies have looked into desired speed and acceleration profiles in free-flow conditions (Ma and Luo, 2016; Twaddle and Grigoropoulos, 2016), on different road surface types and gradients (Shepherd, 1994), with normal bicycles as opposed to electric ones (Schleinitz, 2016) and at wide or narrow cycle lanes (Vansteenkiste et al., 2013). These personal preferences might be constrained at high bicycle traffic volumes and when multiple directions intersect, an effect which is yet to be investigated. The interaction decisions in such situations, their coverage in literature and the corresponding knowledge gaps are the following:

- **steering to avoid colliding with other cyclists**: Steering maneuvers of bi-directional cyclists on collision course have been studied in Yuan et al. (2018), but the interaction with other directions is yet unknown.

- **overtaking cyclists**: Research on cyclists moving in the same direction has looked into following behavior (Andresen et al., 2014), but overtaking decisions have not yet been investigated.

- **yielding to other cyclists**: To the best of our knowledge, there has been no research on yielding decisions at unsignalized crossings where priority rules apply, but are not enforced.

- **accepting a gap in a conflicting stream**: The gap acceptance of cyclists against right-turning vehicular traffic has been studied (Jiang et al., 2013). This, however, might differ significantly when cyclists interact with other cyclists and may also be influenced by whether the intention is to cross or merge.

- **stopping at a red traffic light**: Researchers have analyzed red light running of cyclists at specific intersections across the world and identified influencing attributes that explain this behavior, such as gender, age, amount of conflicting motorized traffic, crossing distance and cycling with company. An overview of these studies can be found in Richardson and Caulfield (2015).

- **positioning when joining a queue**: The formation of multiple channels in queues has been observed at one signalized intersection, stressing the need for a bigger sample (Kucharski et al., 2019). The queue formation process in other situations, like upstream of an open bridge or a reduction of the cycle path width, is not yet studied.

2.2.2 Aggregated cycling behavior

The aggregated behavior of traffic participants is typically captured by the so-called fundamental diagram, which is the relation between average speed, density and flow. Several studies have investigated this relationship for cyclist flows and identified characteristics that

are similar to vehicular traffic and pedestrian flow (Chen et al., 2013; Zhang et al., 2013). Other studies focused on understanding bicycle traffic flow and collected empirical data through:

- **single-file controlled experiments**: They have been conducted outdoors on circular tracks (Navin, 1994; Andresen et al., 2014; Jiang et al., 2016; Mai et al., 2013; Zhao and Zhang, 2017). In this setting, bicycle flow in low and high density situations can be observed, resulting in empirical data covering the full density range of the fundamental diagram. This provided insights into the dynamics of bicycle flow and identified flow characteristics such as stop-and-go waves. However, overtaking was not allowed in these experiments, which is often observed in real-life situations.

- **observing cycling behavior in daily traffic**: Studies have estimated capacity of bicycle paths and resulted in a wide range of values (Botma and Papendrecht, 1991; Li et al., 2015; Greibe and Buch, 2016; Jin et al., 2017a). This might be explained by the differences in infrastructure or bicycle type composition. The influence of electric bicycles has been studied (Wang et al., 2015; Zhou et al., 2015; Jin et al., 2017a), but could not be controlled due to the nature of the empirical data. By controlling the infiltration rate of electrical bicycles, its impact to the overall flow characteristics can be identified more clearly. Furthermore, most empirical data is collected in conditions with low cyclist volumes and lacks observations in the congested regime of the fundamental diagram.

In short, the literature so far provides limited insight into the bicycle flow dynamics for high demand situations when overtaking is allowed and the effect of different attributes, such as the infiltration rate of electric bicycles, on the shape of the fundamental diagram, has not yet been studied.

2.3   Research objectives

Based on the given literature overview, it can be concluded that the research effort to observe and understand cycling behavior is limited. The most essential gap seems to be studying high cyclist volumes, as well as bicycle-to-bicycle interactions at designated cycling infrastructure. With respect to individual behavior, overtaking and yielding have been studied the least. At an aggregated level, overtaking is also important, as it is expected that it can explain the flow differences in the congested regime. Its effect on the shape of the fundamental diagram has not yet been studied, nor has the penetration of electric bicycles.

In order to address these gaps, we focus on bicycle traffic in the absence of other transport modes. Our objective is to collect a novel dataset that captures high cyclist volumes and where overtaking and yielding interactions take place. The aim of this dataset will, then, be to retrieve the characteristics of the fundamental diagram when overtaking is allowed and also to study the effect of bicycle type, an in particular electric bicycles, to the overall flow dynamics. Moreover, the dataset will be used to investigate the attributes that best explain the decisions to overtake and yield.

2.4   Survey on influencing attributes

To investigate the attributes that can explain overtaking and yielding decisions, we conducted an online stated preference survey in the Netherlands in summer 2017. The respondents were asked to name the attributes that influence their decision making in three situations: (i) overtaking or staying behind a single or a small group of cyclists; (ii) going ahead or stopping at a crossing to allow cyclists with priority to merge or cross, and (iii) stopping or continuing at a red traffic signal. The latter was included to check whether the attributes found from observations match the stated ones and as such justify the predictive value of the survey. The specificities of each situation were outlined, and always involved cycling during daytime on road infrastructure designated for cyclists and separated from other traffic. Per situation, a list of attributes was provided to the respondents based on behavioral hypotheses regarding the most influential attributes. Each list contained ten attributes displayed in random order, and three empty fields to enter other attributes. A selection of three to ten attributes was requested per situation. Apart from that, general information about the respondents was collected, such as gender and nationality.

By analyzing the 444 responses, using principal component analysis to reduce dimensionality, the most influential attributes per decision could be obtained. In Figure 2.1 the prevalent attributes for each decision are linked to the corresponding decision (the check marks indicate the attributes that can be studied with our dataset). These decisions are part of the individual behavior, together with steering and pedaling decisions. The schematic fits into the conceptual model of Figure 2.2 which describes cycling behavior at the operational level. According to it, attributes influence the behavior of individuals, who collectively give rise to aggregated behaviors. These behaviors can be observed via microscopic and macroscopic variables, whose relations are visualized in the conceptual model.

Figure 2.1: List of influential attributes per decision according to our survey results. The check marks indicate the attributes that can be studied with the dataset collected in our experiment.

Figure 2.2: Conceptual model of operational cycling behavior. Attributes are linked to individual behaviors, as already shown in detail in Figure 2.1. Collectively they lead to aggregated behaviors. These behaviors can be observed via micro- and macroscopic variables.

The validity of the survey findings is demonstrated by the attributes found significant for the decision to stop at a traffic light as they match those found in literature. However, more data are needed to quantify the effect of the attributes on the overtaking and yielding decisions. A data collection plan is, thus, necessary.

2.5   Development of data collection plan

The research steps to set up the data collection plan are described. First, the data needs and requirements are identified (subsection 2.5.1), followed by the motivation of the choice for the data collection approach and equipment (subsection 2.5.2). A controlled experiment is selected and its set-up is presented, covering the design of the scenarios (subsection 2.5.3) and the cycling track (subsection 2.5.4), the estimation of participants needed (subsection 2.5.5) and the duration required for each scenario (subsection 2.5.6).

2.5.1   Data needs and requirements

As previously mentioned, one of our aims is to retrieve the characteristics of the fundamental diagram when overtaking is allowed and the fleet consists of different bicycle type compositions, as well as to investigate the overtaking and yielding decisions of individuals and to identify the attributes that best explain them. The data type necessary to study individual cycling behavior is trajectories, i.e., cyclist positions in time and a two-dimensional space. Trajectories are the most detailed type of traffic data, which can be aggregated in time or space to study macroscopic variables needed for the construction of the fundamental diagram. By examining trajectories, the use of the cycle path width and the speed adjustments can be studied relative to the position and speed of other cyclists and the environment

(width, curve). The accuracy that is required for the trajectories lies within 10cm which sets requirements for the data collection equipment. Additionally, it is crucial to be able to track and distinguish each individual, while also linking the observations to personal characteristics.

Another requirement is set by the need to capture the fundamental diagram. Therefore, it is necessary to observe low as well as high densities, which can be achieved by controlling the infrastructure setting and bicycle inflow rates. Studying the effect of different bicycle types means that the composition of the fleet should also be controlled. Moreover, controllability is necessary to ensure that the desired cyclist interactions (overtaking and priority negotiation) take place and that the effect of the influencing attributes of Figure 2.1 can be investigated.

2.5.2 Data collection approach and equipment

Three data collection approaches can be used to retrieve trajectory data:

- **observing real-life situations**: Even though this approach can capture the uninfluenced and unbiased behavior, the degree of controllability is very low and does not meet the prescribed requirements.

- **doing an experiment in virtual reality**: Existing bicycle simulators are of unknown validity and behavioral realism. They also do not allow for multiple individuals to cycle simultaneously and interact with each other.

- **doing a controlled experiment in a physical environment**: A controlled experiment allows for a high degree of controllability and, thus, satisfies the requirements.

In a controlled experiment, the number of cyclists using the infrastructure, the routes they take, as well as the design of the infrastructure itself can be controlled. By carefully instructing the participants, specific elements of their behavior, like their choice of speed, can be steered when necessary. Even the external conditions, such as light and wind, may be controlled.

However, the approach has some disadvantages that should be mitigated as far as possible through the experimental design. One of the main disadvantages is the occurrence of the so-called "learning-effect". This means that participants change their behavior over time as their familiarity with the experimental setting increases and they get tired. This can be minimized by varying the layout and tasks that the participants are asked to perform during the day and by shortening their cycling duration.

Another potential drawback relates to data validity and representativeness. It may be argued that the behavior is not realistic due to the fact that participants know they are being observed. We counter this argument based on the fact that the behavior is observed several times and as they need to interact with other cyclists, their consciousness shifts to the riding task and any differences observed in behavior are attributed to intra-personal variability. Moreover, this is intuitive behavior, and the observation equipment will hardly be visible.

Regarding the data collection equipment, as the trajectories need to have high accuracy, overhead video cameras are selected. By placing them above the cyclists, the cameras track their movements with as little occlusion as possible, and continuously in time. To be enable the automated extraction of trajectories from the video images, a red cap is assigned to each participant. This color is chosen because it is easiest to recognize under a wide range of lighting conditions (Daamen and Hoogendoorn, 2003). Finally, to link the observed trajectory to a specific individual, the caps are assigned a unique identification code.

2.5.3   Scenario design

On a microscopic level, the aim is to investigate the effect of the attributes of Figure 2.1 on overtaking and yielding decisions. In the scenario design we can control for two of them, namely the bicycle type and the directionality of the cycle path. Regarding bicycle type, separate runs are scheduled each with a different fleet composition and the scenarios are referred to as "Overtaking". More specifically, there is a run for regular bicycles only, runs that combine regular bicycles with one special type, and a run with all types. In these scenarios there is a one-way flow on the cycle path. For the fleet with all types, the behavior is compared with a run that allows for bi-directional flow.

With respect to yielding decisions, the direction of approaching cyclists is an attribute. Its effect can be investigated by separately studying crossing and merging streams. Therefore, two scenarios are designed, namely "Crossing" and "Merging". As the bicycle type is an attribute, runs are performed with a mixed cycling fleet as well as with regular bicycles only.

On a macroscopic level, scenarios are needed to observe low as well as high densities to construct the fundamental diagram. We implement this by narrowing the cycle path, which obstructs the cyclist flow and leads to queue formation upstream of the narrow section when the demand exceeds its capacity. By varying the width of the narrow path ("bottleneck"), various congested patterns occur, determining both density and speed upstream of the bottleneck. We call it "Active bottleneck" scenario. It consists of different runs, each having another bottleneck width or a different cycling fleet composition, to observe the effect of bicycle types on the fundamental diagram. Specifically, the effect of electric bicycles is investigated by comparing three penetration rates: 0%, 10%, and 20%. These values represent typical values of electric bicycles in urban traffic situations in the Netherlands.

2.5.4   Track design

The layout of the track needs to be carefully designed because it largely determines the behavior that can be observed in the experiment. First of all, cyclists should maintain a speed as close as possible to their normal cycling speed and behave as they would in reality. To this end, a continuous track is selected, where participants make laps instead of short stretches that would require frequent acceleration from, and deceleration towards, standstill. A rounded rectangle shape is preferred over a circular one, because: (i) the cyclists will not be constantly steering in a curve; (ii) there is a straight stretch for overtaking maneuvers, and (iii) the attribute "going straight or turning" for overtaking decisions can be studied.

In terms of dimensions, the length of the straight stretch is set at 40m, which is an adequate length for cyclists to overtake (Yuan et al., 2018). The width of the track is chosen to be 2m. This width ensures that there is enough space for cyclists to overtake and it is also possible to sketch situations with a bi-directional flow (Zeegers, 2004). The radius of the curve should allow cyclists to maintain a comfortable speed without the inside pedal hitting the surface if they lean. For a riding speed of 20km/h, the minimum radius is 7m (Shepherd, 1994).

In order to ensure that the desired interactions take place, different track elements have been integrated into a single track layout, see Figure 2.3. The blue continuous line is the main track, used in all scenarios, where cyclists enter at the top left corner and cycle clockwise. The choice for this cycling direction is based on the norm to cycle on the right-hand side in the Netherlands and as such the inside curve will be taken by the slower cyclists. The inside curve radius is set at 10m, with a quarter of a circle placed on each side and connected with a long straight stretch of 40m and a short one of 16m. The long stretch on the top side gives room for overtaking, while the bottleneck is placed at the bottom side in the Active bottleneck scenario. The short stretch accommodates crossing conditions at a straight stretch rather than within a curve.

Another element is activated to observe crossing behavior (green dotted line in Figure 2.3) where cyclists are riding counter clockwise. With this configuration, there is a bi-directional flow on the top part where the two routes overlap enabling the investigation of the effect of "one- or two-way cycle path" on the overtaking behavior, and also creating two crossing points which increases the amount of observations. An extension of 10m of straight stretch is added at the crossing points and the curve radius is set at 8m, such that the crossing takes place in the middle of the blue track.

A third element is added (black dashed line in Figure 2.3) for the Merging scenario, which is connected to the main track in two locations; one is the off-ramp where cyclists can exit the main track and the other one is the merging point where cyclists join the main flow again. It is worth noting that no markings indicating priority are added on the track to prevent that they influence the behavior.

With respect to controlling the flow, a bottleneck is introduced at the bottom side of the track. It consists of two inflatable mattresses placed next to each other on the track to create a narrow stretch 4m long. The height of the bottleneck is 33cm which blocks pedaling over it but does not hinder steering, creating the impression of an elevated curb rather than that of a wall which could be unsafe to drive through. The bottleneck is moved inwards to decrease the width of the track in that section. This way the cyclists are obstructed, leading to queue formation when the cyclist demand exceeds the capacity of the bottleneck. It is placed downstream the straight stretch (seen from the cycling direction) ensuring that the queue will grow along the straight stretch, and the observations are uninfluenced by the curve. By varying the bottleneck width, various congested patterns occur upstream of the bottleneck.

The bottleneck is set to four different widths, namely 75, 100, 125 and 150cm. These numbers are based on a preliminary bicycle flow experiment that we performed, where the main path width was also 2m and the path was narrowed to a width of 150 to 50cm using steps of 25cm. The 50cm width was found to be too narrow for safety reasons. In order to observe high densities, the flow through the bottleneck should then be reduced in a different manner. The shape of the bottleneck is changed from a small straight stretch to one that cyclists have to meander through, referred to as the "Meander". The two mattresses are placed behind each other with 2m space in between and in such a way that they leave a path of 75cm to the side of the track (Figure 2.4).
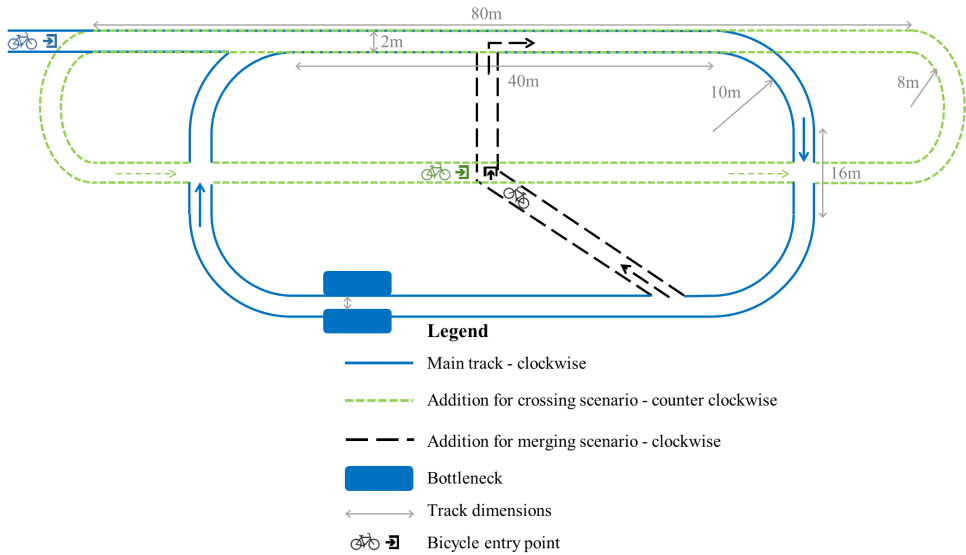
Figure 2.3: Track layout showing in color the elements activated for different scenarios.

Figure 2.4: Construction of meander bottleneck using two mattresses.

2.5.5   Number of participants

The next step is determining the number of participants. We base this primarily on the aim to capture the relation between density, speed and flow. Assuming a diamond queue formation of 2-1-2-1, the jam density is 0.7 cyclists/m^2, which leads to 28 cyclists for a queue length of 20m, which is enough to observe the behavior for the high density and low speed situation.

To maintain a 20m long queue, there need to be as many cyclists joining the tail of the queue as leaving the queue through the bottleneck. The number of cyclists that need to circulate the track depends on the outflow rate of the bottleneck, as well as on the average cycling speed of the circulating cyclists. To estimate the maximum number of participants, the scenario with the highest queue outflow rate should be considered. Based on our preliminary experiment, the outflow rate of the bottleneck of 150cm width is 1.82 cyclists/s. Based on an average cycling speed of 19km/h (Botma and Papendrecht, 1991), 55 additional cyclists are needed. Consequently, a total number of 83 participants is required in the experiment.

2.5.6   Scenario duration and scheduling

The estimation of the duration needed for each scenario is based on the requirement to have enough observations to draw statistically significant findings. In the Overtaking scenario this is translated into giving each cyclist the chance to make at least ten decisions whether to overtake or not (i.e., cycle through the top straight stretch). When the bottleneck is inactive, it takes about 30s to complete a lap, which leads to a required duration of 5min.

With respect to the Merging and Crossing scenarios, the indicator to base the observation calculations on is the attribute "number of approaching cyclists". In order to investigate its effect on the decisions being made, different group sizes, i.e., number of cyclists approaching the negotiation point from each side, need to be observed. As large numbers are appreciated the bottleneck that would constrain the outflow is removed. The time needed to collect sufficient observations of different group sizes is calculated using a simple microsimulation. It assumes a constant cycling speed and simulates dots moving around the track. Once a dot is detected close to the negotiation point, the number of dots present on each approaching stream is counted, while taking into account a physical length of about 2m. If both approaches have a positive number, it is counted as an interaction of a group size coming from the right against a group size coming from the left. After running for a longer duration, the number of encounters of the occurring group combinations at the merging and crossing points is calculated. The result is that the Merging scenario requires 40min and achieves interactions with a maximum group size of 6 against 5 cyclists, and every combination in between. Since the Crossing scenario has two observation points on the track, it requires half the time (20min) for these observations.

In the Active bottleneck scenario, a 5min duration is chosen. This duration enables the estimation of flow, density and speed in continuous and homogeneous conditions in the queue, without lengthening the total duration of the experiment. Also, it accommodates capacity estimation using different aggregation times, which decreases the influence of individual

behavior. Since participants are able to pass the bottleneck multiple times, approximately
5-10 times depending on the bottleneck width, the individual behavior averages out which
benefits the capacity estimation.

In terms of scheduling, the day of the experiment is divided into two sessions, one with
special bicycle types and one without, so that we can observe the behavior of regular bi-
cycles only and compare it to the behavior when special bicycle types are present. In the
latter, the runs with these special types are dominant, checking the overtaking behavior and
the fundamental diagram for different penetration rates. Only two bottleneck widths (75
and 125cm) are kept to limit the total running time. In the session without special bicycles,
there is time to test all the widths and to focus on the Merging and Crossing scenarios. Due
to the fact that the latter require long observation times, we split the duration in batches of
smaller runs of 10min each.

It is estimated that it takes 2min for all cyclists to enter the track in a one-by-one pattern,
and therefore the Overtaking and Active bottleneck scenario runs are scheduled to last 7min.
Since three fleet compositions (no special types, electric and regular bicycles, all types) are
in both scenarios, their corresponding runs are scheduled in continuation, i.e., without any
break. First the Overtaking scenario takes place and then the bottleneck is activated, which
is estimated to take 1min. The activation is performed by introducing a moving bottleneck
on the track, i.e., two persons cycling slowly and next to each other such that they cannot be
overtaken and forming a queue behind them. This way, all cyclists are led as one group up
to the bottleneck, activating it.

Summing up all these times leads to a net cycling time of 90min for each session. To prevent
exhausting the participants, breaks of 15min are scheduled every 3 runs and in between runs
there is a small pause of 5min to initialize the next one. Apart from exhaustion, the learning
effect and boredom need to be prevented. We solve this by alternating the scenarios in the
schedule and by keeping the runs at about 10min each. The planned order of scenario runs
and their properties are summarized in Table 2.1.

2.6 Implementation of experimental design

Having set the requirements and the experiment design, the implementation follows and is
divided into the selection of the location, the recruitment of participants and the set-up of
the measuring and tracking equipment.

2.6.1 Location selection

The selection of the place where the experiment can be executed is based on several criteria.
The most important criterion is that it has enough space to fit the track. The floor area re-
quired for the designed track is 100m x 40m. Moreover, the location should strictly prevent
the presence of other modes. These conditions, along with the fact that a specific track with
this shape and curves will be hard to find, point towards the construction of the track at a
location rather than the use of existing infrastructure. Another benefit of creating the track

Table 2.1: Schedule of scenario runs during the day of the experiment.

Scenario	Bicycle fleet composition				Bottleneck width	Run duration	Time to next run	Session
	Regular	Electric	Racing	Cargo	[cm]	[min]	[min]	
Overtaking	60%	20%	10%	10%	125	7	1	Morning
Active bottleneck	60%	20%	10%	10%	125	5	5	Morning
Overtaking	86%	-	14%	-	-	7	5	Morning
Active bottleneck	75%	25%	-	-	75	7	15	Morning
Overtaking	75%	25%	-	-	125	7	1	Morning
Active bottleneck	75%	25%	-	-	125	5	5	Morning
Merging	60%	20%	10%	10%	-	10	5	Morning
Active bottleneck	86%	14%	-	-	75	7	15	Morning
Crossing	60%	20%	10%	10%	-	10	5	Morning
Active bottleneck	60%	20%	10%	10%	75	7	5	Morning
Active bottleneck	86%	14%	-	-	125	7	15	Morning
Merging	60%	20%	10%	10%	-	10	5	Morning
Overtaking	86%	-	-	14%	-	7	-	Morning
Overtaking	100%	-	-	-	125	7	1	Afternoon
Active bottleneck	100%	-	-	-	125	5	5	Afternoon
Active bottleneck	100%	-	-	-	100	7	5	Afternoon
Merging	100%	-	-	-	-	10	15	Afternoon
Active bottleneck	100%	-	-	-	75	7	5	Afternoon
Crossing	100%	-	-	-	-	10	5	Afternoon
Active bottleneck	100%	-	-	-	150	7	15	Afternoon
Active bottleneck	100%	-	-	-	Meander	7	5	Afternoon
Merging	100%	-	-	-	-	10	5	Afternoon
Active bottleneck	100%	-	-	-	Meander	7	15	Afternoon
Crossing	100%	-	-	-	-	10	5	Afternoon
Merging	100%	-	-	-	-	10	-	Afternoon

is that it can be made obstacle-free to ensure good visibility. Even though the visibility due to obstacles has been found to be an attribute in the yielding decision, it is left out of scope to avoid accidents during the experiment.

Another criterion relates to the controllability of external conditions such as weather and light. These can only be controlled when the experiment takes place indoors. The weather conditions influence cycling behavior, but investigating their effect would require repeating the experiment under different circumstances which is hard to predict and anticipate, as well as costly and difficult to plan with a sufficient number of participants. Therefore, we need to keep the circumstances constant during the whole experiment.

The indoor environment raises two needs. Firstly, the ceiling to be at least 10m high to accommodate tracking equipment and prevent the feeling of cycling in a closed space. Secondly, the surface type should resemble real-world cycling conditions, be safe, and, therefore, be neither slippery nor adhesive.

Last but not least, the location should be easy to find and access, preferably near a crowded and inhabited area. This increases the chances of recruiting enough participants who will show up on time.

Given these criteria, we selected a large exhibition hall in the Ahoy Convention Center, Rotterdam (The Netherlands). The size of the rented hall is 142m x 70m x 12m, which satisfies all the dimension requirements and the floor surface is cement, so similar to cycling

on road surface. Furthermore, it is well accessible by bicycle, connected by public transport and has a car parking.

2.6.2   Participant recruitment

The next step in the implementation is the recruitment of participants. Since it is desired to study the effect of gender and nationality of cycling behavior, anyone is welcome to join. The only restriction is set with respect to age due to ethical reasons, and it is being at least 16 years old. A maximum age threshold is not set, but participants are asked to be physically able to cycle for around 90min including breaks. As reward for the time they spent in the experiment, participants are given a small monetary compensation.

In order to increase the behavioral realism, participants are asked to bring their own bicycle. Upon registration, participants are asked for the bicycle type they intend to bring, as well as for other bicycle types they own. Special focus is placed in the recruitment phase on three special bicycle types (racing, electric and cargo).

Registration is performed through an online form, where availability in time of day (morning/afternoon session) and bicycles is declared. For those that meet the requirements, a confirmation is sent which includes the request to avoid red clothing which obstructs the tracking of the red caps in the camera images. Several platforms are used for the recruitment, such as posts in social media, universities and schools in Rotterdam and advertisements in local newspapers.

2.6.3   Measuring and tracking equipment

As previously mentioned, cameras are placed above the track to record the cyclist movements throughout the day. Due to the lighting conditions of the hall, which were low and variable, high quality cameras had to be used. Two snapshots of the experiment are shown in Figure 2.5. Figure 2.5(a) is a side view (from an overview camera, not to be used for tracking) during a Merging scenario. The cameras are placed at the ceiling next to the lights to improve the image quality and are 10m above the ground. In order to cover the complete straight stretches, three cameras are required on each side with an overlapping area to ensure a continuous trajectory. Two more cameras are placed above the crossing points to observe the cyclist interactions there.

A top view at the location of the bottleneck can be seen in Figure 2.5(b). From this view the trajectories can be extracted by tracking the red cap of each cyclist. As shown in the image, each cap has a pattern of white boxes (like a bar code) on the flap which is unique and linked to the participant characteristics. An additional dot is marked in the middle, to identify looking and cycling direction.

Last but not least, we set up a corner to measure three main bicycle dimensions, i.e., full bicycle length, length from the front wheel to the handlebar and width of the handlebar. This enables studying the effect of different sizes on the behavior in addition to the bicycle types.

(a) Side view of the Merging scenario. Photo by TU Delft/Frank Auperlé.
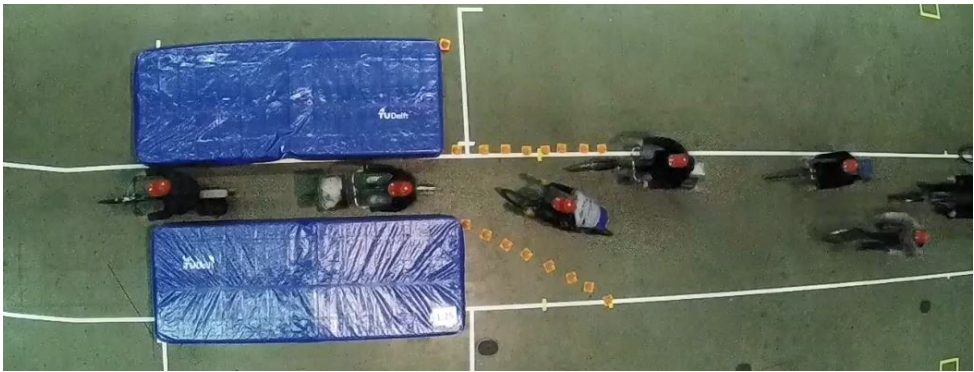
(b) Top view of the Active bottleneck scenario.

Figure 2.5: Camera snapshots.

2.7   Experiment execution and high-level description of data

The experiment took place on 25 April 2018 with 178 participants evenly spread over the morning and afternoon sessions. This section presents the collected dataset, starting with adjustments of the plan that were needed during the day and continuing with the statistics of the participant characteristics and a qualitative description of the data.

2.7.1   Plan adjustments

During the first run in the morning session, it became clear that there were too many cyclists on the track. The queue configuration of 2-1-2-1 that was expected upstream the bottleneck was not observed. Instead, participants anticipated the bottleneck and started braking already at the curve. This resulted into a lower density than anticipated and an overall low speed (congested conditions).

The solution was to create two groups with half of the participants and alternate the group on the track. This way, the long breaks could be skipped as the participants could rest when the other group was cycling. Thanks to this change, it was possible to not only follow the plan, but have time for some additional scenario runs.

Since the narrowing at the bottleneck was anticipated and a dense queue was not naturally arising, we activated it using the moving bottleneck (i.e., the two persons in orange vests in Figure 2.6).
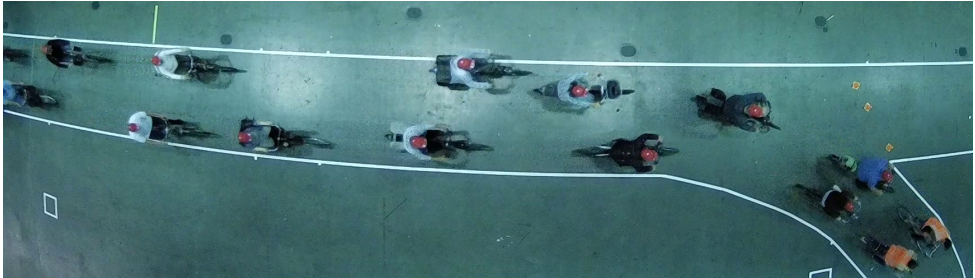
Figure 2.6: Queue formation behind a moving bottleneck.

In the Merging scenario, we initialized with a group starting from inside but the participants self-organized during the runs and dynamically shifted among the two routes. We decided not to obscure this process since it enhances observation of heterogeneity and could even lead to a model on route choice.

2.7.2   Participant characteristics

The descriptive statistics of the participants and their bicycles are summarized in Table 2.2 per session. It can be seen that more males participated in the experiment with a higher share in the afternoon session. The majority of the sample is Dutch and there is a wide range of ages.

With respect to the bicycles, the morning session contained special bicycle types with a high share of electric (35%) and a considerable share of 9% of racing bicycles. Unfortunately, no participants with cargo bicycles could be recruited. In the afternoon, almost all participants had regular bicycles. On average, the bicycle dimensions seem consistent between the two sessions.

2.7.3   Qualitative data description

In total, six hours of videos have been collected which capture the cyclist movements throughout the day. Since there was time left, we tried one more situation. We had one run where we slowly filled up the track with everyone in to study the occurring wide moving jams. The planned scenarios were executed and additional to our expectations, the following phenomena were observed:

Table 2.2: Descriptive statistics of participants and their bicycles per session.

Characteristic	Morning session	Afternoon session
Females	34	30
Males	54	60
Dutch	78	84
Other European	8	2
Non European	2	4
Minimum age	19	17
Average age	52	51
Maximum age	80	89
Standard deviation of age	19	19
Average height [cm]	174	177
Standard deviation of height	10	10
Average weight [kg]	79	77
Standard deviation of weight	15	13
Electric bicycles	31	3
Racing bicycles	8	0
Average bicycle length [cm]	180	180
Standard deviation of bicycle length	6	5
Average handlebar width [cm]	59	59
Standard deviation of handlebar width	6	4

- Participants were braking already upstream the curve which led to lower than expected density.

- Many cyclists were overtaking in curves rather than the top straight stretch.

- Pairs were formed on the track, which blocked overtaking maneuvers (Figure 2.7(a)).

- A variety of yielding decisions was observed regardless of group sizes. Sometimes steering to create space was preferred to stopping (Figure 2.7(b)).

- During the Merging scenario runs, participants alternated between the two routes, leading to a dynamic share and different group sizes interacting at the merge.

- Some of the merging-route cyclists used their arms to indicate they would take the off-ramp and others taking that route would copy (Figure 2.7(c)).

- The right angle at the merging point was not always feasible to follow, so some cyclists went slightly off the track to merge (Figure 2.7(d)).

These observations show that anticipation plays a key role while cycling. In this obstacle-free environment where the curve and bottleneck were in sight, cyclists adjusted their speed in preparation for them. Moreover, speed differences could be better expressed in curves where the cautious cyclists would brake and the rest used this opportunity to overtake. Personal characteristics seem to be dominant with respect to yielding decisions and less so the number of approaching cyclists. Participants respected the rule to cycle inside the cycle

(a) Pair of cyclists obstructing the flow.

(b) Cyclist in black makes space for merging cyclists instead of yielding.

(c) Route indication using arms.

(d) Straying off the path to merge.

Figure 2.7: Examples of observed phenomena.

path, unless it would have led them to unsafe situations. Last but not least, self-organization has been found for cyclists in the form of distributing over different routes and copying the behavior of others. These qualitative findings will be the starting point for future research, additionally to what was already intended with the collected dataset.

2.8   Future research with collected dataset

In this paper, we described the set-up of a large scale controlled cycling experiment and qualitatively presented the collected dataset. The next research step is to process the video data and automatically extract trajectories out of the images, stitch trajectories between consecutive cameras and link to a participant number. This rich dataset will be used to investigate behavior of different bicycle types and personal characteristics, and derive theoretical models that represent the decisions individual cyclists make while cycling and interacting with other cyclists, as well as models that describe the operationalization of these decisions. The dataset will also be used to calibrate and validate these models. Apart from studying individual behavior, we will study macroscopic bicycle traffic characteristics and construct the fundamental diagram for cycling. Such models can be used in future research to assess the quality of different bicycle infrastructure designs under several demand conditions.

Chapter 3

Macroscopic properties of a cyclist stream and the effect of anticipation

The large-scale cycling experiment described in the previous chapter generated a large empirical data set of cycling movements. In turn, this chapter uses a small portion of that data to extract characteristic values for density, speed and flow for different path widths. More specifically, we look at the data of the bottleneck scenarios and examine the macroscopic properties of the bicycle flow for different widths of the narrowing. By extracting individual density and speed, and by analyzing the aggregated quantities and behavioral patterns, this chapter addresses the following question: *How do density, speed and flow relate to each other for uni-directional bicycle flow, and how are these affected by path width and anticipation behavior?*

Results show that the characteristics of bicycle traffic flow are heavily influenced by anticipation. The average cycling speed is not solely linked to how much maneuvering space a cyclist experiences his or herself, but also to the density that this cyclist observes at a certain distance ahead. As a result, similar average speeds can coincide with different density values, which complicates the description of a single fundamental diagram for bicycle traffic flow. The insight that anticipation behavior is an important aspect in bicycle flow dynamics is used in the macroscopic flow model for mixed bicycle–car traffic in Chapter 7.

This chapter has been submitted to a journal and is currently under review.

Abstract

This research provides a deeper understanding of bicycle flow by providing insights into the properties of a cyclist stream for different path widths and uncovering the role of anticipation behavior. We analyze trajectory data from a large–scale cycling experiment. We derive relevant macroscopic properties, i.e., density, speed and flow, and connect these to the path width and usage. Depending on the path width, cyclists move in different configurations (overtaking, staggered and strictly-following). Furthermore, the density–speed relation and density–flow relation are investigated. They are found to be influenced by anticipation behavior, resulting in a more gradual decrease in cycling speed with increasing density and a more gradual increase in flow with increasing density, when compared to the situation without anticipation. Furthermore, we find a minimum speed for cyclist and we find that cyclists can maintain a high flow rate in congested conditions. The obtained insights contribute to the understanding of bicycle flow patterns. Results can be used to develop, improve or validate bicycle flow models, and can be applied in the design cycling infrastructure.

3.1   Introduction

Scientific knowledge of bicycle traffic flow is steadily growing but still limited compared to for example, motorized traffic flow. At the same time, the bicycle usage is growing to the level that urban areas, especially in the Netherlands, are struggling to accommodate all cyclists on their network. This crowdedness causes local congestion and frustration among bicycle users, which decreases the perceived safety and bicycle enthusiasm (De Winter, 2020). To prevent that cyclists are discouraged to cycle and use other, less sustainable, transport instead, it is vital to better manage bicycle traffic. To do so, it is key to unravel the main characteristics of bicycle traffic flow in crowded situations.

These features have been studied in experimental settings, e.g., Zhang et al. (2014) and Jiang et al. (2016), where cyclists are strictly following, meaning that they are not allowed to switch positions. This restriction limits observing the true nature of cyclist flow, including e.g. riding alongside, overtaking, and cycling in staggered formation. This research focuses on three fundamental variables in traffic flow theory, i.e. density, average speed and flow, in the situation where cyclists are allowed to move freely within the path boundaries. Furthermore, the relation between these variables are addressed and how they are affected by anticipation on downstream conditions.

This research takes the macroscopic approach and describes bicycle movements at an aggregated scale, based on empirical data that was retrieved at a large-scale cycling experiment. The bicycle flow will be observed at a narrowing in uni-directional flow. Based on individual speed and individual density, a better understanding of the aggregated quantities, i.e., average density, speed and flow, will be given. Also, insights into the path usage are given for different scenarios. The influence of anticipation is examined by analyzing aggregated data and by zooming in to individual speed data. The key contributions are the new insights into the macroscopic properties of a bicycle stream in the situation where cyclists are free to choose their position on the path.

The paper continues by providing relevant background information in Section 3.2, followed by the research approach in Section 3.3. Section 3.4 presents the results and finally, Section 3.5 reflects on the results by comparing them to other findings, and finally, Section 3.6 presents the main conclusions.

3.2   Related work on aggregated cycling properties and anticipation

The interest in bicycle traffic flow has gradually grown over the past decades. Within the topic, several subcategories can be selected based on the infrastructural setting, e.g., intersection or bicycle path, uni- or bi-directional, and on-street or segregated situation. Here, we focus on uni-directional and segregated paths.

One of the first to report on average bicycle characteristics is Opiela et al. (1980) who connected the speed to available maneuvering space. More than a decade later, Navin (1994) reported on the density–speed relation, showing a linear decrease of speed with increasing density, and the density–flow connection, showing a curved relation with a maximum flow at a density around 3.0 bic/m^2. These results are based on an experiment in single-file motion, which means that participants were instructed to follow and not allowed to overtake others. This setup restricts cyclists in showing their natural behavior and therefore captures only a simplified version of bicycle flow.

Because of its simplicity, the single-file setup is ideal as a first step to unravel the cycling properties that bicycle models need to reproduce. This was done, for instance, in the works of Andresen et al. (2014) and Jiang et al. (2016) to validate microscopic models. Furthermore, the single-file setup enables comparing the results of other traffic forms, e.g., car traffic or pedestrian movements. This comparison has surfaced similar patterns in density–flow relation (Zhang et al., 2014) showing an increase of flow with density in free-flow conditions, and a decrease in flow in congestion. This pattern suggests an analogy in the underlying behavioral mechanism (Zhao and Zhang, 2017). However, is it questionable whether this similarity holds when the instruction to follow for cyclists is relaxed.

So far, two studies have reported on a multi-lane experiment in which cyclists are allowed to use the full width. In Guo et al. (2019), the flow was observed while cyclists moved along a 3-meters wide circular track. They found that the flow increased with track density up to a level of approximately 0.2 bic/m^2, remains constant up to a density of 0.5 bic/m^2, and drops for higher density due to the occurrence of stop-and-go waves. The authors state that the constant plateau in flow is connected to the path usage, since they observed that the number of occupied lanes increased within this density range. The second experiment described in Wierbos et al. (2019) reports on the maximum flow while passing a bottleneck of different sizes. They found that the flow depends on path width, and that the configuration of cyclists differs for different path width. Due to the limited number of observations, a more detailed analysis could not be made. However, the connection between path usage and flow is worth exploring further and will be addressed in this research.

Besides in experiments, bicycle flow has also been studied in real-life situations. Cyclists are not influenced in this setting and thus show their natural cycling behavior. Botma and Papendrecht (1991) report, for instance, on the lateral position of cyclists and the distribution of speed. They concluded that the mean speed is slightly higher on wider paths, and that the lateral distance is smaller when cyclists move in pairs than when cyclists are overtaking. The study of Li et al. (2015) looked at one and two-lane bicycle paths and found that the average speed decreases with increasing density. Furthermore, they observed that a relative large flow could be maintained while the density was high and the average speed was reduced to around 5 km/hr. This indicates that the shape of the density–flow relation is indeed different for the multi-lane setting than for the single-file situation. As explanation, the authors of Li et al. (2015) state that the underlying behavior is more complex in the multi-lane case, which allows them to maintain a small headway even in congested, slow-moving, conditions. This complex behavior has not been labeled by Li et al. (2015), but we believe that it could be described as anticipation. Therefore, we investigate the behavior also in this study.

Anticipation behavior has been studied in car traffic and pedestrian movements, but not yet in bicycle traffic. In car traffic, the phenomenon is described as hysteresis (in, e.g., Treiterer and Myers (1974) and Zhang (1999)). The concept describes that accelerating and decelerating behavior of drivers results in a different pattern in the density–speed relation. Possible explanations mentioned in literature are aggressive and timid drivers (Laval, 2011), a combination of relaxation and anticipation (Deng and Zhang, 2015), and task difficulty, which is connected to the capability of drivers to make decisions while driving (Saifuzzaman et al., 2017). In pedestrian research, anticipation has been addressed in Duives et al. (2014) by studying the movements up- and downstream of a bottleneck. They concluded that anticipation occurs only upstream of a bottleneck. There, pedestrians react upon the upcoming congested conditions within the bottleneck by adopting a lower speed than what is expected under the existing density conditions. Also, Lü et al. (2020) described anticipation as the behavior of pedestrians to slow down in reaction to a potential collision, which results in the combination of low speed and low density. Gulhare et al. (2020) specifically mentioned that the visual information is important in the behavior of pedestrians. When congestion is present downstream, pedestrians maintain at a comfortable distance from one another while moving at low speed. As a result, the density–speed relation differs for the up- and downstream situation. Whether anticipation behavior also influences the density–speed relation bicycle flow is unknown and will be investigated in this study.

In summary, knowledge gaps exists regarding the density–flow and density–speed relation in the situation where cyclists are not restricted to following each other but are also allowed to swerve and overtake. Furthermore, the effect of path usage and anticipation behavior requires further examination. These gaps will be addressed in the continuation of this paper.

3.3   Research approach

This research aims to reveal macroscopic characteristics of bicycle flow, based on microscopic trajectory information. More specifically, we extract individual speed and density before aggregating the data to unveil patterns on a macroscopic level. Section 3.3.1 first describes the experiment in which the trajectory data is retrieved, then Section 3.3.2 describes the steps that are taken to extract the data, Section 3.3.3 describes the definitions of density, speed and flow that are used in this study. And finally, Section 3.3.4 presents the approach to quantify the patterns in, and relation between, the macroscopic variables density, average speed and flow.

3.3.1   Controlled experiment

A large-scale cycling experiment with approximately 200 participants was held at an indoor location in the Netherlands in April 2018. The participants were split up into an afternoon group with conventional bicycles and a morning group with different bicycle types, i.e. racing, electric and conventional bicycles. The cyclists were asked to cycle along a 2-meter-wide track which was narrowed on one side by mattresses, thereby creating a bottleneck. An impression of the situation is given by Figure 3.1, and a selection of the bottleneck situations is presented in Figure 3.2.

The bottleneck size was varied multiple times, resulting in five scenarios: (1) 2.0m or no obstruction, (2) a narrowing of 1.25m, (3) 1.00m, and (4) 0.75m wide, and (5) a meander. In the latter case, cyclists had to pass a narrowing on both sides of the track, resulting in a meandering movement. The scenarios were repeated multiple times in mixed order and are referred to as runs. An overview of the runs that are used in this study is provided in Table 3.1. The participants were asked to cycle similar to how they would move in daily traffic and were allowed to overtake others. In most runs, the cyclists entered the track as a group such that the bottleneck was readily activated. Run 18 is an exception. Here, the cyclists entered the track one by one, thereby gradually increasing the track density. The cycling movements are captured by cameras that are indicated by red dots in Figure 3.3.

Figure 3.1: Impression of the experiment. Photo by TU Delft/Frank Auperlé.

The participants received a financial compensation for their time, and wore red caps while cycling to protect their privacy. Furthermore, the experiment has been approved by the Ethics Committee of the Delft University of Technology. The data used for this study is a selection of the data gathered at a large–scale experiment. The details of the full experiment setup can be found in Gavriilidou et al. (2019).

3.3.2 Data extraction

The cycling movements are captured by downward facing cameras, which register 20 frames per second from a height of 12 meter, resulting in images of 1920x1080 pixels. All participants wear red-colored hats, which are used as reference point for extracting the trajectories. The data set thus consists of head positions that are updated every 0.04 seconds. Figure 3.4 shows the camera images of the lower track, the path alignment, and an example of extracted trajectories. The images display the original camera view and show inaccuracies such as a variable lane width. This is caused by the curvature of the lens and needs correction before the data can be used.

The full list of steps that are taken before the trajectory data is used for further analyses are: 1) lens correction, which corrects the image for curvature of the camera lens; 2) orthorectification, which translates pixel positions to X and Y coordinates in meters; 3) head to ground translation, which relocates the observed red hat positions to ground level. In this process, a uniform head height of 1.79m is assumed. 4) alignment, which corrects the rotation of the camera images caused by slight differences in camera orientation; and) filtering, which removes the trajectories that are false or incomplete ($\sim$0.6%). Figure 3.4 shows the view captured by the cameras (a) and an example of the trajectory data(b), including the camera overlap and positions.

Table 3.1: Schedule of scenario runs during the day of the experiment.

Run #	Bottleneck width [cm]	Participants #	Session
1	125	44	Morning
2	200	35	Morning
3	75	51	Morning
4	125	42	Morning
6	75	45	Morning
8	75	46	Morning
9	125	35	Morning
12	125	45	Afternoon
13	100	44	Afternoon
16	75	45	Afternoon
18	200	1-89	Afternoon
19	Meander	44	Afternoon
20	Meander	45	Afternoon
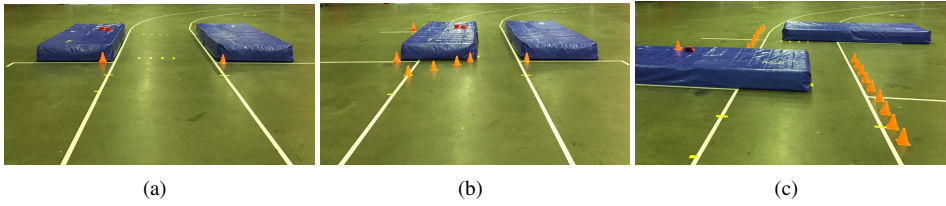
Figure 3.2: Bottleneck situations (a) 2.0m, (b) 0.75m, and (c) meander.
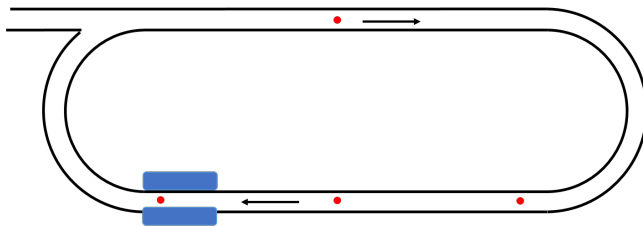
Figure 3.3: Sketch of the track showing the camera positions (red dots) and the driving direction.
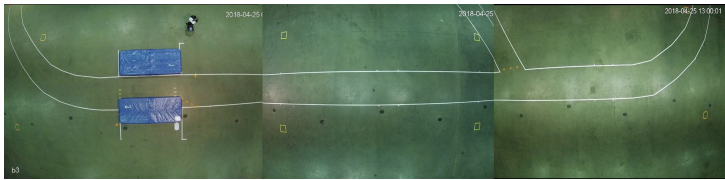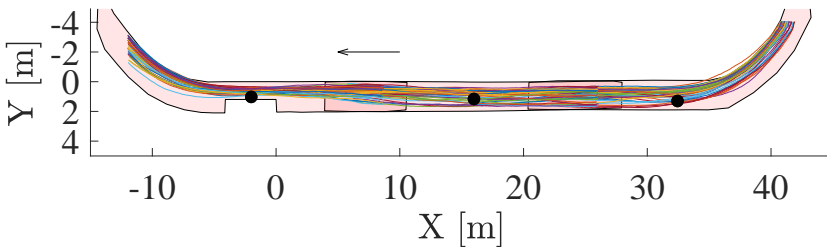
Figure 3.4: View of the three (overlapping) cameras on the lower track (before lens correction was applied) (a), and an example of trajectory data, showing also the positions (black dots) and overlap area of the cameras.

3.3.3   Definitions

This section explains the methods that are used to calculate individual density and speed based on voronoi tessellations, and the different ways to aggregate the variables density, speed and flow.

Individual density and speed

The individual densities are retrieved using the method of voronoi tessellations. This method was proven to be successful in pedestrian research (Duives et al., 2015; Nikolić and Bierlaire, 2018) and was adjusted for bicycle movements to include speed information by Knoop et al. (2020). Here, we use the traditional voronoi tessellation, which means a cyclist gets assigned all space which is closer to this cyclist than to another. Furthermore, the individual space is limited to the path width. An example is given in Figure 3.5a, where the area A_i, depicted in gray, is the voronoi area for cyclist N_i. The individual density k_i at time instant t is calculated by taking the inverse of the voronoi area:

$$k_i(t) = \frac{1}{A_i(t)}. \tag{3.1}$$

The method to retrieve the individual speed is based on the Euclidean distance between the X and Y position on time instant t and those a time step Δt later:

$$v_i(t) = \frac{\text{distance travelled}}{\text{time step}} = \frac{\sqrt{(X_{t+\Delta t} - X_t)^2 + (Y_{t+\Delta t} - Y_t)^2}}{\Delta t}. \tag{3.2}$$

We use $\Delta t = 0.20$ seconds, and in the further analyses a 1-second moving mean of the individual speed, to filter out small fluctuations due to measurements errors in the position.

Aggregated density, speed and flow

We use two methods to aggregate the variables in this research. One is a time average taken at a cross section and the second is an area-based average based on a selected area.

(a)

(b)
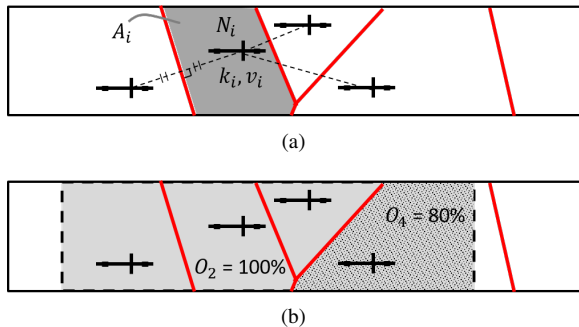
Figure 3.5: Cyclists and their individual area based on voronoi tesselation (a), and examples of cyclists whose individual area has a 100% and 80% overlap with the selected box depicted in gray.

The time-average method is based on the moment a cyclist passes a longitudinal position X. The individual density and speed of all cyclists that pass this line within a chosen time period are registered and aggregated. We use a time period of 30-seconds to smooth out individual variability while still capturing differences due to changing conditions. This method is used to identify the influence of path width to the flow characteristics of bicycle traffic. For every 30 seconds, we select the first cyclist that passes the cross section. The interval time (T_{int}) is the time between first cyclists of consecutive periods and forms the basis of our aggregation. Note that depending on the passage moment, the interval time can be shorter or longer than 30 seconds. The average speed ($\bar{v}$) is calculated as the harmonic mean of the individual speeds of all cyclists that pass within the interval time, see Eq. 3.3 The average flow ($\bar{q}$) is based on the number of passing cyclists divided by the interval time, see Eq. 3.4.

$$\bar{v} = N_{\text{pass}} \left(\sum \frac{1}{v_i} \right)^{-1} \tag{3.3}$$

$$\bar{q} = \frac{N_{\text{pass}}}{T_{\text{int}}} \tag{3.4}$$

$$\bar{k} = \frac{\bar{q}}{\bar{v}} \tag{3.5}$$

The area-based average variables, denoted by capital letters, are density $\overline{K}$, speed $\overline{V}$ and flow $\overline{Q}$. They are calculated by taking the mean of the individual data within a selected area. The benefit of this approach is that it allows for identification of instantaneous characteristics and is therefore better suited to analyze the density–speed and density–flow relation. Throughout this research we set the size of this box to 5 x 2 meters (length x width). Since the edges of the voronoi areas are not straight, we need to account for the edges of our selected box. For this, we calculate the overlap O of the voronoi cells with the selected box, see Figure 3.5b. Also, we need to take into account that cyclists can be outside the box themselves, but their voronoi area overlaps with the box of interest. For this, we calculate the fraction of the box f_i. This is based on the overlap O_i between the voronoi area of cyclist i and the box of interest. Then, f_i is calculated as the ratio of O_i to the box area A_{box}, see Eq 3.6. All f_i together sum up to one ($\sum f_i = 1$).

$$f_i = \frac{O_i}{A_{\text{box}}} \tag{3.6}$$

The calculation of the mean density within the box at time instant t is then:

$$\overline{K}(t) = \sum_{i \in E} f_i(t)k_i(t) \quad \text{and} \quad E = \{i \in \mathbb{Z} \mid f_i > 0\}. \tag{3.7}$$

The mean speed u within the box of interest at time instant t is, similar to the mean density, weighted by the overlapping voronoi areas:

$$\overline{V}(t) = \sum_{i \in E} f_i(t)v_i(t) \quad \text{and} \quad E = \{i \in \mathbb{Z} \mid f_i > 0\}. \tag{3.8}$$

The flow within the box of interest on time instant t is determined by straightforward multiplying the mean density and mean speed:

$$\overline{Q}(t) = \overline{K}(t) \cdot \overline{V}(t). \tag{3.9}$$

3.3.4 Approach

Our aim is to identify the characteristics of bicycle traffic in terms of density, speed and flow, and to relate these characteristics to path width and anticipation. To reach this goal, we compare the data of different scenarios in which a bottleneck is included to narrow the path. This narrowing varies between 2.00 meter (no obstruction), 1.25 meter, 1.00 meter, 0.75 meter and a meander. In the latter scenario, cyclists have to pass a narrowing of 0.75 meter on both sides of the track, resulting in a meandering movement in between. The following analyses are performed:

1. We investigate the influence of path width to the average density $(\bar{k})$, speed $(\bar{v})$ and flow $(\bar{q})$. This data is based on the 30-second averages of cyclists passing the line X = 0m, which is at the entrance of the narrowing.

2. We investigate the path usage of individual cyclists to identify movement patterns on the macroscopic level for different path widths. For this, we analyze the Y position of cyclists on the path that pass the cross-section X = -1m (inside the narrowing) and connect the positioning of cyclists to typical flow conditions based on the individual density and speed data.

3. We investigate the relation between density and speed, and density and flow based on area-based averages. For every second, we plot the density $(\bar{K})$ against speed $(\bar{V})$ and flow $(\bar{Q})$, resulting in lots of scatter. To better visualize the relation, we plot the median value for speed and flow for certain bins in density. The bin size depends on the number of observations, meaning that more data points will result in a more detailed curve. The data of scenarios with different path widths will be separated such that the effect of the narrowing can be identified.

4. We investigate the occurrence of anticipation by comparing the scatter plots of area-based density–speed data at four sections of the track, i.e. at 0-5m, 10-15m, and 30-35m upstream the bottleneck, and on the opposite side of the track. The effect of anticipation is expected to be highest at a distance before the narrowing, because cyclists have time and space to react, while this effect is less expected near the narrowing where the behavior is foreseen to be merely density driven. The data on the opposite side of the track is expected to be uninfluenced, since cyclists do not yet see the queue in front of the narrowing.

5. We investigate the macroscopic properties of bicycle flow by looking at the evolution of individual cycling characteristics along the track. For this, we compare individual data at ten cross sections along the lower track, which are five meters apart. At each cross section, we record the individual speed and density of passing cyclists as well as their speed difference to the two most surrounding cyclists. The latter is a measure for overtaking movements, since this requires a speed difference. All results are visualized in box plots, which show the variability of cycling characteristics in space.

3.4 Results

This section presents the results of the five analyses listed above. The full findings are listed first, followed by summary in section Section 3.4.6.

3.4.1 Speed, density and flow for different path widths

To investigate the influence of path width, we examine the average speed, density and flow for different situations, as shown in Figures 3.6 and 3.7. Visualized with box plots are the distribution of the 30-second averages at the bottleneck entrance (a) per scenario and (b) specified into run numbers. The runs are not consecutive because they are performed in mixed order and other scenarios were done as well, which are not used in this research. The no-obstruction scenario is included as reference; it does not have a narrowing, thus the path is two meters wide.

The average individual speed ($\bar{v}$) is shown in Figure 3.6a and shows an increase with increasing path width when comparing the median values. As expected, the speed is lowest in the scenario with the meander, and highest when the path is unobstructed. Furthermore,

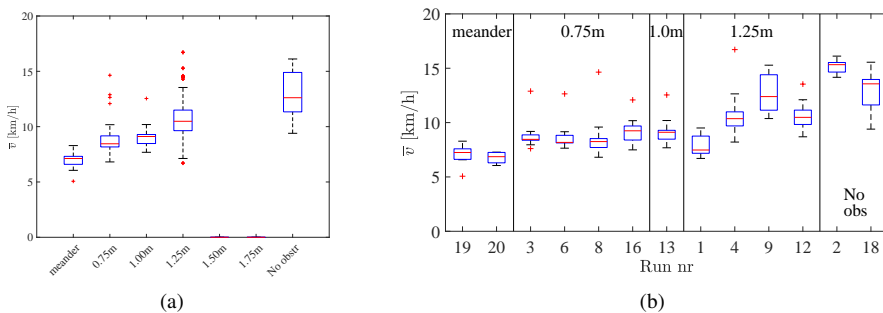

(a)   (b)

Figure 3.6: Box plots of 30sec-average speed across the line X = 0m for different bottleneck widths combined (a) and split up in individual runs in (b).

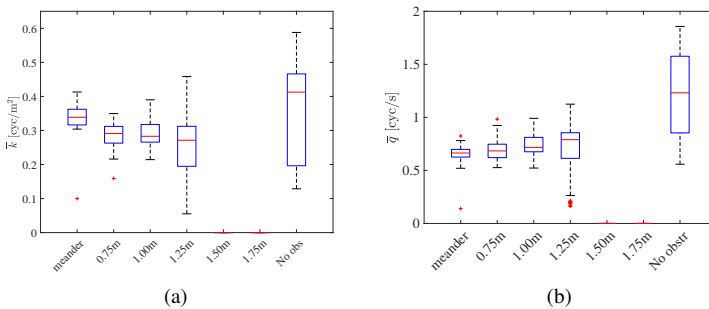(a)   (b)

Figure 3.7: Box plots of (a) individual density and (b) flow across the line X = 0m per scenario.

the speed variation increases with path width, hinting that cyclists have more opportunity to cycle at different speeds on wider paths. This indicator is visualized by the box plot height, where a compact box plot means that cyclists have similar speed while passing the narrowing and a large box indicates that more speed variation is observed. A similar pattern is visible when looking at the individual runs in Figure 3.6b, which shows that the average speed is around 10 km/h in all runs of the 0.75m scenario, while this varies between variation 8 and 14 km/h when the path is 1.25m wide. The larger speed variation in the latter scenario indicates that cyclists have more opportunity to cycle at different speeds, which is related to the path usage and the opportunity to overtake and is further discussed in Section 3.4.2 and 3.4.5. The unobstructed scenario shows a difference of 3 km/h between run 2 and 18. This gap is related to the total number of cyclists on the track, which is much smaller in run 2 (35 cyclists) than in run 18 (88 cyclists), indicating that the cyclists in run 2 have more opportunity to cycle at their desired speed.

The individual density of cyclists within the narrowing are shown in Figure 3.7a. Remarkably, the density is highest for both the meander ($\bar{k} = 0.22$ cyc/m^2) and unobstructed scenario ($\bar{k} = 0.24$ cyc/m^2), and drops to $\bar{k} = 0.18$ cyc/m^2 in the 1.25m case, while a continuous decrease with width was expected. This result is explained by two factors. First, the voronoi method that is used to calculate the individual density is based on the available physical area. When the path width decreases, the available space reduces resulting in a higher density even when the space between consecutive cyclists remains equal. This explains the increase in average density from the 1.25m scenario to smaller cases. Second, the higher density values in the 1.25 and 2.00m-scenarios can be explained by the total number of cyclists on the track, which is 88 in run 1 and 18. Most other runs hold 45 participants, except for run 2 with 35 cyclists. The variation in number of participants was done intentionally to force differences in cycling conditions, i.e. free flow and congestion. As expected, having more cyclists on the track results in a higher density and lower average speed.

Similar to the speed results, the variation in average individual density is higher in the 1.25m and 2.00m scenario (0.10–0.32 cyc/m^2), than in the cases with a smaller narrowing (0.16–0.25 cyc/m^2). This relates to the fact that cyclists are able to move abreast in the 1.25m case and wider, while merely staggered and following formations are observed in the smaller scenarios. Also, a steady queue is observed in the scenarios smaller than 1.25m, resulting in a constant longitudinal spacing between cyclists and thus a steady density level. Queues are less frequently observed in the 1.25 and 2.00m scenario, resulting in a fluctuating demand at the entrance of the narrowing. This results in varying distance between cyclists and thus a larger variability in density.

The median values of the average flow slightly increase when the bottleneck opening is wider, see Figure 3.7b, starting with $\bar{q} = 0.66$ cyc/s in the meander and increasing to $\bar{q}$ = 0.79 cyc/s in the 1.25m case. The flow in the unobstructed scenario steeply increases to 1.23 cyc/s in the 2.00m scenario, which shows that the relation between flow and path width is not linear. Figure 3.7b also shows that runs with a narrow bottleneck, i.e. meander and 0.75m, have a more constant flow, indicated by a compact box plot, than those for the wider ones, i.e. 1.25m and without obstruction (2.00m). This relates to track density and path usage; cyclists moving abreast in high demand situation (run 18) result in a higher flow

value than cyclist that are following in low demand situation (run 2). Since run 18 has many cyclists on the track and is unobstructed, the median flow of this run can be considered as the minimum boundary for the capacity, which is 1.5 cyc/s on a 2.00m-wide path.

3.4.2   Path usage

To better understand the patterns in average speed, density and flow, we now look at the path usage and the positions of cyclists in different scenarios, see Figure 3.8. Visualized on the left-hand side are the frequency distribution of the Y positions, and the personal density of cyclists while passing a line which is one meter inside the narrowing. This hence shows at which lateral position cyclists cross, and to which extent this depends on density. Visualized in the middle are the Y positions and individual speed at the same cross section. Screenshots of cyclists passing the narrowing are included on the right-hand side. Based on Figure 3.8, the following observations are made:

- 2.00m: Cyclists mostly occupy two lanes and move alongside each other, where the left lane is slightly faster than the right lane. Occasionally, three lanes are formed where cyclists move alternately alone and in pairs. When density is low (<0.1 cyc/m^2), cyclists move alone and occupy the right or middle lane, which is consistent with the Dutch rule to keep right. The highest density values of 0.5–0.6 cyc/m^2 are observed near the track edges, which coincides with cycling alternately in threes and in pairs. Here, the middle cyclist has a larger personal space than the outer cyclists, which are bounded by the track edges. This space restriction is less prominent to the center of the track, resulting in less observations of high-density for cyclists occupying the middle lane.

- 1.25m: Cyclists pick position in the middle of the narrowing for low density, using one lane, and fan out to the sides for in higher density, using two lanes. In most cases, these lanes are not used simultaneously but cyclists move in a staggered configuration where e.g. a cyclist on the right lane is followed by a cyclist in the left lane some moments later, as shown in Figure 3.8f. Once in a while, a pair of cyclists move next to each other through the narrowing. The highest cycling speed are obtained when density is smaller than 0.25 cyc/m^2. Most lowest cycling speeds (<6 km/hr) are found between 0.10–0.35 cyc/m^2, which is a lower value than expected based on first order traffic theory and because it partially overlaps with the range of higher speed. There are two explanations for this: First, it results from an inefficient merging process just upstream of the bottleneck where a cyclist had to stop before entering the narrowing. When passing the entrance, the cyclist is still accelerating and leaves a gap with its predecessor, which causes both the low speed and relatively low personal density. Second, the cyclists that pass with higher density are confident that they can pass the narrowing at this high speed because the conditions downstream are favorable. Therefore, they temporarily tolerate a higher density, while maintaining a high speed.

- 1.00m: Cyclists pass the narrowing in two different configurations. The two patterns are (a) keeping the same middle lane in a following mode, and (b) moving alternately in left and right lane in a staggered formation. Cyclists are no longer observed to move abreast. Compared to wider path widths, the spread in observed speed is much

(a)

(b)

(c) Scenario 2.00m

(d)

(e)

(f) Scenario 1.25m

(g)

(h)

(i) Scenario 1.00m

(j)

(k)

(l) Scenario 0.75m

(m)

(n)

(o) Scenario Meander

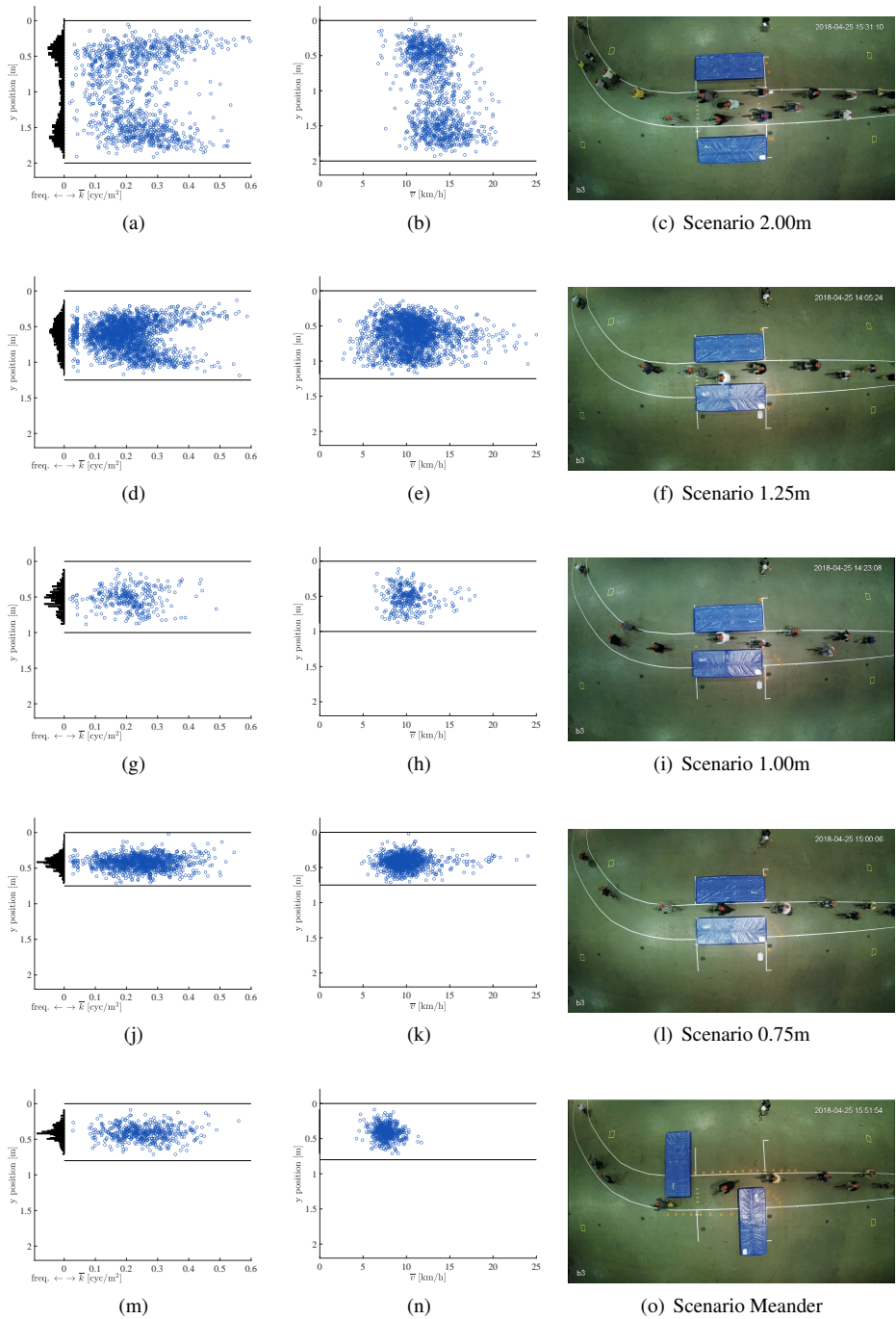*Figure 3.8: Y positions and individual density (left) and cycling speed (middle) of cyclists passing the cross-section X = -1m. On the right are screenshots of cyclists passing the narrowing.*

smaller, indicating that the narrowing creates a steady demand and cyclists move in synchronized manner, adapting to the speed of cyclists near them. Cyclists in the left lane keep a smaller distance to the track edge. Possibly, this is related to cycling confidence since, in general, more careful cyclists tend to keep right, and more confident cyclists are found in the left lane.

- 0.75m: Cyclists pass the narrowing in strictly-following mode, using only one lane. The variation in Y position is mainly an artifact of the method for trajectory extraction, which is based on the red hats. When cyclists are pedaling, their heads slightly move to the side where they apply force. The highest cycling speeds are obtained in low density conditions, while the speed is lowest between 0.20–0.35 cyc/m^2.

- Meander: Cyclists again have a strictly-following configuration, maintaining a slightly larger spacing than in the 1.00m-scenario. Now, little difference in speed is observed in low and high density conditions. This is explained by the fact that all cyclist have to slow down to successfully maneuver through the meander.

3.4.3 Density–flow and density–speed relationship

Average speed, density and flow rate are correlated in 1st order traffic flow theory. Based on this theory, a relation between density–speed and density–flow is expected for particular widths of the path. Figure 3.9 shows the area-averaged density–speed and density–flow plots for different path widths combined along a 5-meter stretch inside the narrowing. On the left-hand side, all data is visualized with the darker colors indicating smaller path widths. On the right-hand side, the median line of all data is plotted. Based on these figures, four observations are made:

- The speed decreases with increasing density for most widths, except the meander which has a constant low speed. The speed reduction with density is a logical consequence of having less physical space to move. For the meander, the observed density range is small, indicating that the cyclists pass the bottleneck at a constant distance from each other and maintain a cautious pace.

- The scatter in speed data reaches a minimum at approximately 5 km/h for all widths, and can therefore be considered as the minimum cycling speed. The existent of a lower boundary is explained by the characteristic of bicycles to tumble over when speed is too low. Speeds below 5 km/h are observed, but only when cyclists use their feet to maintain balance and push themselves forward.

- The density, speed and flow values are highest in the 2-meter scenario, and decrease for narrower path widths, except for the 1-meter scenario. The near consecutive order can be explained by the path usage. The number of lanes that cyclists use reduces when path width decreases and the distance between cyclists increases, which results in a lower flow. Furthermore, when the flow through the narrowing is smaller, cyclists have to adapt by reducing their speed while passing the narrowing.

- The median lines for the 1.25m and 1.00m scenario are similar, indicating similar underlying behavior. This is consistent with the observed configuration in both cases.
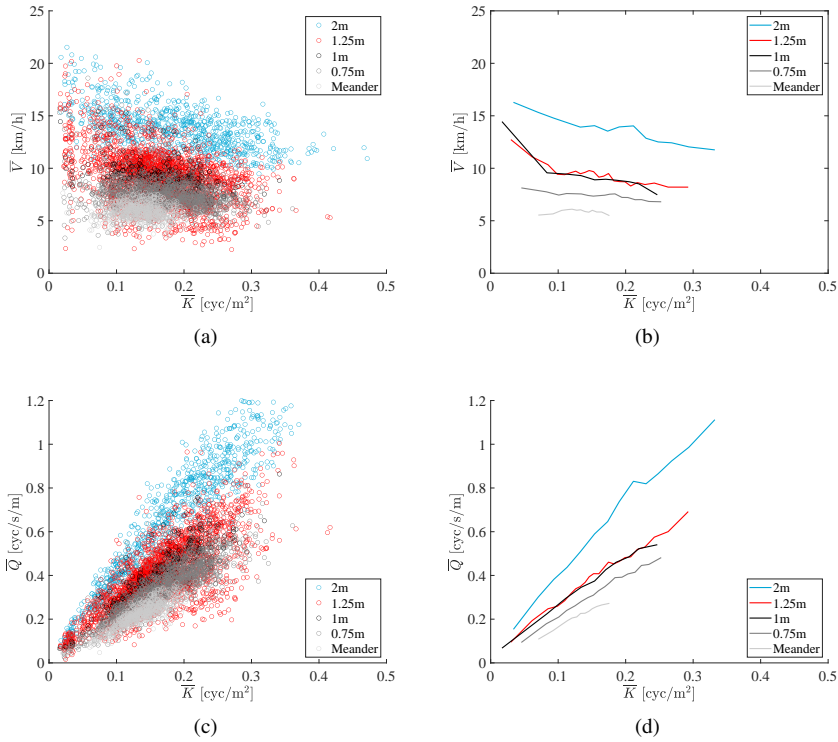
Figure 3.9: *Area-based density–speed plots (upper panels) and density–flow plots (lower panels) for different path width based on 1-sec averaged data inside the narrowing.*

Cyclists alternately occupy the left and right lane and do not overtake. Once in a while, cyclists move pairwise in the 1.25m scenario, which is not observed in the 1m scenario. The frequency at which this happens is not high enough to affect the flow rate, but it could explain the wider density range that is observed in the 1.25m scenario.

- The density–flow plots show a steady increase with density, and do not have a maximum within the observed density range. On the one hand, this indicates that capacity is not reached, and that the flow conditions within the narrowing are not congested, while congestion does occur further upstream. On the other hand, the maximum observed density could indicate the ideal circumstances in which smooth flow is achieved. This means that the maximum flow value for each path width can be considered as the capacity, i.e. 0.27 cyc/s/m (meander), 0.48 cyc/s/m (0.75m), 0.54 cyc/s/m (1.00m), 0.69 cyc/s/m (1.25m) and 1.11 cyc/s/m (2.00m).

We now combine the data of all scenarios and look at locations upstream of the bottleneck and the path is 2.00-meter wide. Figure 3.10 shows the area-average data at three stretches

on the track, i.e. X = 5-10m, and X = 25-30m on the side of the narrowing, and half way on the opposite side of the track. The distance to the bottleneck thus increases from (a) to (c). Since the bottleneck causes congestion upstream, it is expected that a congested branch is visible in the density–speed and density–flow plots upstream of the narrowing.

Based on Figure 3.10, three observations are highlighted. First, the data of the 5-10m section is comparable to that within the narrowing by not showing a capacity point or congested branch. Most likely, the cyclists have already prepared themselves for passing the narrowing by merging, or adapted speed to prepare for merging, resulting in a smooth flow pattern. Second, the observed density range is higher in the 25-30m section than closer to the narrowing. This indicates that cyclists occupy the full width and merging has not yet occurred. The median line increases with increasing density and does not show a capacity point. This can possibly be explained by anticipation behavior, which prevents a complete breakdown of the bicycle flow. Instead of coming to a complete stop, cyclists try to maintain their forward-momentum by slowing down in advance so they can continue moving (slowly). Third, the data on the opposite side of the track (Figure 3.10f) show a steady relation up to $\overline{K} = 0.15$ cyc/m^2, and changes shape for higher values. Although flow still increases, it can be said that the bicycle flow changes regime from free-flow to congested conditions at $\overline{K}$ = 0.15 cyc/m^2. However, the flow continues to increase for higher density, indicating that congestion in bicycle traffic does not coincides with a drop in flow.

(a) X = 5-10m   (b) X = 25-30m   (c) X = opposite side

(d) X = 5-10m   (e) X = 25-30m   (f) X = opposite side
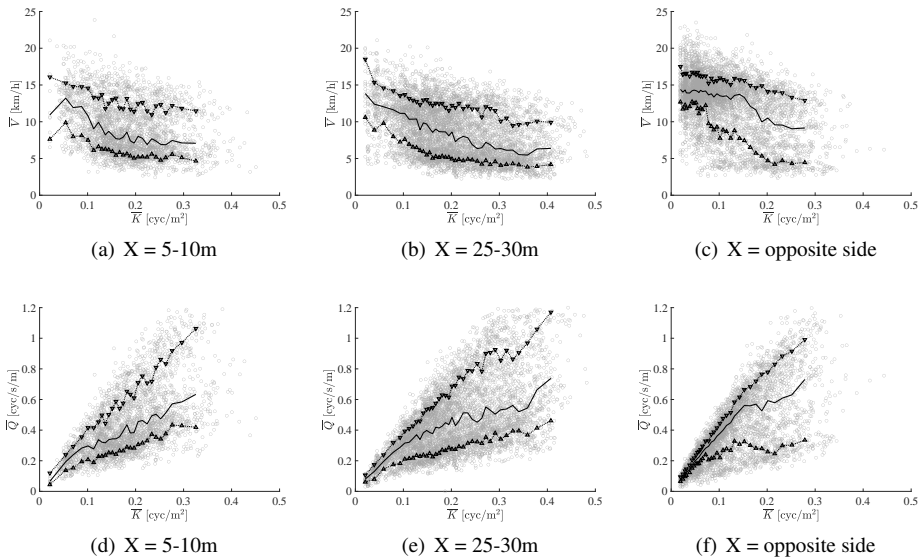
Figure 3.10: Area-based density–flow data for three stretches on the track, based on 1-sec averaged data of all runs. The solid black line indicates the median and the lines with triangles are the quartiles.

3.4.4   Influence of anticipation

To investigate the effect of anticipation behavior, we zoom in to a single run and look at the density–speed relation in four different stretches. Anticipation behavior encompasses that cyclists not only react to density in their direct surrounding but also react to the conditions further downstream. In our experiment, this is the upcoming narrowing, the associated queue, and the available space downstream of the narrowing. We look at one specific run at multiple location on the track, as shown in Figure 3.11. It shows the area-average density–speed data for run 16, which has a bottleneck width of 0.75m, at four different stretches. The first one (a) covers a stretch on the opposite side of the track, while the other three cover the track at a distance of 25-30m (b), 10-15m (c), and 0-5m (d) upstream of the narrowing.

The data show a wide variation in density and velocity between different locations. The spread is smallest in (a) and (d), while a much wider spread is observed in (b) and (c). This difference can be explained by varying stages of anticipation: Cyclists on the opposite side of the track (a) show no anticipation; they do not see any obstruction ahead and thus cycle at their desired speed. The density variation at (a) occurs due to differences in clustering, varying from a cyclist moving alone, to a pair of cyclists who form a temporary moving bottleneck. The spread in average density and speed is largest for stretch (b), where similar

(a) opposite side of the track

(b) 25-30m upstream

(c) 10-15m upstream

(d) 0-5m upstream
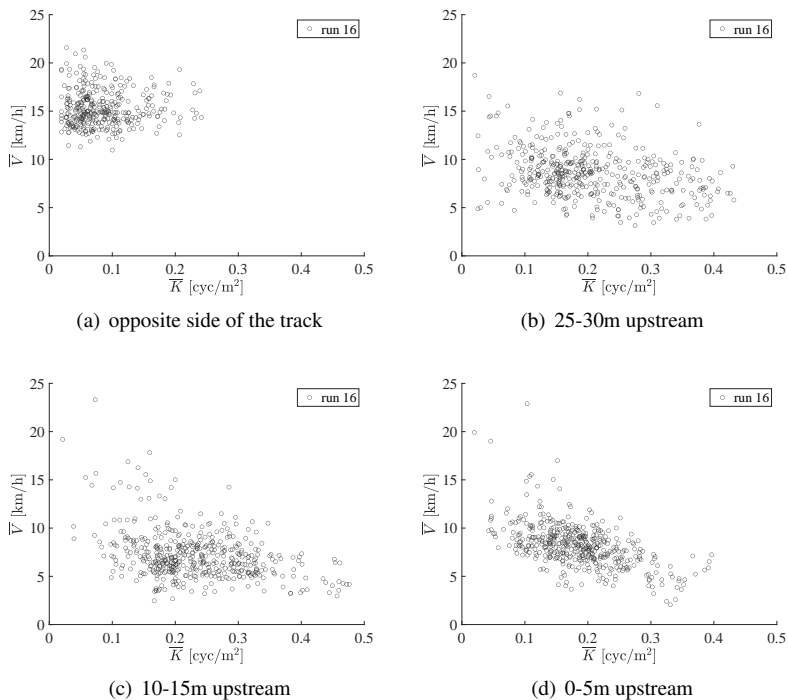
Figure 3.11: Area-average density–speed within four stretches on the track based on 1sec data.

speed values coincides with a large range of density and vice versa. For example, an average speed of 5 km/hr is observed when density ranges between 0.1 and 0.4 cyc/m^2, while at the same range also speeds occur of 10 to 15 km/hr. This is a typical result of anticipation behavior, because cyclists either reduce speed (or simply stop pedaling) because they see others braking in front of them and already adapt their own speed, resulting in low speed and large spacing (thus low density), or they continue at high speed because they see an available spot in the queue further downstream. To reach that spot, they temporarily accept a higher density while overtaking others, resulting in high speed and high density. Moving closer to the bottleneck in stretch (c), the speed variation is smaller than in (b), especially for $\overline{K}$ larger than 0.2 cyc/m^2. In stretch (c), most gaps are filled and cyclists prepare for merging, resulting in a synchronized flow within the queue, in which participants react to they direct surrounding. Occasionally, cyclists overtake others that are preparing for merging, increasing the (spread in) average density and speed in the process. It is, however, unclear whether this behavior should be considered as anticipation or aggressiveness. In stretch (d), just upstream of the narrowing, cyclists react mostly to the conditions around them, i.e. density, and show little to no anticipation. They have to adapt their speed to others in order to pass the narrowing, resulting in less scattered density–speed data.

Although not illustrated in Figure 3.11, cyclists also show anticipation within the narrowing by adapting their speed to the conditions downstream. When the area behind the bottleneck is occupied, speeds are low and vice versa. When the area downstream is empty, cyclists temporarily accept a higher density and move at a higher speed through the narrowing than expected based on their individual density.

3.4.5   Bicycle flow properties along the track

To better grasp the macroscopic properties of bicycle flow, we now look at the evolution of cycling characteristics along the track. For this, we aggregate the individual properties of cyclists passing ten cross sections along the lower track, which are each 5 meters apart. Figure 3.12 shows the resulting box plots of individual density k (left), individual speed v (middle) and the difference in speed with its neighboring cyclists (right). For the latter, the individual speed is compared with the average speed of its two surrounding cyclists. We discuss the data of three runs, i.e. 1.25m (run12), 0.75m (run 16) and meander (run 20), and start with the density and speed data.

As expected, the density and speed data vary along the track in opposite pattern. Since cyclists cannot disappear from the track, a change in density must coincide with an opposite response in speed or vice versa. Less expected is the curved shape in the median density and speed data, which becomes more pronounced with decreasing bottleneck width. The extremes, so the lowest speed and highest density, are located well before the narrowing, which is situated at X = 0m. Furthermore, the extremes occur at slightly different X position. The highest density is observed around X = 15 and 20m, while the lowest speed values are observed further downstream around X = 10 and 15m. This mismatch confirms that bicycle the density–speed relation is influenced by anticipation behavior.
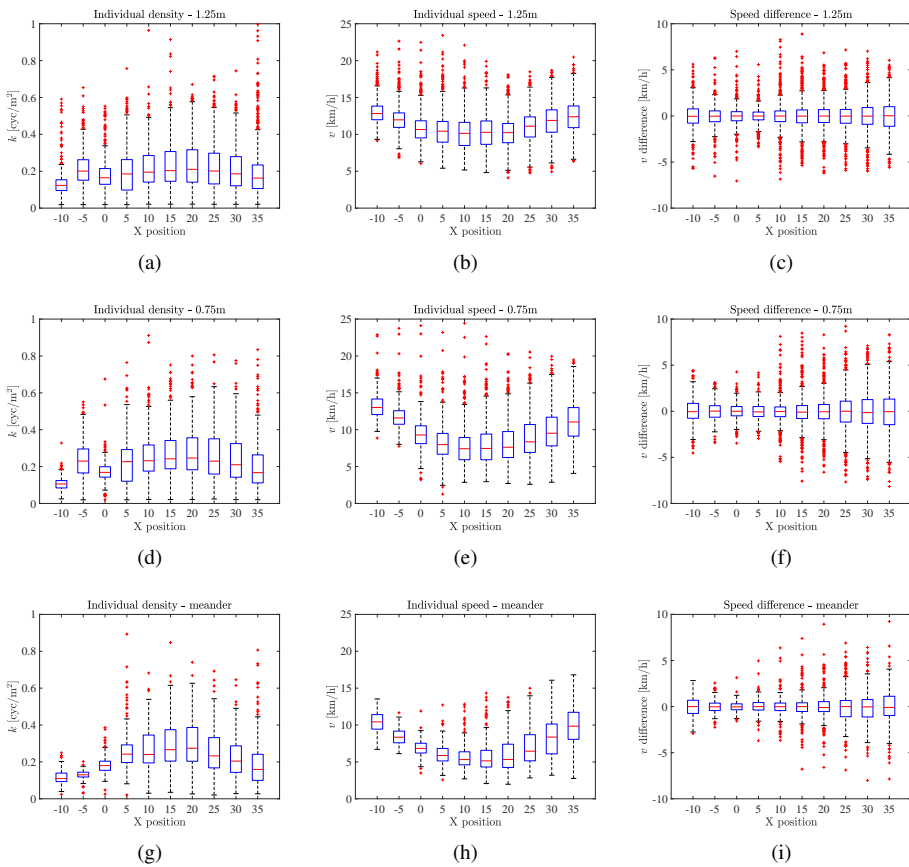
Figure 3.12: Box plot of individual speed, density and speed difference at different cross sections along the track for run 12 (upper), run 16 (middle) and run 20 (lower).

An explanation for the curved pattern is that cyclists already prepare for merging and move to one lane well before the narrowing. As a result, the density just upstream of this merging point is highest, while speed is lowest at the point of merging itself. Further downstream, cyclists accelerate again, resulting in higher speed and lower density for X below 5 meter. Upstream of the merging area, cyclists are joining the queue and thus reduce speed and increase their individual density when moving from X is 35 to 20m. This process is visualized with snapshots in Figure 3.13, which shows an area in which cyclists are merging, a slow moving cyclist which acts as a moving bottleneck for following cyclists, while others on the left can still overtake, thereby creating an area of high density.

The overtaking movements are captured by the speed differences in the left panels of Figure 3.13. Although the variation is small, the box plots are most compact between X = 0 and 5m, while the speed variation increases further upstream (best visible by looking at the quartiles). This coincides with the observation in Section 3.4.4 that cyclists move at similar

speed just upstream of the narrowing, while overtaking (high speed and density) and slowly moving cyclists (low density and low speed) are observed at the queue tail. Furthermore, the speed differences within the bottleneck is are slightly larger in the 1.25m scenario than in the meander, which coincides with different path usage. In the first scenario, cyclists move in a staggered formation, while the meander only allows for a strictly-following configuration. Using two lanes instead of one, gives cyclists more opportunity to go at slightly different speed and e.g. prepare for an overtaking movement after leaving the narrowing.
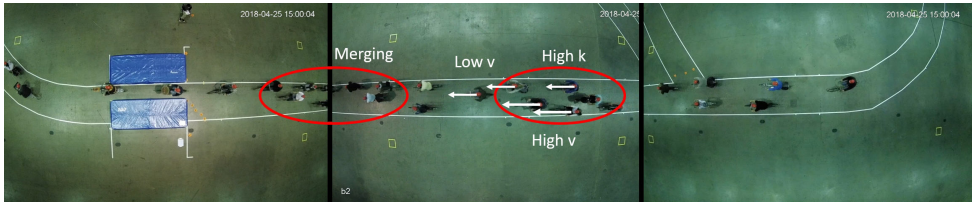
(a)

Figure 3.13: Snapshots of merging process

3.4.6   Result summary

1. Narrowing the path leads to a decrease in average individual speed ($\overline{v}$) and flow ($\overline{q}$), while the average individual density ($\overline{k}$) shows the opposite pattern. Furthermore, the density, speed and flow do not linearly increase with path width, and thus depend on other factors as well.

2. The overall speed decreases when path width reduces. When the width is greater or equal to 1.25m and multiple lanes are occupied, cycling speed is higher in the left lane than the right. On a 2.00m wide path, cyclists form 2 to 3 lanes, and overtake each other. For path widths smaller than 1.25m, cycling abreast is no longer observed and cyclists move in following or staggered configuration. To recall, cyclists move in a staggered formation when a cyclist on e.g. the right lane is followed by a cyclist in the left lane some moments later. This is primarily the case at a 1.25m path; when the path is 1.00m or smaller, cyclists are strictly following each other. As a result, the longitudinal spacing is larger in the following mode than in the staggered formation.

3. Path width influences the overall speed ($\overline{V}$), density ($\overline{K}$) and flow ($\overline{Q}$) by influencing the available cycling lanes and possible cycling configurations. The speed decreases with density, while the flow increases with density. The density–flow relation does not show a capacity point, since the flow continues to increase with increasing density. On a 2.00-meter wide path, the density–speed and density–flow relation are influenced by anticipation, resulting in a gradual transition from free-flow to congested conditions. When anticipation is absent, a clear transition between regimes occurs at a density of 0.15 cyc/m^2.

4. Anticipation behavior in bicycle flow is characterized by a wide variation in the density–speed diagram. On the one hand, anticipation occurs when the density downstream is high and cyclists stop pedaling well before reaching the queue, resulting

in the combination of low speed and low density. On the other hand, cyclists may temporarily accept a higher density when the conditions downstream are favorable, resulting in the combination of high density and high speed.

5. The properties of a cyclist stream vary along the track and depend on the infrastructural setting. In case of a narrowing, cyclists anticipate upon the upcoming obstruction by starting to merge around 10 to 15 meters before the narrowing. The lowest speed occurs at the point of merging, while the highest density values are obtained just upstream of this merging point.

3.5   Discussion

This section reflects on the obtained results by comparing them to findings in literature. Our findings are based on a large data set that was collected in a large-scale cycling experiment. This setting has limitations, since participants cycle indoors and might behave differently in real-life situations. For instance, the absence of a side curb might affect the path usage. However, the data is collected over a full day and the data set size is therefore large enough to capture cycling behavior that is likely to match that of outdoors. The data set size can explain some difference with comparable research in literature. This study shows that narrowing the path leads to an increase in density, and a decrease in speed and flow, which is in alignment with those in Wierbos et al. (2019). However, the flow values are smaller with median values between 0.6 cyc/s for a 0.75m path and 0.8 cyc/s for a 1.25m path in this experiment than the outflow capacities reported in the mentioned research, which reports 0.9 cyc/s and 1.5 cyc/s, respectively. The difference in flow possibly results from the sample size. In this research, we have observed the flow during 6 to 10 minutes per run, compared to 20 to 60 seconds in the other experiment.

We find similarities and differences when comparing the density–flow relation in this research to that in Guo et al. (2019). They reported an increase in flow for the density range 0–0.2 bic/m^2, a plateau of approximately 0.58 bic/s/m between 0.2–0.5 bic/m^2 and a decrease in flow for higher density. We roughly found a similar relation up to a density of 0.4 bic/m^2, although the boundary is found at 0.15 bic/m^2 instead of 0.2 bic/m^2. We did not have sufficient observations for density larger than 0.4 bic/m^2 to conclude a relation in that range. The differences could also results from other factors, such as cultural behavior (Asian versus Dutch) or bicycle size. Also, the position of riders could play a role which is more upright on typical Dutch bikes than on MTB type of bikes where the rider is bent forward and the eyes have a lower position.

Furthermore, we found that anticipation behavior leads to a gradually increasing density–speed relation, and the abrupt change in flow regime as observed in Guo et al. (2019) is only visible in our data when anticipation is absent. The situation-dependent difference in density–flow relation is also observed in pedestrian research (Duives et al., 2014; Gulhare et al., 2020) before and after a bottleneck situation. This suggests that the underlying behavior might be similar, which is worth investigating in future studies.

The path usage in this research is similar to that observed in Wierbos et al. (2019), going from a staggered formation and occasionally moving abreast in the 1.25m scenario, to solely staggered formation at a 1.00m width and following configuration at a width of 0.75m. Furthermore, the staggered configuration shows similarity to the 'zipper effect' in pedestrian flow under saturated conditions. This term describes that pedestrians move in lanes which are partially overlapping. Since they cannot physically overlap one another, pedestrians move at small longitudinal distance from each other and at similar speed. This configuration causes that the capacity does not increase linearly with the bottleneck width, but shows a stepwise increase instead (Hoogendoorn and Daamen, 2005). It is likely that this effect also plays a role in our research, since we found that the bicycle capacity does not scale linearly with the bottleneck width.

3.6   Conclusion

This research has revealed the macroscopic properties of a bicycle stream based on a large-scale cycling experiment. The main characteristic variables density, speed and flow have been investigated, as well as the influence of path width, positioning of cyclists on the path, and occurrence of anticipation behavior. The main findings of this research are listed in the following overview:

- Narrowing the path leads to an increase in density and simultaneous decrease in average speed and capacity at the bottleneck location. The density, speed and flow do not scale linearly to the path width.

- Cyclists form other configurations on paths of different widths, e.g., overtaking, staggered, or strictly-following, which influences the ability to cycle at their desired speed.

- The minimum cycling speed is around 5 km/h.

- Cyclists maintain a high flow while density is high also. As a result, the density—flow relation does not show a distinct capacity point, but rather displays a plateau of high flow in congested conditions.

- A change in regime, from free-flow to congested conditions, is observed at a density of approximately 0.15 cyc/m^2. This critical point does not coincide with a maximum in flow but marks the boundary to a different steepness in flow increase.

- Anticipation upon an upcoming high density area occurs as two opposite reactions in cycling behavior. On the one hand, cyclists stop pedaling when approaching a congested area, resulting in the combination of low speed and low density. On the other hand, cyclists temporarily accept a higher density when the conditions further downstream are favorable, i.e. available space ahead, resulting in the combination of high density and high speed.

- The density–speed relation and density–flow relation are found to be influenced by anticipation behavior. Its occurrence leads to a more gradual decline in speed with increasing density, while the flow shows a more gradual increase.

The insights into cycling behavior that are obtained in this study form an important step in the understanding of bicycle flow and can be used to better manage bicycle traffic in urban areas. For example, the knowledge gained on the influence of path width can be used to design road diversions when part of a bike path needs maintenance. Furthermore, the data on path usage can for instance be used to validate outcomes of microscopic bicycle models, while new macroscopic models can be developed using the insights into the relation between density, speed and flow and the role of anticipation.

Chapter 4

Capacity, capacity drop and relation of capacity to the path width

This chapter elucidates bicycle traffic flow by studying the aggregated movements of cyclists before and after the onset of congestion within the setting of a controlled bottleneck flow experiment. It quantitatively describes the relation between capacity and path width, provides a qualitative explanation of this relation by analyzing the cyclist configuration for different path widths, and considers the occurrence of a capacity drop in bicycle flow. By doing do, it answers the following research question: *How does path width influence the maximum flow on a uni-directional bike path?*

Using slanted cumulative curves and regression analysis, we find that the capacity of a bicycle path increases linearly with increasing path width. A steady drop in flow is observed after the onset of congestion, indicating that the capacity drop phenomenon also occurs in bicycle traffic. This phenomenon has been described for motorized traffic, but never before for bicycles.

Abstract

Bicycle usage is encouraged in many cities because of its health and environmental benefits. As a result, bicycle traffic increases which leads to questions on the requirements of bicycle infrastructure. Design guidelines are available but the scientific substantiation is limited. This research contributes to understanding bicycle traffic flow by studying the aggregated movements of cyclists before and after the onset of congestion within the setting of a controlled bottleneck flow experiment. The paper quantitatively describes the relation between capacity and path width, provides a qualitative explanation of this relation by analyzing the cyclist configuration for different path widths, and studies the existence of a capacity drop in bicycle flow. Using slanted cumulative curves and regression analysis, the capacity of a bicycle path is found to increase linearly with increasing path width. A steady drop in flow is observed after the onset of congestion, indicating that the capacity drop phenomenon is observed in bicycle traffic. The results presented in this paper can help city planners to create bicycle infrastructure that can handle high cyclist demand.

4.1   Introduction

The worldwide trend of urbanization leads to an increasing demand of people traveling from A to B within the city bounds. To handle this growing stream of travelers and prevent overloading of the road network, there is a need to transport people in a sustainable manner (United Nations, Department of Economic and Social Affairs, 2018). Using the bicycle is a good option as long as the infrastructure allows a safe and quick journey. However, the current understanding of bicycle traffic is rather limited leaving municipalities and practitioners with questions on how to create a cycling network that can handle a high cyclist demand.

Before looking at the network level, the traffic dynamics on a single bicycle path must be better understood first. More specifically, the capacity of a bicycle path is of interest as well as how capacity relates to the path width. If the cyclist demand exceeds the capacity, congestion will occur which might impact the maximum flow along the bicycle path. This phenomenon, called the capacity drop, is observed in motorized traffic but has not been reported yet for bicycles. Insight into this phenomenon for cyclists will contribute to the overall understanding of bicycle flow and help practitioners to design cycling infrastructure that is sustainable in a future with increased bicycle demand.

This research contributes to understanding bicycle traffic by analyzing the aggregated movements of cyclists before and after the onset of congestion. The work done within the setting of a controlled bottleneck experiment to minimize the influence of other traffic modes.

In the ensuing of this paper, Section 4.2 gives an overview of the literature, Section 4.3 explains the set-up of the experiment, Section 4.4 describes the resulting data set, Section 4.5 presents the methodology to analyze the data, Section 4.6 presents the results, which are then discussed in Section 4.7.

4.2 Background

Bicycle traffic has been the subject of research for more than three decades but the understanding of bicycle flow dynamics has progressed only little. In earlier years, Botma and Papendrecht (1991) and Navin (1994) have studied bicycle flow and have estimated the capacity of bicycle paths, which have motivated a range of similar studies (Andresen et al., 2014; Li et al., 2015; Jin et al., 2017b). The reported capacity values show a large range between 2,600 and 8,100 cyc/hr. These differences, linked to the underlying cycling behavior, are not yet fully understood. Differences may occur due to the large variation in infrastructure such as the path width but this has not been tested yet. To better compare the reported capacity values, the relation between capacity and path width should be better comprehended.

To better grasp the dynamics of bicycle flow, Chen et al. (2013) and Zhang et al. (2013) have looked into finding similarities to the dynamics of motorized traffic and pedestrian flow. The comparisons show similar flow characteristics such as the occurrence of stop-and-go waves. Also, after scaling the speed and density with the mode-specific free-flow speed and length, a similar shape of the fundamental relation between density, speed and flow has been retrieved. Jiang et al. (2016) have looked specifically into bicycle flow and have found no evidence for a capacity drop. The capacity drop is a phenomenon that is frequently observed in car traffic flow after congestion occurs at a bottleneck. Due to the increased distance between drivers induced by acceleration, the discharge rate of the traffic jam can be lower than the free flow capacity before the onset of congestion due to an increased distance between drivers (Cassidy and Bertini, 1999). The magnitude of the drop is determined by the intra-driver differences in preferred acceleration (Yuan et al., 2017) and for vehicular traffic capacity drops ranging from 3% to 30% are reported. The earlier mentioned study by Jiang et al. (2016) is based on single-file movement of cyclists, which restricts the normal cycling behavior. Whether the capacity drop exists when cyclists are allowed to overtake is still an open question.

In pedestrian research, the relation between capacity and bottleneck width is described by Hoogendoorn and Daamen (2005). They have found that pedestrians moving uni-directionally through a narrowing organize themselves in dynamic layers and move in a staggered fashion. This zipping behavior leads to a step-wise relation between capacity and bottleneck width; depending on the number of effective lanes that fit on the path, capacity increases in discrete steps. Similar behavior could be present in bicycle flow but this has not been studied so far.

In this work, we investigate the relation between capacity and path width. To this end, we carry out a cycling experiment with a realistic one-directional bicycle flow in which overtaking is explicitly allowed to occur. This allows for observing the free flow capacity as well as the queue discharge rate. In this setting, the capacity drop phenomenon might be observed in the same way as in vehicular traffic. More details of the experiment are given in the following section.

4.3   Experiment

The experiment is held on a closed terrain to exclude the disturbance of other traffic participants such as cars or pedestrians. The cycling movements are recorded on a straight stretch so that cyclists can move at their free speed without being restricted by the road curvature. The experiment has been approved by the Ethics Committee of the Delft University of Technology. Further details of the track lay-out and camera placement are described in Section 4.3.2 and 4.3.3 but before elaborating on that, the paper continues with explaining the experimental design in Section 4.3.1.

4.3.1   Design

The experiment consists of a group of cyclists that move along a uni-directional bicycle path. An obstacle is placed on the path that creates a bottleneck by narrowing the path and enables the occurrence of congestion, see Figure 4.1. The obstacle limits the flow since fewer cyclists fit on the path. However, the bottleneck is only activated when the cyclist demand exceeds the capacity, leading to congestion at the upstream side of the obstacle. To ensure the activation, participants should arrive at the bottleneck cycling at their desired speed with a sufficient rate.

The capacity for different path widths can be determined before congestion sets in by varying the bottleneck width and ensuring a sufficient demand on the 2 m-wide path approaching the obstacle. If the capacity drop phenomenon occurs in bicycle traffic, the observed flow through the bottleneck will drop to the queue outflow after the onset of congestion.
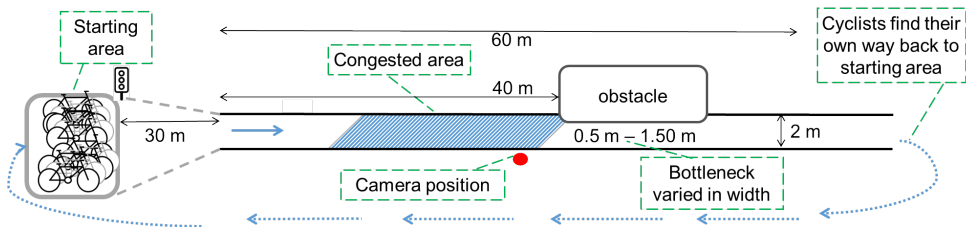
Figure 4.1: Sketch of the track design.

4.3.2   Set-up and execution

The experiment has been held in March 2018 on the Green Village terrain of Delft University of Technology in The Netherlands. The surface consists of 2-by-2 m concrete slabs over a total length of 60 m, creating a clear cycle path of 2 m width which was further indicated by orange cones, see Figure 4.2a. The participants, gathered in a starting area before the entrance of the track, start cycling after a start sign is given. The space between the starting area and the entrance of the cone-marked path is approximately 30 m as illustrated in Figure 4.1. Multiple test runs confirmed that a length of 25 m is sufficient for individual cyclists to reach their desired speed from standstill. However, the start-up process of a group of 34 cyclists might take longer. While we have not tested this hypothesis, we deem a total length

of 70 m sufficient for the group to reach the bottleneck location at the desired speed. To ensure a high arrival rate at the bottleneck location, which is needed to find capacity, the cyclists start from a waiting area much wider than the 2 m path and they are focally encouraged to start cycling simultaneously. This is to prevent that the process of acceleration to the desired speed, leads to stretching of the group configuration. Furthermore, the cyclists are instructed to cycle as they would normally do when leaving from a controlled intersection. After reaching the end of the 60 m stretch, the participants are asked to gather again at the starting point to prepare for the next run.

The obstacle, consisting of two inflatable air mattresses wrapped in a blue cover, is placed at approximately 2/3 of the straight stretch. The height of the obstacle is 33 cm which will block the pedaling over it but does not hinder steering which could be unsafe. Five scenarios are tested involving different bottleneck widths, varying between 0.50 and 1.50 m in steps of 25 cm. The order in which the scenarios are executed is randomized to reduce the behavioral adaptation. This results in the following order in which the scenarios are tested: 1.50, 0.75, 1.00, 1.25 and 0.50 m. Each scenario is repeated three times in a row to check for consistency.

4.3.3 Observations

In total two cameras are placed on either side of a 11 m-high pole, which is positioned next to the track at the upstream side of the bottleneck. Camera 1 is the main camera and captures all bicycle movements from a near top-down angle on the stretch between 10 m upstream and 2 m downstream of the bottleneck entrance (Figure 4.2a). Camera 2 is placed as backup and records the cyclists over a stretch of 18 m with an angle towards the upstream side. The placement position at the other side of the pole creates a gap in the track recording due to occlusion by the pole (Figure 4.2b).

The recruitment of participants has been done primarily via a master course at the university, resulting in a group of 34 people. A short questionnaire has been handed out before starting
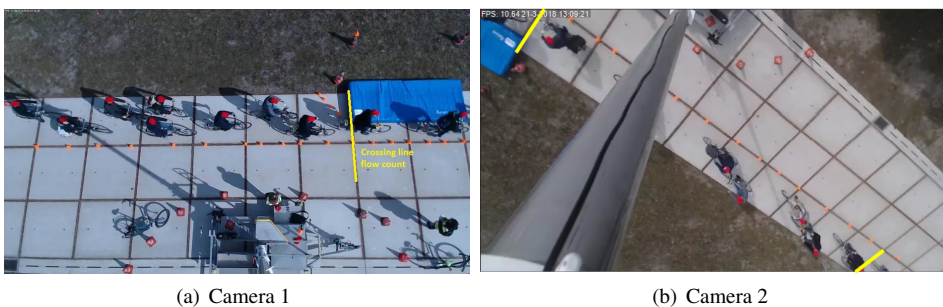
(a) Camera 1   (b) Camera 2

Figure 4.2: View of camera 1 (a) taken from a run with a 0.75 m wide bottleneck, and camera 2 (b) showing a situation with a 1.50 m-bottleneck. The crossing lines in yellow are used for the flow counts.

the experiment to collect socio-demographic data on age, gender, nationality, bike type and cycling experience. For privacy reasons, the survey data is anonymized and participants have been asked to wear a red cap during the experiment to minimize face-recognition.

4.4   Data set description

A total of 34 people participated in the experiment and based on the survey result we know that the group consists mainly of students who use the bike on a daily basis. One participant stated that his/her cycling frequency is once per month; all others cycle on a daily basis. The percentages of male and female participants are 76% and 24% respectively and every participant joined with a bike that they are familiar with. Most of these bikes are classified as a regular bike which includes a wide range of bikes with different braking systems (hand-brake or back-pedal brake) and one or multiple gears. Three exceptions are mentioned explicitly because they might lead to different behavior: 1) a foldable bike, which has a different physical shape, 2) a fixed gear bike, which has a different acceleration pattern, and 3) a racing bike, which has a different pose and desired speed. The details on age and nationality of the participants are presented in Figure 4.3. These descriptive data might be useful when comparing our results to future studies.

(a)   (b)
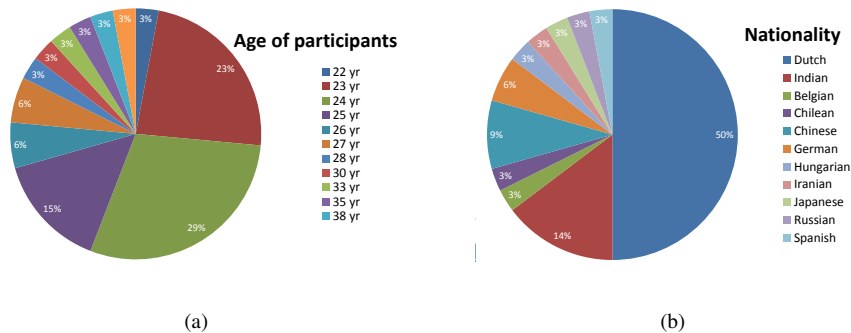
Figure 4.3: Socio-demographic data of the 34 participants.

A total of 14 runs are recorded and in most runs 34 participants joined. Some runs have 31 or 33 people because participants dropped out while other runs have 35 cyclists as one of the organizers has joined in as well. An overview of the runs is presented in Table 4.1. The third run of the scenario with a bottleneck width of 0.50 m (run 50-3) has been canceled because of safety reasons. The path is so narrow that some cyclists are touching the obstacle with their pedal or moving the cones creating a potentially unsafe situation for the following cyclists.

Next section describes the process and choices that are made to extract the data from the video recording.

Table 4.1: Details of the runs that were performed during the experiment.

Run #	Scenario name	Bottleneck width (m)	Participant #	Duration (s)
1	150-1	1.50	34	27
2	150-2	1.50	34	22
3	150-3	1.50	34	21
4	75-1	0.75	34	36
5	75-2	0.75	34	35
6	75-3	0.75	34	38
7	100-1	1.00	34	31
8	100-2	1.00	34	30
9	100-3	1.00	34	31
10	125-1	1.25	34	27
11	125-2	1.25	34	28
12	125-3	1.25	31	20
13	50-1	0.50	35	52
14	50-2	0.50	34	47
15	50-3	0.50	canceled	-

4.4.1   Data extraction

All cycling movements are captured by the main camera 1 and the backup camera 2, see
Figure 4.2. The recording frequency of camera 1 fluctuates around 15 frames per second
due to frame-skipping, while backup camera 2 operates with a lower frequency of around 10
frames per second. The frame rate fluctuation results in irregular position shifts of cyclists
between frames, making a frame-by-frame analysis of bicycle displacements difficult. To
minimize this error, only the first frame of every second is used for further analysis.

The camera recordings were programmed to save every 15 minutes while maintaining a
continuous data stream. However, this process did not function properly resulting in gaps of
two to three minutes between recordings in which data was lost. As a result, the scenarios
50-1 and 50-2 were not fully captured by main camera 1, and backup camera 2 was used for
the data extraction instead.

The data extraction of the flow is done manually by counting the number of cyclists that have
passed the bottleneck entrance in each second as indicated by the yellow lines in Figure 4.2.
If a cyclist is situated across a boundary, the center of a bicycle, in between the two wheels,
is used to determine its position. As pointed out by Steffen and Seyfried (2010), there are
downsides to using this definition. The continuous nature of the cycling movement is lost
due to the discretization of space and time. The space discretization leads to a volatility in
the data set since the cyclists who are moving across a boundary are either in or out based on
the bike's center point, while in truth they are spread across the crossing line. Furthermore,
the resulting data depends on the chosen aggregation time. This error can be reduced by
averaging over time but at the cost of the data resolution. In our case, we base the further
analysis on the moving mean of 3 s and leave a more detailed analysis for future research.

4.5   Data analysis plan

The objectives of the paper are to quantitatively describe the relation between capacity and path width, and to check the existence of a capacity drop in bicycle flow. To meet the objectives, both free flow capacity and queue discharge rate for the different bottleneck widths need to be estimated. First, we will present the method we use to find the individual capacities; then we describe the process to determine the path width dependency of capacity.

4.5.1   Estimating capacity

A first indication for capacity is obtained by visualizing the time it takes for all cyclists to pass the bottleneck. This is done by constructing a cumulative flow curve for each run. This curve indicates how many cyclists have passed a particular location as function to time. Hence, the cumulative flow number N is constructed by adding up all the flow counts of the previous time steps. The slope represents the number of cyclists that pass the bottleneck per time step, which equals the flow $q = \frac{dN}{dt}$. The steeper the curve the higher the flow, so capacity coincides with the steepest curve. The cumulative flow curves for the different runs are presented in Figure 4.4. The moment that the first cyclists enters the narrow section is chosen as the starting time (t=0). The first 10 s are chaotic and the lines are difficult to distinguish. This part can be ignored since the main message of the figure relates to the range between 10 and 50 s. It illustrates that for narrower bottlenecks (gray and purple colors) the time needed to let all cyclists pass increases compared to the wide bottleneck widths (black and red colors). In the widest bottleneck (150 cm) it takes at least 21 s, while the passing time in the narrowest bottleneck (50 cm) is at most 52 s.
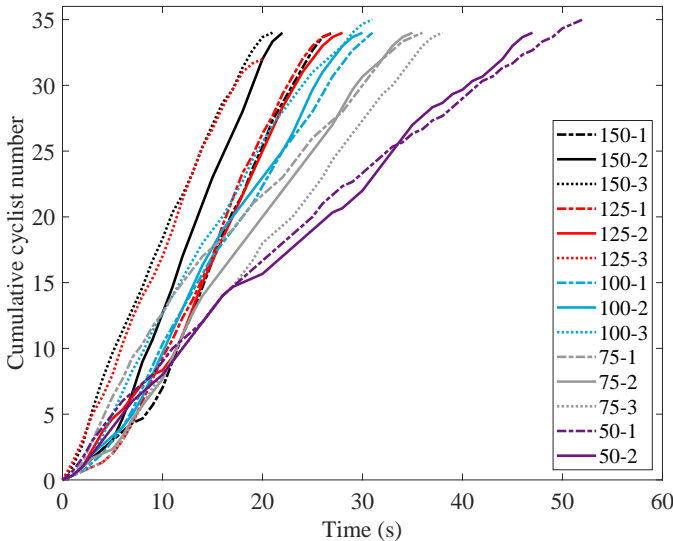
Figure 4.4: Cumulative curves of the runs with bottleneck widths between 0.50 and 1.50 m. The legend refers to the scenario names as given in table 4.1.

To obtain the capacity value, a so-called slanted cumulative flow curve is used, indicated by $\tilde{N}$. This means that a constant reference flow (q_0) is subtracted from the cumulative flow count (N) resulting in the following expression:

$$\tilde{N} = N - \int q_0 dt \tag{4.1}$$

By changing the reference flow, one can slant the curves in such a way that the $\tilde{N}$ is constant. This is done manually by choosing different values for q_0. The advantage of this is that the capacity value can be determined accurately and there is no influence of aggregation time. To remove noise we use a three-second moving average.

Capacity values are determined for each run separately. We find a value for both the free flow capacity as well as the queue discharge rate. Hence, we find two values for which there is a constant value of the slanted cumulative flow curve. If a capacity drop exists, two steady plateaus should be identified in the slanted curve. The highest value coincides with the free capacity and should occur before congestion occurs, while the lower value is the outflow capacity which would occur after the onset of congestion. The difference between the two capacity values is the capacity drop.

Figure 4.5 shows graphically the working of the methodology for the run 75-1, resulting in a capacity value of 1.45 cyc/s and queue outflow of 0.83 cyc/s. Other determined capacity values are presented in Section 4.6.
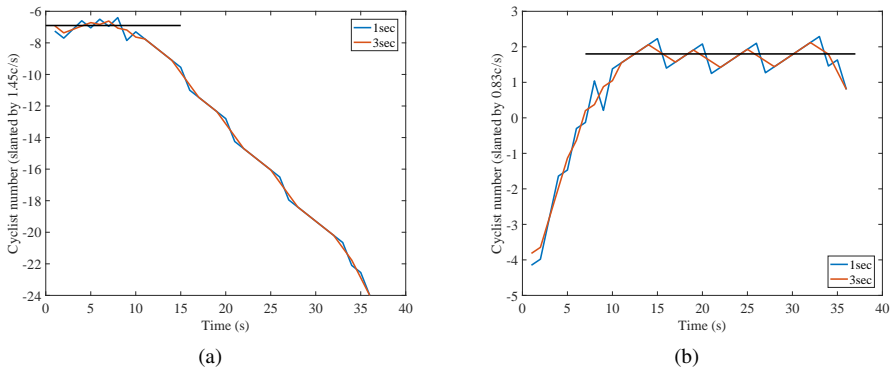
Figure 4.5: Example of slanted cumulative curves to determine capacity (a) and queue outflow (b) (run 75-1). The blue line is based on the 1-s data and the red line is the 3-s moving average; the black lines are added to illustrate the horizontal plateau.

4.5.2 Quantifying the path width – capacity relation

When the capacity and outflow are determined for all bottleneck widths, the dependency to path width can be quantified using linear regression analysis. This will result in the

following capacity equation:

$$C = C_0 + \beta d. \tag{4.2}$$

Where C is the capacity in cyc/s of a d-meter wide path. Furthermore, β is the regression co-efficient which coincides with the slope of the regression line when the equation is plotted. The physical interpretation of this coefficient is that an additional meter of path width coincides with an increase in capacity by β cyc/s. The regression constant C_0 is the y-intercept of the capacity equation. Hypothetically, this gives the capacity of a path of 0 m width, which is an unrealistic situation. Therefore, C_0 does not have a physical interpretation.

4.5.3   Qualitative description of the width–capacity relation

The dependency of capacity to path width is expected to stem from the underlying cycling behavior. This can be assessed by providing a qualitative description of the cyclists configuration while passing the bottleneck.

To describe the position of cyclists, the path is divided into lanes and sublanes using the description of Botma and Papendrecht (1991) to determine the cyclist headway. A cyclist occupies a lane which is approximately as wide as its steer. These individual lanes are not fixed to the path but have a dynamic position on the path based on the cyclist wheels. The path itself is divided into fixed sublanes of 15.6 cm width. These sublanes are used to describe the lateral position of the cyclists. If the wheels of following cyclists have a displacement of 15.6 cm or more, the cyclists are assigned to a different sublane. Since the individual lanes at the path edges cannot be shifted, the total number of sublanes on a path is equal to the path width divided by 15.6 minus two. A lane is assigned 'effective' when it is used by the cyclists.

4.6   Results

In this section we present the results. We first report on the quantitative analyses of the capacity before discussing qualitatively the relation between path width and the observed flow configurations.

4.6.1   Capacity and capacity drop

For all runs, both a capacity value as well as a queue outflow are obtained using slanted cumulative curves. All estimated flow are combined into one graph, see Figure 4.6. The line is a visualization of the regression fit and the measurements are indicated by points. It shows a positive trend of flow with increasing bottleneck width. The smallest capacity value of 0.90 cyc/s is obtained in the 0.50 m scenario, while the largest value of 2.4 cyc/s coincides with a run in the 1.50 m scenario. A similar trend is found for the outflow with the smallest value of 0.56 cyc/s and largest value of 1.99 cyc/s in respectively a 0.50 m and 1.50 m run.

Fitting the relationship as mentioned in Section 4.5.2 results in equation 4.3 for capacity C_{cap} and equation 4.4 for the outflow C_{out}.

$$C_{cap} = 0.475 + 0.0111d \tag{4.3}$$

$$C_{out} = 0.042 + 0.0118d \tag{4.4}$$

The models have an R^2-value of 0.896 for capacity and 0.949 for the outflow, which is a strong result. It means that the obtained equations can explain 89.6% and 94.9% respectively of the observed variance in estimated capacity and outflow.

The slope of the equations presented in Figure 4.6 quantifies the dependency of capacity to path width, which is what we set out to find. For an additional meter of path width in the range of 0.50 to 1.50 m, the capacity increases by 1.11 cyc/s and the queue outflow increases by 1.18 cyc/s. These slopes are remarkably similar and the difference is only 0.07 cyc/s, indicating that a constant drop in flow occurs after activation of the bottleneck. In the range of 0.50 to 1.50 m path width, the flow drops 0.45 cyc/s when the cycling conditions change from free flow to congested. These results provide evidence that the capacity drop phenomenon exists in bicycle traffic.

4.6.2 Cyclist configuration and its connection to capacity

If cyclists would behave like vehicles, the capacity would be dependent on their following distance and the number of lanes. For our bottleneck widths there are either one or two lanes
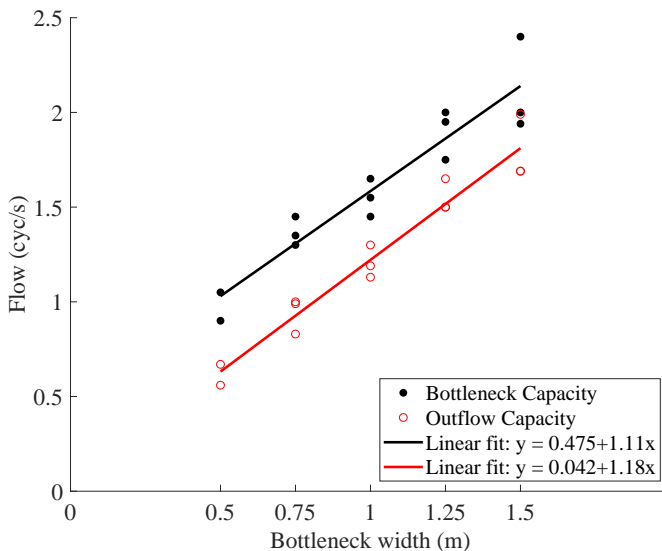

Figure 4.6: Estimated capacity values for each of the 14 runs. The black dots are the bottleneck capacities observed before congestion, while the red dots represent the queue outflow capacities that are observed after the onset of congestion. The two lines visualize the regression fits.

since the standard lane width is between 0.75 and 1.00 m. This lane number is insufficient to explain the variation in capacity. The positive dependency of capacity to path width can be explained by qualitatively analyzing the cyclist configuration while passing the bottleneck, using sublanes and effective sublanes as introduced in Section 4.5.3. This leads to the observations described in writing below, followed by an interpretation. A visualization of the different configurations is presented in Figure 4.7, illustrating examples of observed patterns.

- 2.00 m: Four effective sublanes are observed on the main path while approaching the bottleneck location. A maximum of two sublanes are occupied simultaneously, leading to a staggered formation in the lateral direction. Cyclists are not completely positioned side-by-side, but show a slight displacement in the longitudinal direction as well.

- 1.50 m: While passing the widest bottleneck, sufficient space is available to continue cycling side-by-side but the number of effective lanes reduces to about three of which two can be occupied simultaneously. People on the right side occupy the same lane, while the ones on the left side can still vary their position in the lateral direction, occupying different sublanes.

- 1.25 m: Enough space remains available to cycle side-by-side but the choice in lateral position is limited. The cyclists on the left and right path are now using the same lane as their predecessor. Most people place themselves such that the saddles are not located side-by-side but the front and rear wheel can be completely overlapping when looking at a cross section.

- 1.00 m: The width is reduced such that cycling side-by-side is impossible and only one effective lane is occupied at the same time. In lateral direction, the placement is such that the rear and front wheel can be side-by-side, meaning that 2 effective lanes are used simultaneously. This enables cyclists to maintain a small distance to each other in longitudinal direction.

- 0.75 m: Only single-file movement is observed with only a small variations in lateral placement. Whether this displacement exceeds 15.6 cm and therefore uses one or two effective lanes cannot be judge based on the video images at this stage. It can be observed that the distance between cyclists increases compared to the 1.25 m path.

- 0.50 m: Again, only single-file movement is observed but now cyclists have an identical placement on the path, using the same effective lane. The longitudinal placement of cyclists increases even further compared to the previous bottleneck size.

When visualizing the qualitative description of cyclist configuration for different bottleneck width, the sequence in Figure 4.7 shows resemblance to a merging process. The lateral distance between effective lanes gradually decreases until the path width does not allow cyclists to use multiple sublanes simultaneously, and the longitudinal distance between cyclists increases. Since merging is a gradual process, it can explain the linear expression of the relation between path width and capacity.
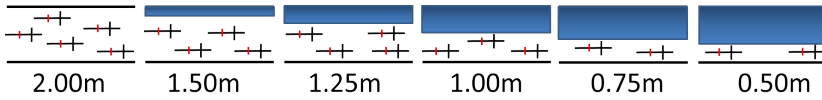
Figure 4.7: Sketch of cyclist configuration while moving from left to right along a path of different widths.

4.7 Discussion

The mentioned capacity values and queue discharge rates for the different bottleneck widths are obtained by conducting a bottleneck experiment with 34 cyclists. The group composition and socio-demographic characteristics of its participants, such as age or cycling experience, as well as the experimental setting, i.e. the artificial bicycle path and bottleneck situation, may influence the capacity values. The results reported in this paper are therefore preliminary and should be validated in future research. This has not been done at this stage since the existing empirical data for bicycle flow is limited and no similar experiment has been conducted so far. In the future, it would be interesting to compare the findings to observations in real world situations and to check the sensitivity to different types of bike paths and different group characteristics such as age or cycling experience.

The obtained linear expression of the capacity equation is explained in this paper by the resemblance to a merging process based solely on configuration of the cyclist while passing the bottleneck. Besides positioning, the average speed is also expected to influence the capacity. Although the speed is not quantified, the behavior observed in the video images provide indications that the average speed upstream of the bottleneck decreases with decreasing path width, i.e., cyclists "anticipate" the approaching bottleneck and therefore reduce their speeds. This is reflected by an increase in observed swaying movements to prevent falling over and, as speed reduces further, people placing a foot on the ground for extra stability resulting in stepping rather than cycling behavior. The bicycle self remains in motion but the individual speed reduces close to zero when a foot is placed temporarily on the ground.

The cyclists anticipate their turn to pass the bottleneck entrance and accelerate before actually passing it. Therefore, the speed through the bottleneck is already higher than in the queue, and the flow observed at the bottleneck entrance is the queue discharge rate. The change from capacity to queue discharge rate is best visualized in the curves of the runs with 0.75 m bottleneck width in Figure 4.4. The flow is highest in the first 10 to 15 s (steep slope) and reduces to a steady flow (steady slope) afterwards.

A learning effect for the various bottleneck widths can be considered by looking into the duration of the consecutive runs, see Figure 4.8. Remarkably, the second run is typically shorter than the first run of each experiment, which might indicate a learning effect as cyclists become more familiar with the track. This trend however is less clear when comparing the third to the second run. Furthermore, it is not resembled in the obtained capacity values.
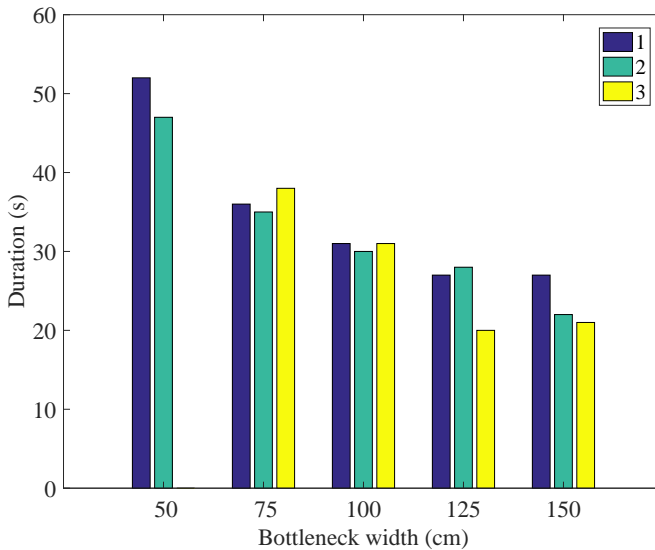
Figure 4.8: Total duration of the three consecutive runs within each bottleneck scenario.

The highest values for free flow capacity however are observed in the 3rd, 1st, 2nd, 2nd and 1st run of the different scenarios, while the highest outflow are observed four times in the 2nd run and once in the third. This indicates that the learning effect is not consistently present.

Another explanation of the different run duration is the arrival pattern of the cyclists at the bottleneck location. Due to stretching of the group caused by speed differences or delays in the start-up process, the first cyclists arrived in a few seconds before the rest of the group and thereby lengthened the total duration time. The effect of this stretched arrival pattern is illustrated by a flatter slope in the first 5 s of the cumulative curve in Figure 4.4.

The estimated relation between path width and capacity value can be used to find maximum flow values outside the range of 0.50-1.50 m. However, the bottleneck width of 0.50 m was difficult for the cyclists to pass and the third iteration of this scenario was canceled for this reason. A path width smaller than 0.50 m would be even more challenging and unrealistic in daily practice. Therefore, a 0.50 m path width is considered to be the minimum and as a consequence, the regression model should not be used to find capacity values for paths smaller than 0.50 m. This restriction does not apply to extrapolation for larger path widths when assuming that the usage of the path does not change. However, future research is advised to confirm that extrapolation is indeed allowed.

The non-zero y-intercept of the capacity equation indicates that observed capacity values on a certain path width, cannot be standardized to a capacity per meter by simply dividing it by the total path width. Instead, the result obtained in this study of 1.11 cyc/s per meter width can be used. By doing so, the wide range of capacity values reported in literature might be narrowed down, leading to a clearer advice for road planners.

4.8   Conclusion

A cycling bottleneck experiment has been set up to study bicycle path capacity. The experiment involved a group of cyclists moving along a 2-m wide path which included an obstacle to create a bottleneck by narrowing the path. The size of the bottleneck was varied between scenarios ranging between 0.50 and 1.50 m width and each scenario was repeated three times. The flow before activation of the bottleneck (free flow capacity) and the flow after the onset of congestion (queue discharge rate) were analyzed.

An important finding of this paper is that the capacity was found to be linearly dependent on the cycle path width. In fact, the capacity increases by 1.11 cyc/s for every additional meter path width in the range of 0.50-1.50 m. The queue outflow was also found to be linearly dependent on path width with an increase of 1.18 cyc/s/m. Both values can be used as reference value to compare capacities of cycling paths of various width. The queue discharge rate was found to be consistently lower than the free flow capacity and the drop magnitude was 0.45 cyc/s for cycle paths widths between 0.50-1.50 m. This confirms the existence of the capacity drop phenomenon in bicycle traffic.

The linear relationships for both the free flow capacity and the queue discharge rate have yielded a non-zero constant. Therefore, the capacity values found for a certain path width cannot be standardized to a capacity per meter by simply dividing it by the total path width. This complicates the comparison of capacity values reported in literature, which typically focus on a single bottleneck width each. The result obtained in this study, which provides both the slope and the axis intercept, can be used to correct and compare capacities across different path widths. By doing so, the wide range of capacity values reported in literature might be narrowed down.

A qualitative analysis of the cyclist configuration has shown that the bicycle path capacity does not work with lanes as in car traffic, but sublanes can be formed. Hence, the capacity does not increase in large steps for one or two lanes only but smaller increases in cycle path width already lead to an increase in number of sublanes and the capacity therefore gradually increases.

Further next steps in the research involve the retrieval of individual trajectories to enable the analysis of the density-flow relation based on individual localized densities. Furthermore, the obtained insights into bicycle flow dynamics will be used in the development and calibration of a macroscopic bicycle flow model. The development of such a model will enable the estimation of city-wide cyclist demand and, in the long term, help mitigate bicycle congestion.

Part II

Empirical research into bicycle flow at controlled intersections

Chapter 5

Jam density, merging cyclists and queue discharge rate

The focus of this dissertation now shifts to controlled intersections. Since cyclists typically accumulate at these places, they are an ideal setting to study macroscopic cycling behavior. This chapter provides insights into the queue dynamics of bicyclists by analyzing the queue discharge process. More specifically, it quantifies how closely individuals are queued up together and its impact on the maximum flow at the intersection. Furthermore, the chapter describes how this process is affected by cyclists who merge into the queue during the discharge phase. It thus addresses the research question: *What is the influence of jam density and merging cyclists on the queue discharge rate at a controlled intersection?*

Results show that the queue discharge rate increases as queue density increases. Furthermore, cyclists who merge by overtaking contribute to the queue discharge rate, while cyclists who merge from a perpendicular direction hinder the discharge process, thereby decreasing the bicycle flow at the intersection. The impact of merging cyclists is quantified via a newly-introduced bicycle-equivalent (BE) value. This chapter's insights can be used to develop measures that minimize delay at intersections. This topic is further explored in Chapter 6 by influencing the queue configuration.

Abstract

An increasing number of people use the bicycle for urban trips resulting in local congestion at intersections, especially during peak hour. Understanding the queue dynamics is key to find the correct measures that can reduce the delays for cyclists without affecting other traffic modes. To this end, the discharge process of bicycle queues are studied, focusing on the impact of jam density to the queue discharge rate and how this process is affected by cyclists that merge into the queue during the discharge phase. The impact of merging cyclists is captured by a newly introduced bicycle equivalent (BE) value. This direction-specific BE value is used to convert a merging cyclist into a cyclist that is waiting in the original queue. Results show that the queue discharge rate increases with increasing density of the queue. Furthermore, cyclists that merge by overtaking contribute to the queue discharge rate, while cyclists who merge from a perpendicular direction hinder the discharge process, thereby decreasing the bicycle flow at the intersection. The insights can be used to develop measures which minimize delay at intersections and to design efficient infrastructure for bicyclist.

5.1 Introduction

Bicycles are gaining popularity as a mode of transport, especially in Western European countries and regions with a positive policy towards cycling (Winters et al., 2017; Heinen et al., 2010). Around 27% of all daily trips in the Netherlands were made by bicycle between 1995 and 2005 (Pucher and Buehler, 2008), and this increased to 32% in 2016 (Ton et al., 2019). Besides this development in usage, also the distance traveled per trip expanded, leading to more cyclists on the roads (KiM, 2019). The increased bicycle traffic has led to local congestion at intersections during peak hour, even though the Dutch cycling infrastructure is well developed. Little is known about the dynamics of bicycle flow and more research is required to identify measures that can help prevent future bicycle congestion.

This study focuses on the queue dynamics at a controlled intersection to gain insight into the factors that influence the queue discharge rate, e.g. jam density. Cyclists have freedom in choosing their position on the road, especially when joining a queue. Depending on how compact the people position themselves, a bicycle queue can have different densities. When moving, the density relates to flow according to the fundamental diagram in traffic flow theory. If and how such a relation holds for jam density and queue outflow is open to question.

Furthermore, it is unclear how so-called "merging cyclists" affect the outflow (Figure 5.1). These merging cyclists are additional cyclists that merge into the flow during the queue discharge process for example, by overtaking the queue from behind, or joining the queue from the side. The influence of merging cyclists is linked to the layout of the intersection and number of approach directions. If there are open spaces in the queue to absorb the additional cyclists, the merging behavior might have a positive effect on the overall flow. However, if the merging behavior obstructs the queue discharge process, the overall capacity might reduce. This leads to the following question: What is the impact of jam density and merging cyclists on the queue discharge rate at an intersection?
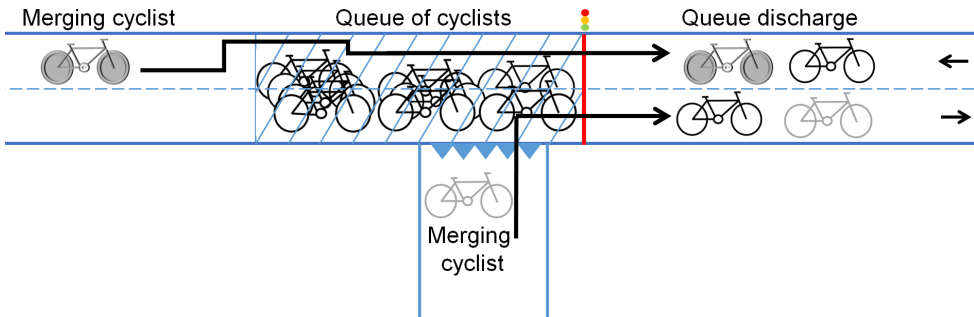
Figure 5.1: Sketch of a queue discharge process: the original queue is indicated by the cyclists in the hatched area, the arrows indicate merging cyclists who skip part of the queue and join the discharge before the queue is cleared.

This study aims to quantify the influence of jam density and merging cyclists to the queue discharge process. We do so by analyzing the queuing events of a real-life intersection with multiple approach directions. The results of this case study are then qualitatively validated in a small-scale controlled experiment. This setting allows us to keep the group composition constant, which reduces the intrinsic variability of the observed discharge times. The results are expected to differ quantitatively from the real-life case study due to the different infrastructural setting and group composition. However, they will suffice to validate the sign of the influence of jam density to the queue discharge time and discharge rate. The acquired knowledge can be used to evaluate existing infrastructure with respect to cyclist delay, or to design new intersections where the delay for cyclists is reduced. The results will be of interest especially for countries with high bicycle volumes, such as the Netherlands or Denmark.

The paper is build up as follows: Section 5.2 provides background information on bicycle traffic flow and equivalent units, Section 5.3 describes the research methodology, Section 5.4 describes the case study which is used to analyze the queue discharge process. Section 5.5 shows the results of the analysis, and Section 5.6 gives details of the experiment that was used to validate the case study results. The paper ends with a discussion of the results in Section 5.7 and conclusions in Section 5.8.

5.2   Related Work

Cyclists have the freedom to choose their lateral position on the road because a bicycle lane is generally wider than the bicycle itself. This enables cyclists to overtake other people or to cycle in pairs within one lane (Botma and Papendrecht, 1991; Hoogendoorn and Daamen, 2016). At intersections, this freedom results in queues that are less organized than the queues in motorized traffic. A queue of motorized vehicles is structured in lanes, whereas cyclists in a queue are grouped closely together and form a cluster pattern (Wang and Wei, 1993). How this cluster pattern effects the queue discharge process is yet unclear.

The flow characteristics of bicycle and motorized traffic are comparable under certain conditions (Navin, 1994). Similar concepts such as speed, flow and density relations can be used to describe the flow on a macroscopic level (Zhang et al., 2013). Typical characteristics are among others capacity, critical density, and jam density. Only a few values have been reported on jam density, all varying around 0.6 bic/m^2 (Navin, 1994; Deng and Xu, 2014; Goñi-Ros et al., 2018). The reported maximum flow, or capacity, shows more variation. The highest number has been reported by Navin (1994) who performed experiments in 1974 in Vancouver (Canada) and compared the findings to data from real-life situations, resulting in an estimated capacity of about 4,000 bic/h/m for a 2.5m wide cycle path. Botma and Papendrecht (1991) studied bicycle data in The Netherlands, estimating a capacity between 2,600 and 3,600 bic/h/m for a 2.5m wide cycle path. Hoogendoorn and Daamen (2016) reported the lowest capacity value of 1,531 bic/h/m based on a new bicycle headway model with the remark that this value might be an underestimation of the actual capacity because the cyclists did not use the full width of 3m-wide path. Li et al. (2015) looked into mixed bicycle traffic consisting of around 80% electric bicycles and reported a capacity of around 3,300 bic/h/m. An explanation for the wide variation could be a different definition for maximum flow, namely saturation flow and capacity.

The saturation flow is the maximum number of cyclists that pass the stop line of an intersection within one unit of time, whereas the capacity takes into account the signal time, resulting in a lower value than saturation flow (Chen et al., 2014). Seriani et al. (2015) analyzed the saturation flow at Travistock Square (London, UK) and Pocuro (Santiago de Chile) and found that the saturation flow at Travistock Square depended on the time of day; a maximum of around 4,300 bic/h/m was observed in morning peak hour, while the results were 25% lower for the afternoon peak hour. The saturation flow showed a linear dependency on lane width at Pocuro, ranging between 2,000 bic/h/m on a 1m lane and 2,350 bic/h/m on a 2m lane. Jin et al. (2015) also found that the width of a cycle path did not significantly influence the capacity per meter, implying that the total capacity of a cycle path scales linearly to the width of the cycle path. The time interval used to calculate capacity was found to influence the results significantly and with a linear downward trend; the estimated capacity decreased when a larger time interval was used for the estimation. Besides path width and measuring interval, also the configuration of the cyclists in the queue might be of influence to the capacity.

Bicycle queue formation has been studied by Cao et al. (2011) which resulted in two models to describe the relation between queue length, jam density and density distribution. It was observed that initially only a portion of the lane width was used for the queue, but when a critical queue length was reached, the additional cyclists would overtake the queue and start to fill the gaps. This process indicates that queues of similar lengths can have different average queue densities. How these merging manoeuvres such as overtaking influences the queue discharge process however, have not yet been studied.

The discharge process of a bicycle queue has been studied by Goñi-Ros et al. (2018), specifically looking at macroscopic characteristics in queuing events without merging cyclists. They found that a higher jam density results in higher discharge flow and shockwave speed. Furthermore, they observed a wide variation between queuing events, which highlights the

stochastic nature of bicycle traffic flow. This finding is also stressed in Yuan et al. (2019), who estimated the bicycle flow capacity of an intersection based on the saturation headway and number of virtual sublanes. The observed number of sublanes was less than the theoretical number, leading to a decrease in saturation rate of 27–43%. The high variety in reported values for capacity and saturation flow might also be explained by several factors such as infrastructure design, weather conditions and heterogeneity in bicycle or bicyclist type. Although it might be interesting to look into these factors, it is out of scope here. We focus on the influence of jam density to the flow, and aim to capture the influence of merging cyclists in equivalent units.

In motorized traffic, equivalent units are used to account for heterogeneity. The traffic flow at an intersection with multiple approach directions can be considered as heterogeneous, since the overall flow consists of multiple sub flows with different characteristics. This heterogeneity makes it difficult to compare flow characteristics such as queue discharge rate. The comparison is made easier when the impact of different factors are described in the same reference unit. The most common reference is the passenger car equivalent (PCE), which was first introduced by the 1965 Highway Capacity Manual (Roess and Prassas, 2014). Each vehicle type has a specific correction factor (PCE value) to convert a mixed traffic stream into a uniform flow of PCEs.

Alternative reference modes have been proposed as well to retrieve a homogeneous description of heterogeneous flow. Cao and Sano (2012) proposed a motorcycle equivalent (ME) to translate mixed traffic conditions in Hanoi, Vietnam, into a unified motorcycle flow. A mixed flow of bicycles and mopeds was normalized in bicycle equivalents (BE) units by Chen et al. (2011). It was found that mopeds have a BE value larger than one under high-density conditions, and a BE value smaller than one under low-density conditions. Other research focused on retrieving BE values for different infrastructure and varying mixing ratios for motorized and non-motorized cyclists. The BE value for mopeds was found to depend on lane width, slope of the road, density and moped percentage (Chen et al., 2012). The impact of electric bicycles has been captured in a fixed bicycle equivalent value of 0.666 (Jin et al., 2015), based on observations in free flow, stable and restricted flow conditions. Equivalent units have not been used before to describe bicycle flow at an intersection with multiple approach directions. We apply this concept to capture the influence of merging cyclists to the queue discharge rate.

5.3   Methodology

This Section 5.3.1 describes method used to find the influence of jam density to the discharge time and queue discharge rate. Section 5.3.2 describes the method to include the effect of merging cyclists and introduces the bicycle equivalent unit.

5.3.1 Analysis of the influence of jam density on the queue discharge process

The influence of the jam density to the queue discharge process is captured via the queue discharge time and discharge rate. The method to determine these variables are discussed first, followed by the method to determine their relation.

The density of a queue depends on its dimensions and the number of cyclists in it. For a queue of fixed length, a waiting area can be defined as the length multiplied by the width of the cycle path. The jam density is then calculated by the number of cyclists in the waiting area (N_q) divided by the fixed dimensions of the waiting area (A):

$$k_{\mathrm{j}} = \frac{N_q}{A}. \tag{5.1}$$

The duration of the queue discharge process is the discharge time, which is the time interval between the first and the last cyclist in the queue to exit the waiting area: $T_{\mathrm{dis}} = T_{\mathrm{last}} - T_{\mathrm{first}}$. The queue discharge rate (q_{dis}) is the number of cyclists (N) that pass the exit line of the waiting area during the discharge time:

$$q_{\mathrm{dis}} = \frac{N}{T_{\mathrm{dis}}}. \tag{5.2}$$

Here, N consists of the cyclists in the queue and the additional cyclists that merge into the queue during the discharge process. If the merging cyclists influence the queue discharge process, both the discharge time and queue discharge rate will be affected.

Since the cumulative flow N is less volatile than the flow, we choose to show the effects of jam density in this cumulative flow plane. If the queue discharge rate was independent of queue density, the total discharge time (T_{dis}) would scale proportionally with the number of cyclists:

$$T_{\mathrm{dis}} = \frac{N_q}{q_{\mathrm{dis}}} = \frac{Ak_j}{q_{\mathrm{dis}}}. \tag{5.3}$$

Figure 5.2 shows how T_{dis} would relate to the jam density if this was the case. We will analyze the various observed queuing events and show them in this plane. If the queue discharge rate is independent on the jam density, the various points will follow one of the colored lines. If not, the points will cross several lines. We will perform a linear regression of these points, of the form

$$T_{\mathrm{dis}} = T_0 + \beta k_j. \tag{5.4}$$

Where T_0 indicates the offset. We expect a value for β larger than 0. A value for T_0 equal to zero would indicate that the discharge time is proportional to the jam density k_q (and N), see Equation 5.3. However, when the T_0 value is larger than 0, it would indicate that the term $1/q_d$ decreases with density, and hence the queue discharge rate increases with the queue density.

5.3.2 Analysis of the influence of merging cyclists

We will extend the analysis above to include also the affect of merging cyclists on the queue dissipation process. This impact of merging cyclists is quantified using multiple linear regression analysis. Since the queue discharge rate depends on the discharge time in our definition, see Equation 5.2, we focus the analysis on the queue discharge time, and later use the bicycle equivalent unit to quantify the effect of the different merging directions. The expression of the multiple linear regression analysis is:

$$T_{\text{dis}} = T_0 + \mu N_q + \sum \alpha_i N_i. \tag{5.5}$$

Here N_q is the number of waiting cyclists in the queue, N_i is the number of cyclists merging into the queue from direction i, T_0 is the regression constants, and μ, α_i are the regression coefficients, corresponding to direction i. The regression coefficients of the different merging directions are tested on a 95% significance level and only the directions that lead to the model with the highest adjusted R-squared value should be included. The standardized regression coefficients of the final model are used to evaluate and rank the influencing factors for discharge time. A standardized coefficient is expressed in standard deviations (σ) and indicates how many standard deviations the discharge time will change due to the increase of one standard deviation of the independent variable.

Scaling the regression coefficients (α_i) to the main influencing factor (μ) gives an indication of the impact of the different influencing factors. This process of scaling is similar to the concept of passenger car equivalent, which is a measure for the impact factor of different classes in heterogeneous (motorized) traffic (Transportation Research Board, 2000). For bicycle traffic, a bicycle equivalent (BE) is introduced as a measure for the impact of merging cyclists from direction i relative to the impact of the cyclists in the original queue:

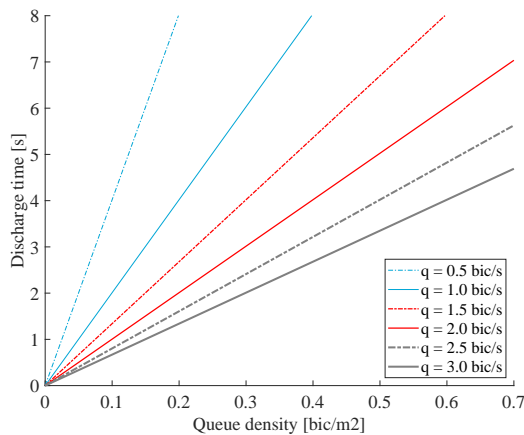$$\text{BE}_i = \frac{\alpha_i}{\mu}. \tag{5.6}$$

Figure 5.2: Template to visualize the relation between jam density and queue discharge rate.

The bicycle equivalent value BE_i represents the impact that a merging cyclist from direction i has on the discharge time. A BE value larger than 1 indicates that the merging cyclist has an increased impact on the discharge time, hindering the waiting people more than if the cyclist were standing in the original queue. A BE value smaller than 1 indicates that the merging cyclist has less influence than if they were standing in the waiting area.

Using the BE values, the total number of cyclists in Equation 5.2 can be recalculated to the reference unit or bicycle equivalent unit (beu). This results in a uniform expression for queue discharge rate in beu/s,

$$q_{beu} = \frac{N_{beu}}{T_{dis}} = \frac{N_q + \sum (BE_i N_i)}{T_{dis}}. \tag{5.7}$$

Merging cyclists with BE value larger than 1 indicates that the overall influence on the outflow in bic/s is negative. The negative impact on discharge time is larger than the positive gain of an additional cyclist in the total cyclist count N. After correcting for this impact, their contribution changes to positive in the queue discharge rate expressed in beu/s. Merging cyclists with a BE value smaller than 1 results in a positive influence to the outflow when expressed in bic/s but this influence is reduced when the outflow is expressed in beu/s.

5.4   Case study

The methods described in Section 5.3 were tested in a case study for which the data was collected in October 2014, see Hoogendoorn and Daamen (2016). The location is the Mekelweg−Jaffalaan - intersection, which is part of a busy cycling route between the city center and the university campus in Delft, the Netherlands. Video data were collected over a period of 2 weeks, covering an intersection where bicyclists have priority over cars. The stream of cyclists in morning peak hour was controlled by human traffic controllers who stopped the stream of cyclists periodically to help car traffic cross the cycle path. An overview of the situation is provided in Figure 5.3. Due to the proximity to the university, the flow consisted predominantly of students who cycled on a regular basis and might have been rushed to get to their classes in time.

The video was analyzed, looking specifically at the moments at which the bicyclists were stopped and released again by the traffic controller. During the blocked periods, a queue of cyclists formed in front of the intersection using occasionally the full width of the cycle path (3 meter), including the lane for the opposite direction. In the images, a waiting area was defined and drawn by the white lines in Figure 5.3b. The size of the waiting area (A, 6.7m x 3m) was chosen such that a clear count of the number of cyclists could be made based on the video images, so its size was limited by the presence of the tree. The events were recorded only when the queue length reached the end of the waiting area or exceeded this length, resulting in a total of 106 queuing events. The number of cyclists within the waiting area was determined manually, resulting in different queue densities depending on how compact the cyclists had positioned themselves. After the traffic controller released the flow, the queue discharge time was determined as the time interval between the first wheel passing the exit line and the second wheel of the last cyclist (of the original queue) passing

the exit line. With this method, the initial start-up time of the cyclists was not included in the discharge time. The bicyclists did not have any interaction with vehicles during the discharge time, and interaction with pedestrians was very limited. Based on this knowledge, we assumed in the analysis that the discharge process was only influenced by cyclist-cyclist interaction.

The observed jam density ranged between 0.2 and 0.6 bic/m^2 with a mean of 0.4 bic/m^2 and standard deviation of 0.086 bic/m^2, see Figure 5.4. The time to empty the waiting area ranged from 2 to 7 seconds with a mean of 4.6 s and standard deviation of 0.92 s. Before the last cyclist of the original queue left the waiting area, additional cyclists could merge into the queue from different directions. The merging cyclists were counted from different directions (see Figure 5.3b) being the cycle path from the Jaffalaan which has a 90 degree angle with the waiting area (1), overtaking from behind (2) and a shortcut direction across the side walk (3). Furthermore, the presence of cyclists going in the opposite direction was recorded (4) as well as the cyclists coming from direction 5. Only the queues in the morning peak hour were captured and analyzed. At that time of the day, the majority of the flow was directed towards the university building (to the right in Figure 5.3) and almost no oncoming cyclists were present coming from direction 4. The number of additional cyclists per discharge period varied between $0 - 6$ cyclists for direction 1, $0 - 4$ cyclists for direction 2, and $0 - 2$ for direction 3. During the selected queuing events, no bicyclists were observed coming from direction 5.

(a) Example of queuing event, the cyclists within the two white lines are counted to determine jam density.

(b) Influencing directions

Figure 5.3: Example of the video data (a) with the waiting area defined by the white lines. The black arrows indicate the different directions in which additional cyclists can influence the queue discharge process (b).

5.5 Results of case study

The results of the analysis of the case study data are discussed, starting with the influence of jam density on the discharge time and queue discharge rate, followed by a quantification of the influence of merging cyclists, which leads to queue discharge rate expressed in bicycle equivalent units.

(a) Frequency distribution of jam density   (b) Frequency distribution of queue discharge time
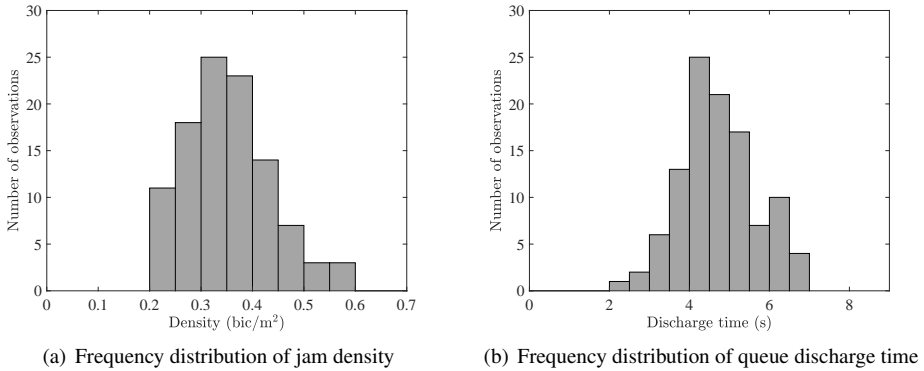
Figure 5.4: Frequency distributions.

5.5.1 Influence of jam density

The observed queue discharge times are plotted against jam density in Figure 5.5. The scattered dots show a positive trend, which is captured by the linear fit (black line). The results show that discharge time increased gradually with jam density, which can be interpreted as a time penalty for density. On the other hand, the queue discharge rate also increases when cyclists stand closer together in the queue, which indicates that the queue dissipation process is more efficient. Linear regression analysis results in the following regression model:

$$T_{\text{dis}} = 2.70 + 5.05 k_j. \tag{5.8}$$

The regression equation is statistically significant ($F(1,104) = 30.4, p < .001$) with an R-squared value of .226. This means that the discharge time increases with 5.05 seconds for every bic/m^2 increase in jam density, and that the equation explains about 23% of the variance in observed discharge time. The model is improved when also including the effect of merging cyclists.

5.5.2 Influence of merging cyclists

Other explanatory factors for the observed variation in queue discharge time are cyclists that merged into the queue during the discharge process. The multiple regression analysis showed that only the number of waiting cyclists in the queue (N_q), number of merging cyclists from direction 1 (N_1) and merging cyclists from direction 2 (N_2) had a significant influence on the discharge time. The influence of merging cyclists from direction 3 (N_3) and oncoming cyclists (N_4) was not statistically significant and has therefore been excluded from the final regression analysis. Table 5.1 provides the results of the Pearson correlation. It shows that the correlation between discharge time and both N_q and N_1 are around 0.50, indicating that these variables had a moderate and positive impact on the discharge time. The correlation between discharge time and merging cyclists from direction 2 is lower, around 0.25, indicating that N_2 had a possible positive impact on discharge time, but the connection was weak. The correlation between N_q and N_1, N_q and N_2 and N_1 and N_2 is smaller
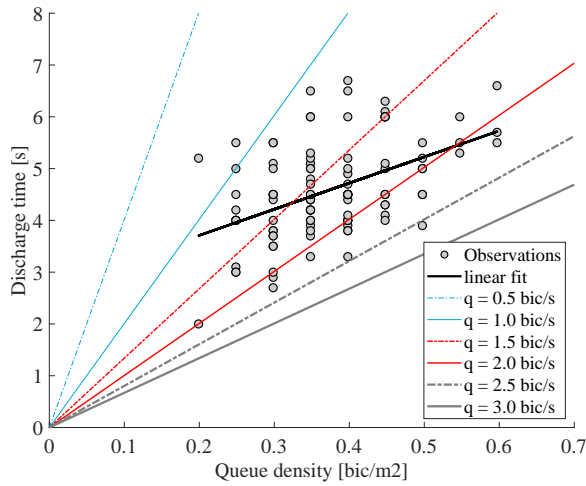
*Figure 5.5: Observed discharge time and jam density (dots) and the linear regression fit
(black line). The lines starting from the origin indicate different flow in bic/s
over the full width of the cycle path (3 meter).*

than 0.20, indicating that the relation was very weak and that the variance of one variable
was unlikely to explain the variation of the other variable. The p-values of the correlation
results are shown in Table 5.2. The values below 0.05 are statistically significant, meaning
it is 95% certain that the variations in both variables are not unrelated. In other words, the
variables N_q, N_1 and N_2 were likely to explain a part of the variance within the observed
queue discharge time.

The regression model that fits the data best is captured by the following equation:

$$T_{\text{dis}} = 2.06 + 4.84k_j + 0.32N_1 + 0.20N_2. \tag{5.9}$$

The standardized regression coefficients, which are used to determine the ranking, for N_q,
N_1 and N_2 are respectively 0.46, 0.44 and 0.21. This indicates that the number of waiting
cyclists in the queue is the variable that explained most of the variation in discharge time,
closely followed by the number of merging cyclists from direction 1. The R-squared value
of the regression equation (9) is .499, indicating that about 50% of the variance in discharge
time was explained by the model.

Table 5.1: Pearson correlation matrix.

	T_{dis}	N_q	N_1	N_2
T_{dis}	1	-	-	-
N_q	0.476	1	-	-
N_1	0.515	0.065	1	-
N_2	0.261	-0.045	0.184	1

Table 5.2: P-values of the correlations.

	T_{dis}	N_q	N_1	N_2
T_{dis}	1	-	-	-
N_q	<0.001	1	-	-
N_1	<0.001	0.508	1	-
N_2	0.007	0.648	0.059	1

The regression model for discharge time shows that the influence of merging cyclists depended on the direction of the merge. The impact of the direction with respect to the influence of the jam density was captured by the bicycle equivalent (BE) value. A BE value of 1.31 was found for bicyclists that merged by taking a sharp turn (∼90 degree angle, direction 1) and a BE of 0.83 was found for cyclists that overtook from behind (direction 2). This means that merging behavior from the side disrupted the discharge process and caused a delay to the last cyclist in the original queue, whereas merging behavior from behind affected the discharge time less. Using the BE values, the effect of merging cyclists from different directions was recalculated to a uniform expression for merging flow, expressed in bicycle equivalent units. The results are visualized in Figure 5.6, showing an increase in queue discharge rate with both increasing jam density and corrected merging flow. The observed queue discharge rate ranged between 1.3 and 3.3 bic/s over a 3 meter wide cycle path, which translates into 1,500 to 4,200 beu/h/m. These estimates were valid only during the discharge process itself, which lasted up to 7 seconds in this study. It is unlikely that this high flow can be maintained for a full hour in real traffic conditions, but for comparison reasons the rates are expressed in an hourly rate. The large variation in queue discharge rate was explained by different combinations of jam density and merging cyclists. The lower values were related to low jam density values and low merging flow, whereas the highest queue discharge values were achieved by a high presence of merging cyclists. The maximum value of 4,200 beu/h/m was found at a jam density of 0.4 bic/m^2 and merging flow of 1.75 beu/s.
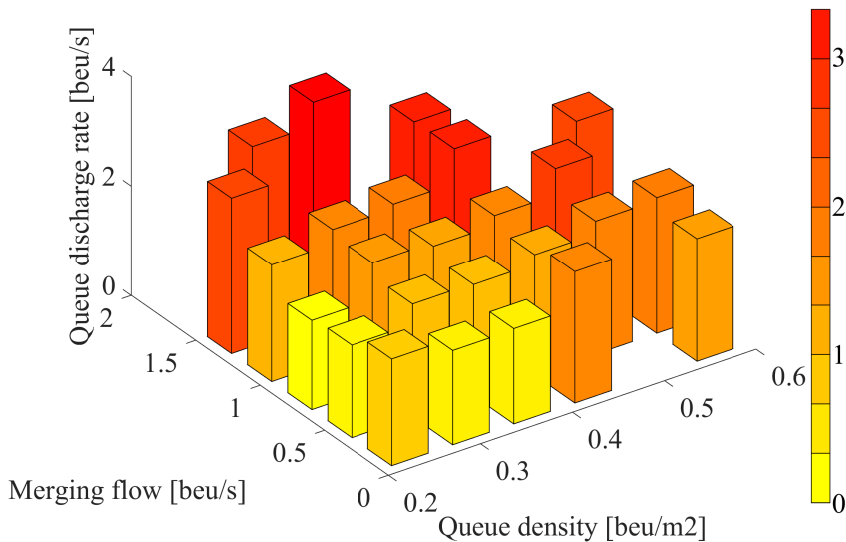

Figure 5.6: Queue discharge rate at different jam density and merging flow, expressed in bicycle equivalent units.

5.6   Validation experiment

The results of the case study show a positive relation between jam density and queue discharge time, as well as a positive influence of jam density and merging cyclists to the queue discharge rate. These findings are validated in an experimental setting which allows to control the group composition by using the same set of cyclists for each queuing event. By doing so, the variability in observed queue discharge time, caused by differences between cyclists, e.g. bicycle type, experience, etc., is reduced.

The setup of the experiment was as follows. We asked a group of 20 cyclists to cycle as they would normally do in daily life and to stop when they reached a mimic traffic signal. While approaching the intersection and the signal was red, the cyclists were free to pick their position while forming a queue. An example of such a queuing event is shown in Figure 5.7a. Once the sign turned green, the cyclists started cycling again and the queue cleared. The group of cyclists approached the mimic intersection multiple times, while mixing the ordering every time such that differences in cycling style would not be dominant. The track did not include a side path, meaning that merging cyclists could only influence the queue discharge process by overtaking. The track width was varied between two and three meters to get different jam density values. Recall that the path in the case study was a two-way cycle path of 3-meter width and that this full width was only used in the dense queues.

The group of participants consisted primarily of students from an American university who were in their twenties. A questionnaire learned that about half of the participants use a bike several times per week in their daily life, while a small portion indicated that they never cycle. Nevertheless, they indicated that their cycling confidence during the experiment was good. All cyclists participated on a rental bike which they had time to become familiar with in the days prior to the experiment.

The procedure to retrieve jam density, queue discharge time and discharge rate was similar to that for the case study. The only difference is the dimension of the waiting area. A fixed queue length of 7 meters was chosen instead of 6.7m such that the boundary was clearly distinguishable by an existing cross-line on the path, see Figure 5.7b. The total length of the queue was 8 to 15 meter and thus exceeded the length of the waiting area in each run. A total of 7 runs were recorded, which is deemed sufficient to qualitatively validate the positive effect of jam density to the queue discharge rate.

5.6.1   Experiment results

The combined jam density and discharge time of the experiment are shown in Figure 5.8. Two initial observations can be made based on it: First, we find the points further to the right so the jam density is higher in the experiment than what was observed in the case study. And second, the points are higher up in the graph so more time is needed to clear the queue, resulting in larger queue discharge times.

The observed discharge times at $k_{jam} = 0.64$ bic/m^2 is widespread, which can be explained when looking at the discharge process. The queue that took approximately 10 seconds to

clear was influenced by a cyclist that had difficulty to start cycling and was overtaken in the process, while the cyclists in the queue that only needed 6 seconds to clear were restarting to cycle so fast that a gap appeared to the cyclists behind them in the queue, indicating that the process was faster than anticipated.

For validation of the relationship, we also show the regression line, which is given by $T_{dis} = 4.63 + 5.29 k_{jam}$ and R-squared = 0.212. It shows that also in the controlled experiment, the queue discharge rate increases with jam density. However, the overall flow is lower than in the case study. In the experiment, the flow increases from 1.2 to 1.4 bic/s, while in the case study a discharge rate of 1.5 bic/s was reached. Although the number of observations are limited, the discharge rate shows a positive response to an increase in jam density. As expected based on the different group composition, the regression model from section 5.5.1 is unable to predict the discharge times for the higher jam density values in the experiment. On the other hand, the experiment results do show that the queue discharge time and rate are indeed positively influenced by the density of the queue.

Merging by overtaking was observed only on two occasions in the experiment. In both runs, there was exactly one cyclist that merged into the original queue, and several partial overtaking manoeuvres, which were not completed before passing the stopping line. These two merging events are too limited to validate the method proposed in section 5.3.2. Nevertheless, it is interesting to mention that merging by overtaking is also observed in an experimental setting.

(a)   (b)
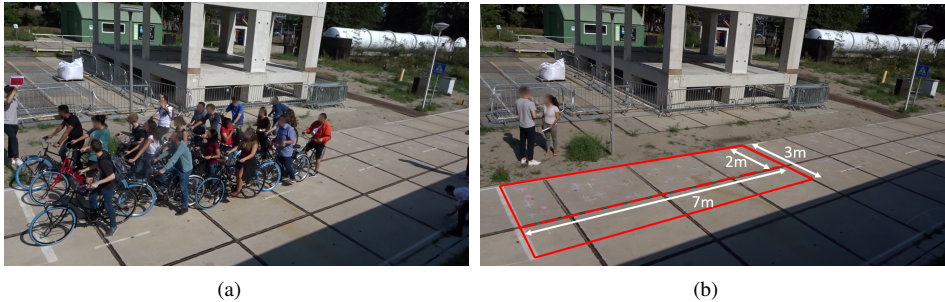
Figure 5.7: Example of a queueing event in the experiment (a) and cleared path showing the waiting area indicated with red lines (b).

5.7   Discussion and future research

Both the case study results and the experiment findings show that a positive relation exists between the jam density and both the queue discharge time and discharge rate for a queue of fixed length.

The trend lines in Figure 5.8 show that the discharge rates in the case study increases from 0.8 to 1.5 bic/s, and in the experiment increases from approximately 1.2 to 1.4 bic/s for the
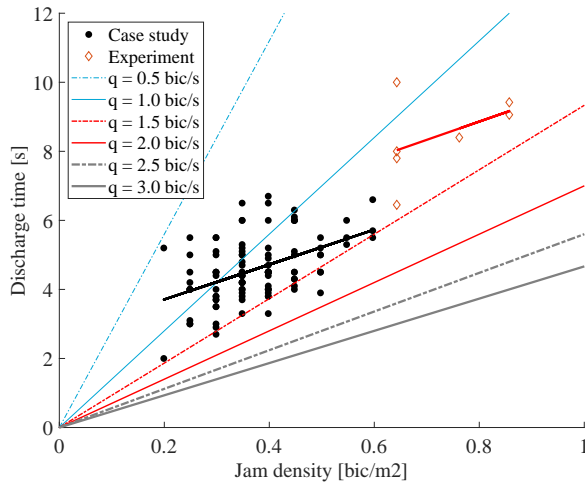
Figure 5.8: Combined results of case study and experiment.

total width of the path. When extrapolating the flow to an hourly saturation rate, the results for the case study roughly increase from 1,000 to 1,800 bic/h/m, while the experiment give rates between 1,400 and 1,700 bic/h/m. These results are below the lowest saturation rate of 2,000 bic/h/m that was reported in literature by Seriani et al. (2015). A possible explanation for this could be the absence of hastiness in the experiment.

The analysis of the case study results identified three factors that influenced the time for clearing a queue of fixed length, being the number of cyclists in the queue, merging cyclists from the side, and merging cyclists from behind. Merging behavior from the side disrupted the discharge process and caused a delay to the last cyclist in the original queue, whereas merging behavior from behind affected the discharge time less. Unfortunately, the number of observed overtaking manoeuvres in the experiment was too small to validate the impact of merging cyclists and more research is needed before it can be used in practice. Furthermore, it would be interesting to study more locations to fine the effect of geometry, population, weather and other factors in the future research. Possibly, other means of data collection could contribute in this, e.g. GPS-trajectories (Christian et al., 2019), mobile phone data (Ghahramani et al., 2020) or drone counts (Kim, 2020).

The queue discharge rate increased with increasing jam density. This indicates that a higher discharge flow can be obtained if cyclists create a denser queue. Further exploring this dependency to jam density would be interesting e.g. to optimise the throughput at an intersection. Does the positive influence of jam density to the flow maintain when cyclists queue up closer together, or is there a maximum? Furthermore, more behavioral research is needed to find the best way to nudge cyclists into queuing up closer together in a real-life situation. Other possible research directions are: Allowing for a dynamic queue length instead of a fixed length, as well as analyzing the exact spatial configuration of the queue to identify the relation to the merging flow. Open spaces in the queue (local density minima) could initiate

merging behavior from different directions. Personal characteristics, i.e. age, gender, level of fitness, can be included to retrieve a more specific impact factor for merging cyclists, as well as specifying the type of bicycle, i.e. electric, regular or cargo.

5.8   Conclusion

This study analyzed the queue discharge process of cyclists at a controlled intersection, focusing on how jam density and merging cyclists influence the discharge rate. The jam density was found to positively influence the queue discharge rate. Furthermore, it was found that cyclists who merged by overtaking contributed more to the observed discharge rate compared to cyclists that were standing in the original queue. Cyclists that merged from a direction perpendicular to the queuing direction were found to hinder the discharge process, decreasing the observed discharge rate. The positive relation between jam density and queue discharge time and discharge rate was validated in a controlled experiment.

The results of this study contributes to the development of bicycle models which help in assessing new plans for bicycle infrastructure layout or measures to minimize delay at intersections.

Chapter 6

Queue configuration, jam density and the effect on discharge rate

The previous chapter showed that a higher jam density creates a higher queue discharge rate. In theory, higher jam densities are feasible than those currently observed in practice. This leads to our hypothesis that the delay at intersections can be further reduced when cyclists are encouraged to queue up closer together. To explore this, we carried out an experiment in which the queue configuration was influenced to increase jam density. This chapter presents ways to increase the queueing density, analyzing the effect on the queue discharge process both quantitatively and qualitatively. The research question connected to this chapter is as follows: *Can the jam density of bicycle queues be influenced by managing the queue build-up and if so, does the relation between jam density and discharge rate hold for higher jam density values?*

Results show that increasing the jam density indeed increases the queue discharge rate. This also holds for jam density values that exceed those observed in normal queuing conditions. The efficiency of the queue discharge process, captured by the discharge rate, was found to increase by 40% when cyclists queue up closely together. Qualitative comparison of the queuing positions and discharge patterns showed that the discharge sequence is largely determined by the queuing position, and that cyclists keep a distance from each other in both time and space during the queue discharge phase. When applied in practice, these findings can be used to update the signal length and green phases for all traffic, thereby reducing congestion in urban areas.

Abstract

Congestion in bicycle traffic is a daily occurrence at many urban intersections. It is known that a higher density in the queue leads to a higher discharge rate. In theory, higher jam densities than those currently observed in practice are feasible. This leads to our hypothesis that the delay at intersections can be further reduced when cyclists are encouraged to queue up closer together. To explore this option, we carried out an experiment in which the queue configuration was influenced to increase the jam density. This paper presents ways to increase the queuing density, up to twice the density found without instructions. Results show that increasing the jam density does indeed increase the queue discharge rate; this also holds for jam density values that exceed those observed in normal queuing conditions. The efficiency of the queue discharge process, captured by the discharge rate, was found to increase by 40% when cyclists queue up closely together. Qualitative comparison of the queuing positions and discharge patterns showed that the discharge sequence is largely determined by the queuing position, and that cyclists keep a distance from each other in both time and space during the queue discharge phase. When applied in practice, these findings can be used to update the signal length and green phases for all traffic, thereby reducing congestion in urban areas.

6.1   Introduction

Using the bicycle to travel from A to B is popular in countries with a well-established cycling culture, such as the Netherlands and Denmark. Bicycle usage in the Netherlands is increasing (Harms and Kansen, 2018), which is a positive trend from a health and sustainability point of view (Forsyth and Oakes, 2015), but it also raises challenges. For some, the challenge is to understand cyclists to further promote cycling (Harms et al., 2016), while others are investigating ways to reduce delays for cyclists (Paulsen and Nagel, 2019). The urban infrastructure is struggling to handle the increased bicycle traffic flow, especially during the peak hours, resulting in congestion. Congestion predominantly occurs at controlled intersections which act as bottlenecks for cyclists, resulting in queues and delays. Cyclists have to wait more than one cycle length before they can traverse the intersection, which occurs on a daily basis in Amsterdam, Utrecht and other cities in the Netherlands with high cyclist volumes.

A possible solution to reduce congestion is to ensure that more cyclists are able to pass the traffic signal during the green phase. Simply lengthening the green time would negatively affect the other traffic which is undesirable. Another option could be to optimize the queue discharge process, e.g. the queue discharge rate and average speed of cyclists during the queue dissipation. Previous research (Goñi-Ros et al., 2018; Kucharski et al., 2019; Wierbos et al., 2020) has shown that the queue discharge rate is positively influenced by the jam density, which is the average number of stopped cyclists per squared unit of space. Although more factors could play a role here as well, this effect of jam density implies that the queue discharge process can be optimized by increasing the density of the queue.

The maximum observed jam density in practice is below what should be possible in theory, based on the physical dimension of bicycles. To reach higher jam densities, the queue formation process must be influenced e.g. by encouraging people to queue up closer together or providing predetermined waiting positions. It is, however, unknown whether creating denser queues can be achieved in practice and if so, whether the positive relation between jam density and queue discharge rate then holds. These questions are addressed in this study by means of a controlled experiment in which the participants are asked to perform multiple repetitions of cycling, forming a queue, and continuing to cycle after a signal turns green. In the meantime, different instructions were provided on how to form the queue. The discharge process was recorded on video and analyzed for each configuration to identify the impact of the configuration and resulting jam density on the queue discharge rate and discharge speed.

The paper continues with providing additional background information on macroscopic quantities and other findings in bicycle queue formation in Section 6.2. Then, Section 6.3 describes the experiment setup, the data analysis plan, and the experimental execution. Section 6.4 gives the results and its interpretations. Section 6.5 shows the practical implication of the main finding, and Section 6.6 discusses the results and gives direction for future research. Section 6.7 closes the paper by presenting the main conclusion.

6.2 Background on macroscopic quantities and queue formation

The literature on bicycle traffic flow has gradually expanded over the past several years. Earlier work primarily focused on single file movements and uninterrupted bicycle traffic flow, reporting on e.g. mean speed and gap acceptance, speed, volume and passing movements (Botma and Papendrecht, 1991) and capacity and level of service (LOS) (Navin, 1994; Allen et al., 1998). More recently, the traffic dynamics of bicycle traffic flow are further studied by means of large-scale bicycle experiments, either focusing on single lane movements to enable comparison with car traffic (Mai et al., 2013; Zhang et al., 2013; Jiang et al., 2016; Zhao and Zhang, 2017), or multi-lane bicycle flow to investigate the characteristics of bicycle traffic flow when overtaking is allowed (Gavriilidou et al., 2019; Guo et al., 2019).

Besides the uninterrupted behavior, traffic flow at intersections has gained increasing attention since they are the main bottlenecks for bicycle traffic flow. One of the first analyses on cycling behavior while approaching an intersection was done by Opiela et al. (1980), reporting on arrival patterns, approach speeds, and crossing gap acceptance characteristics. In the dissipation phase of a queue, important aspects are the capacity, queue discharge rate and the jam density. The capacity is the maximum number of cyclists that can pass the intersection per unit of time, usually converted to one hour, while taking into account the cycle length. The capacity therefore depends on the green interval and total cycle length (Wang et al., 2011). The queue discharge rate, or saturation flow, is the average number of cyclists that pass the traffic signal per unit of time. This flow is only measured during the green interval and does not take the waiting time into account, resulting in a higher value than the capacity.

Reported values of saturation flow show a wide variation which can be related to e.g. time of day, width of the path, topography or bicycle type. The influence of bicycle type on the capacity was studied by Zhou et al. (2015); Jin et al. (2015). They found that the presence of electric bikes besides conventional bikes increases the capacity, while cyclists transporting cargo decrease the capacity. Jin et al. (2015) introduced a bicycle equivalent unit to convert the capacity of a mixed stream of bicycles into a standardized flow of conventional bikes. Seriani et al. (2015) observed that the saturation flow during the morning peak hour exceeds that of the afternoon peak for sites in London and Santiago de Chile. Furthermore, a near linear relation was obtained between path width and saturation flow, meaning that the saturation flow nearly doubles when the path width changes from one to two meters. Raksuntorn and Khan (2003) studied the queue discharge rate at four intersections in different American cities and found that cyclists form multiple adjacent queues when the path width increases. Furthermore, the saturation flow shows a step-wise increase with the formation of a new lane. The differentiation into lanes is also described by Botma and Papendrecht (1991) who used theoretical sublanes to identify whether a cyclist is constrained by a cyclist in front or not. This qualification is used to determine the headway of a cyclist, which in turn is useful to estimate capacity as was done by Hoogendoorn and Daamen (2016) by proposing a bicycle headway model. Recently, Yuan et al. (2019) introduced a new method based on empirical data to determine the number of sublanes for bicycle traffic. They found that the observed number of sublanes is less than the theoretical number, which results in a reduction of the capacity estimate. Furthermore, the observed number of sublanes, as well as other variables e.g., start-up time and saturation headway, were found to be highly stochastic.

The jam density is the result of the queue formation process, which in turn results from the cyclists' decisions on where to stop (Gavriilidou et al., 2019). During this process, cyclists spontaneously form multiple channels which results in different dimensions and density of the queue. A higher jam density leads to an increase in queue discharge rate as was found by Kucharski et al. (2019) based on queues of 2 to 7 cyclists in Krakow and Goñi-Ros et al. (2018) who observed queueing events with 7 to 19 cyclists at an intersection in Amsterdam. These findings imply that the efficiency of the queue discharge process increases when the jam density is higher. However, it is unknown whether higher discharge rates are indeed obtained for higher jam density and under which circumstances denser queues could be formed.

For pedestrian movements it is known that a bottleneck results in a loosely formed queue, whereas a train boarding leads to a densely formed queue (Kneidl, 2016). These situations have not been categorized for bicycle movements yet but one can observe in Amsterdam that a queue at an intersection is less dense than the queue of cyclists in front of a ferry. At intersections, the reported jam densities in literature vary between 0.56–0.65 bicycles/m^2 (Deng and Xu, 2014), 0.20–0.60 bicycles/m^2 (Wierbos et al., 2020) and 0.31–0.65 bicycles/m^2 (Goñi-Ros et al., 2018). In theory, higher jam density values should be possible and leading to less congestion. However, it is unknown if the jam density can reach a higher value in practice and if so, whether the positive relation between jam density and discharge rates holds for jam densities exceeding 0.65 cyc/m^2. This specific knowledge gap is the topic of our study. We aim to understand the link between the density of the

queue and the discharge process, especially in situations with a high jam density. A key aspect in reaching these higher density values is to find effective ways to influence the queue formation process.

6.3 Research approach

The primary aim of this study is to investigate whether the jam density can be positively influenced by giving different queuing instructions to the cyclists. And if so, we aim to quantitatively describe the influence of jam density on queue discharge rate for the observed jam density range. The secondary aim is to better understand the underlying processes of the queue discharge. Section 6.3.1 describes the setup of the controlled experiment, section 6.3.2 presents the data extraction and analysis plan, split up into the primary and secondary aims, and section 6.3.3 describes the experimental execution.

6.3.1 Experimental setup

The behavior is studied in the setting of a controlled experiment because we are interested in density values that have not yet been recorded in real-life situations. In the experiment, we ask a group of cyclists to cycle on a two-meter-wide path until they reach a stop line where a person is holding a red 'STOP' sign or a green 'GO' sign, mimicking a traffic signal. When the sign indicates STOP, the cyclists stop and form a queue; when the sign states GO, the cyclists restart cycling and the queue dissipates. A sketch of the setup is shown in Figure 6.1. The movements between the stop line and 17m upstream are captured by a camera that captures the movements at a rate of 25 frames per second. Figure 6.2 shows the view of the camera. The experiment is held in a closed terrain which has no gradient and is free of other traffic to minimize external influences. The design of the experiment was tested and approved by the ethics committee of Delft University of Technology.
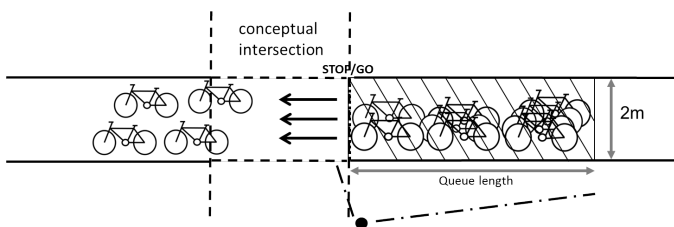
Figure 6.1: Draft of the experiment setup. The dotted line indicates the stop line, the black dot is the camera position, and the dash dotted lines visualize the camera view.

We repeat the sequence of arriving, queuing and clearing multiple times while providing different guidance on how to form the queue. First, no queuing instructions are given to capture the uninfluenced behavior. Then, we start to intervene and ask the participants to queue up more closely, without giving further information on how to do this. Then, we ask them to queue up on pre-assigned spots in pairs, in threes or a mixture. These spots are indicated with colored markings on which the cyclists place their front wheel. Each

Figure 6.2: Snapshot of the camera view.

formation has its own symbol and color, as shown in Figure 6.2. Figure 6.3 shows the
different queuing formations that were tested:

(a) In pairs, staggered

(b) In threes and side by side

(c) In threes and v-shape where the middle cyclist is placed slightly backwards

(d) Alternating in pairs and in threes

(e) In threes with a shift

These configurations are chosen such that the density is higher than the highest jam density
of 0.65 bic/m^2 (Goñi-Ros et al., 2018) that has been reported so far. In theory, the config-
urations (b) and (c) result in comparable jam density but the queue discharge rate might be
different since the configuration can influence the process to start moving. More configura-
tions are possible, especially when relaxing the constrained of a 2m-wide path. However,
the capacity does not scale linearly to the width of the path (Wierbos et al., 2019). Changing
the path width would thus affect the discharge rates and is expected to diffuse the effect of
jam density. For this reason we look only at different configurations within a fixed path
width. Following the findings of Gavriilidou et al. (2019), a bicycle length of 1.80cm and
handle bar width of 60cm is used to place the markings on the path. An additional 10cm is
added on each side for every cyclist, resulting in a lateral spacing of 80cm when the cyclists
are placed in threes and side-by-side. Each configuration is repeated thrice to capture the
fluctuations that will occur due to the stochastic nature of cyclists' behavior. Furthermore,

(a) $k_j = 0.67$ bic/m^2 (b) $k_j = 0.75$ bic/m^2 (c) $k_j = 0.75$ bic/m^2

(d) $k_j = 0.90$ bic/m^2 (e) $k_j = 1.00$ bic/m^2
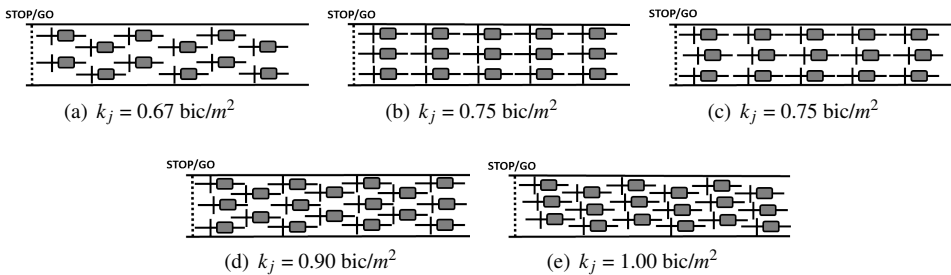
Figure 6.3: Tested queue configuration with theoretical jam densities.

we encourage cyclists to change order every time to minimize the influence of personal preferences in speed and reaction time.

6.3.2   Data extraction and analysis methods

The sequence of arriving, queuing and continuing cycling is called a run hereafter. We split the analysis of all runs into two parts, in line with our primary and secondary objectives.

Jam density and queue discharge rate

The primary objective is to quantify the relation between the jam density (k_j) and the queue discharge rate (q_d) for high jam density situations. To this end, the jam density and queue discharge rate need to be determined. The former is determined using the length of the queue, which is recorded for each run and measured after the experiment has finished. Since the number of participants is kept the same, a dense queue results in a shorter queue than a queue with low density. The jam density for each run is therefore determined by the number of cyclists within the queue (N) and the dimension of the queue (A), which is the queue length (l) times the path width of two meters:

$$k_j = \frac{N}{A} = \frac{N}{2l} \tag{6.1}$$

The data extraction for the queue discharge phase is done using the lateral cross-section technique described in Knoop et al. (2009). This technique extracts the pixels along a cross-section of each video still and merges the slices from consecutive frames into a new figure. We take the stop line for our cross section, see the yellow line in Figure 6.4a. The resulting image shows the passing times and lateral positions of the cyclists, see Figure 6.4b. When a cyclist passes with a low speed, the wheel will occupy the cross-section for a longer time period and therefore has a larger size in the image then a wheel of a fast-moving cyclist. The position and time of the wheel centers are identified and indicated with red dots. Figure 6.5a is an example, showing the passing moments of all cyclists of a run.

The queue discharge rate is determined using the individual passing moments of the cyclists and combining them in a cumulative curve. To minimize the influence of individual fluctuations in e.g. reaction time and speed, we perform a linear regression analysis, resulting in the following model:

$$N = q_d(t_i - L). \tag{6.2}$$

Here, N is the cyclist number, q_d is the queue discharge rate in cyclists per second, t is the time in seconds at which the Nth-cyclist passes the stop line and $L = \frac{t_0}{q_d}$ is a constant which depends on the queue discharge rate and the start-up time t_0 of the first cyclist. The slope of the regression line is the measure for the average queue discharge rate which we use for our further analysis $\frac{\Delta N}{\Delta t} = q_d$, see Figure 6.5b. The jam density and queue discharge rate for each run are then coupled and a regression analysis is performed to quantify the influence of the jam density on the queue discharge rate.

(a)   (b)

*Figure 6.4: Example of a queue showing the cross-section (yellow) and queue length (white)
that is used for the analyses (a) and the constructed image in space and time (b)
showing the lateral position and passing time of all front wheels indicated with
red dots.*

(a)   (b)
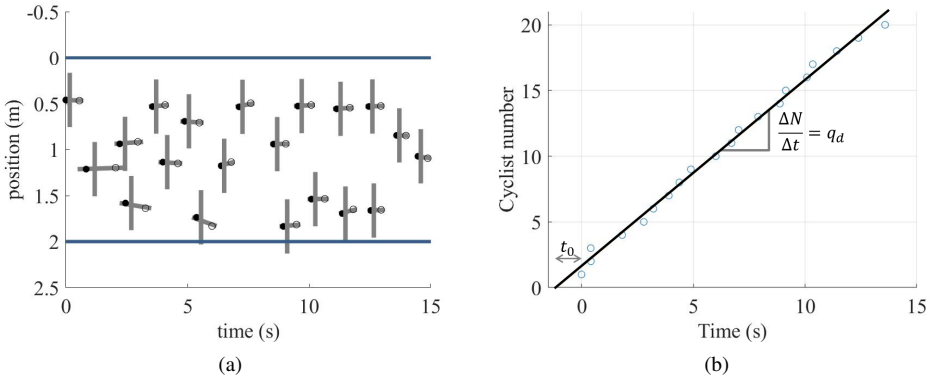
*Figure 6.5: The digitized version of 6.4b showing the lateral position and passing time of
all bikes (a). The front wheel is indicated with the filled dot, the rear wheels
with the open dot. (b) shows an example of the regression analysis to obtain the
queue discharge rate.*

Speed and queue configuration

The secondary objective is to better understand the underlying processes of the queue discharge. To this end, we perform two analyses. First, we investigate the individual and average speeds of cyclists during the queue discharge process and second, we compare the queue configuration to the discharge pattern.

The individual speeds (v_{d}^i) are extracted using the passing times (t) of the front and rear wheels and the distance between the two wheels (r), which equals the average length of a bike, i.e. 1.80m (Gavriilidou et al., 2019), minus twice the radius of a wheel, which is approximately 0.35m for an 28-inch wheel, $r = 1.80 - 2*0.35 = 1.10$m:

$$v_{\mathrm{d}}^i = \frac{r}{t_{\mathrm{rear}}^i - t_{\mathrm{front}}^i}. \tag{6.3}$$

The average speed V_d during the queue discharge phase is the harmonic mean of the individual speeds:

$$V_\mathrm{d} = \left(\frac{1}{n}\sum_{i=1}^{n}\frac{1}{v_\mathrm{d}^i}\right)^{-1} , \qquad (6.4)$$

in which n is the total number of cyclists that are participating in that run. A regression analysis is performed to grasp the influence of the jam density on the average speed during the discharge.

To grasp the underlying mechanisms of the obtained relations, we qualitatively describe the different queue configurations and their effects on the observed patterns during the discharge phase. This is done by following each cyclist during the discharge process and comparing it to the queue position with the speed, ranking and lateral placement on the path while passing the stop line. Different colors are used to visualize the position of cyclists in the queue matched to their ranking in the discharge phase.

6.3.3 Experiment execution

The experiment was held at the Green Village terrain which is a living lab and test facility of Delft University of Technology. The terrain was closed for visitors to eliminate possible disturbance by other traffic. The experiment was held on the 7th of August in 2019 which was a dry and partly clouded day with a moderate breeze (4 Beaufort). These wind conditions are common in the Netherlands and are not expected to have influenced the outcomes. A total of 20 people participated in the experiment of which the majority was student, between $20 - 25$ years old and held the American nationality. Twelve of the twenty participants were male, implying that the group consisted predominantly of young male adults. All cyclists participated on a classic 'oma fiets'-type of bike with single speed and back-pedal brakes, which is commonly used in the Netherlands. These rental bikes had been used in the days before the experiment so everyone had time to become familiar with this type of bike. The participants were asked to fill in a short questionnaire about their cycling experience and confidence while cycling. The results are presented in Figure 6.6. 40% of the participants indicated that they use the bike multiple times per week which is below the European average of 85% that is reported in Prati et al. (2019). On the other hand, the participants rated their confidence while cycling on average an 8.3, on a scale of 1 to 10. Furthermore, the age at which they learned how to cycle was on average at age 6. So although their cycling frequency is below average, their confidence and familiarity with riding a bicycle is high.

The sequence of arriving, queuing and clearing was repeated 23 times. Most runs were consecutive so the cyclists continued cycling in between runs. The cyclists were only stopped when new queuing instructions had to be given. By mistake, configuration (b) 'side-by-side in threes' was not repeated 3 times as initially planned but only twice. On the other hand, the runs without instructions and 3-2-3 on indicated positions (d) was repeated four times because the first cyclists of the group had already passed the point were new instructions could be given. An overview of all runs is presented in Table 6.1.

Table 6.1: Details of the runs that were performed during the experiment.

Run #	Configuration	Instructions	Jam density bic/m^2	Discharge rate $bic/s/m$
1		None	0.62	0.59
2		None	0.67	0.54
3		None	0.67	0.57
4		None	0.69	0.54
5		Queue up closely	1.18	0.68
6		Queue up closely	1.09	0.71
7	(a)	In pairs	0.71	0.64
8	(a)	In pairs	0.71	0.61
9	(a)	In pairs	0.72	0.67
10	(b)	Side by side in threes	0.85	0.66
11	(b)	Side by side in threes	0.81	0.70
12	(c)	In threes and v-shape	0.77	0.58
13	(c)	In threes and v-shape	0.79	0.66
14	(c)	In threes and v-shape	0.71	0.50
		Break		
15	(d)	3-2-3	0.99	0.70
16	(d)	3-2-3	1.11	0.78
17	(d)	3-2-3	1.11	0.71
18	(d)	3-2-3	1.07	0.80
19	(e)	3-3-3 with shift	0.99	0.67
20	(e)	3-3-3 with shift	0.99	0.68
21	(e)	3-3-3 with shift	0.99	0.72
22		Queue up normal and feel comfortable doing	0.95	0.65
23		Queue up closely	1.31	0.81

6.4 Results

This section describes the findings of the analyses by first zooming in on the relation between jam density and the queue discharge rate in Section 6.4.1, and then describing the speed and comparison of the queue configuration and discharge patterns in Section 6.4.2.

6.4.1 Relation jam density and queue discharge rate

The observed jam density values range between 0.6 and 1.3 bic/m^2, as can be seen in Figure 6.7. The normal runs without queuing instructions resulted in the lowest jam densities between 0.6 and 0.7 bic/m^2, which are in agreement with the value of 0.65 bic/m^2 reported in literature (Goñi-Ros et al., 2018). The jam density increased when we began to provide
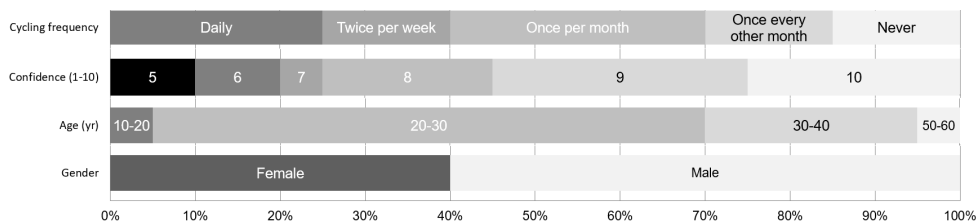
Figure 6.6: Results from the questionnaires filled in by 20 participants.
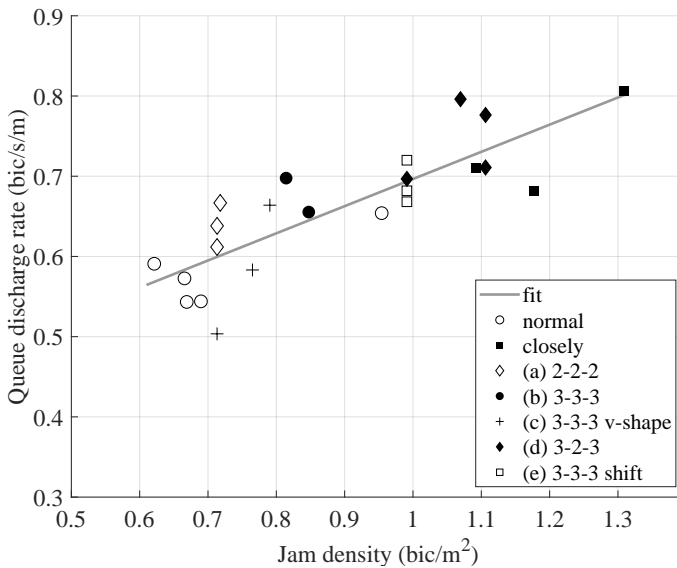
Figure 6.7: Jam density and the queue discharge rate.

instructions on how to form the queue. Meanwhile, the variation in jam density is small for runs with similar instructions, which can be expected since we asked cyclists to queue up on pre-assigned spots. The exception are the runs without instructions and where cyclists were asked to queue up closely. Here, the cyclists where free to pick their own position, which resulted in a higher variation in jam density. When ordering the jam densities from low to high, we roughly find the following order: No instructions, in pairs (a), in threes with v-shape (c), in threes side by side (b), in threes with a shift (e), alternating 3-2-3 (d) and queue up closely. The latter instruction resulted in jam densities between and 1.3 bic/m^2, which is close to twice the uninfluenced jam density. These results show that the density of a queue can indeed be positively influenced by giving instructions.

Three other results regarding jam density are highlighted: First, the configurations (b) and (c) were expected to result in similar jam densities. However, the results of the experiment show a slight difference; configuration in threes with v-shape (c) resulted in slightly lower densities than when the cyclists were queued up side-by-side (b). Second, the configuration where cyclists queued up in threes with a shift (e) was expected to result in higher density than when the cyclists alternately queue up in pairs and threes (d). However, the results from the experiment show the opposite although the differences are small. Apparently, the available space can be used more efficiently in the 3-2-3 setup. Last, one of the normal runs resulted in a higher jam density than expected. This run was done near the end of the experiment, so after the cyclists had been asked to queue up closer together. It is unclear whether this result is caused by an increasing familiarity with the experiment setting or if the participants got used to queuing up close together which changed their perception of normal.

The obtained queue discharge rates vary between 0.5 and 0.8 bic/s/m and increases with increasing density. In uninfluenced queuing conditions, the discharge rate varied between 0.54 and 0.60 bic/m/s, which is below the expected value of 0.65 bic/s/m from literature (Goñi-Ros et al., 2018; Wierbos et al., 2020). This might be explained by the level of experience in cycling. Some participants indicated that they rarely cycle in daily life, which could increase the reaction time and acceleration process. Another factor of influence could be the absence of haste in the setting of a controlled experiment and that no other cyclists were coming from behind. The highest queue discharge rates were obtained in two runs with a 3-2-3 configuration of the queue and a run in which the cyclists queued up closely. Most other runs show a queue discharge rate between 0.6 and 0.7 bic/s/m, except for a run with configuration (run e), in threes and in v-shape. The video recordings showed that two consecutive cyclists were talking to each other in the queue. Due to inattention of the front cyclist, the reaction time to restart moving was increased and the cyclists behind were delayed resulting in a lower discharge rate.

The jam densities and discharge rates combined show a positive relation, which confirms that the discharge flow can be positively influenced by increasing the density of the queue. Linear regression analyses to the data results in the model: $q_d = Q_0 + \beta k_j$ with regression constant $Q_0 = 0.36$ bic/s and the coefficient $\beta = 0.34$ m^2/s. The R-squared value of the model is 0.70. The regression analyses was also performed for a quadratic fit, but this model resulted in a lower R-squared value. The obtained model means that when 20 cyclists are waiting at a controlled intersection on a 2m wide path, the minimum green time needed to clear the queue is approximately 18 seconds for a queue of jam density of 0.6 bic/m^2, while this decreases to 13 seconds when the jam density is increased to 1.2 bic/m^2. Doubling the jam density will therefore lead to an efficiency gain in the discharge process by approximately 40%.

The obtained positive relation between jam density and queue discharge rate is in agreement with literature. However, the magnitude of the relation is different. The positive response of the queue discharge rate to increasing jam density is stronger in Goñi-Ros et al. (2018) for jam densities between 0.3 and 0.65 bic/m^2 than the impact on queue discharge rate in the density range of 0.6 – 1.3 bic/m^2 of our study. The difference could result from the different setting, namely a real-life situation versus a controlled experiment. Alternatively, the relation between jam density and queue discharge rate is not linear but follows a quadratic or different relation instead where the positive relation flattens for higher jam density.

6.4.2   Speed and queue configuration

The average cycling speed during the queue discharge phase varied between 5 and 8 km/hr, and decreases with increasing density, see Figure 6.8a. This data is highly influenced by the start-up process of the first cyclists, as can be seen in Figure 6.8b. Here, the individual speeds of all cyclists are plotted, together with the moving average of a run with a pairwise configuration and 3-2-3 configuration (high density). This shows that the first 8-12 cyclists are still accelerating while passing the stop line, while the later cyclists have more or less reached a constant speed. The moving averages of two runs are highlighted to illustrate the differences between runs, showing that the speed is higher in runs with a pair-wise queuing
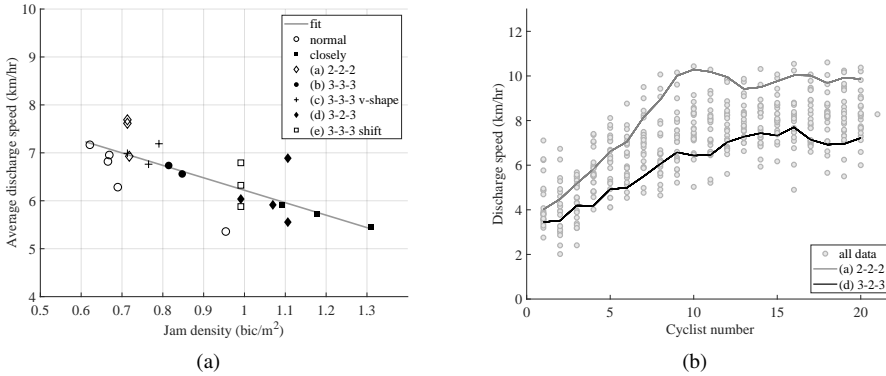
Figure 6.8: Results of the experiment, with (a) the queue discharge rate and (b) the average speed that cyclists had while passing the stop line.

configuration and lower in a setting with alternately pairs and threes which has a high density.

When combining the average discharge speed and the jam density, Figure 6.8a shows that the average discharge speed decreases with increasing jam density. Linear regression analyses on the average speed data results in the model: $v_d = V_0 + \alpha k_j$, with regression constant $V_0 = 8.82$ km/hr and the coefficient $\alpha = -2.60$ (km/h)/(bic/m^2). The R-squared value of the model is 0.57. This negative relation can be explained by the observation that cyclists have less space to manoeuvrer in a dense queue, resulting in reaction behavior instead of anticipation behavior. In low density queues, cyclists can anticipate upon the movement of someone in front and already decide to start moving as well, while in a dense queue, the cyclists must wait until the person in front has moved away until they have space to start pedaling.

The qualitative analysis of the queue configurations and the discharge patterns of all runs have led to insights into the cyclists' behavior. Based on the queue configurations only, two observations are made: First, in the runs without instructions, the cyclists used the total width of the path but there was a slight tendency to stop more to the right-hand side of the path. Second, some cyclists chose a spot close to others, while other cyclists preferred to leave a gap of 1 to 2 meters. This last preference was overruled when cyclists were asked to queue up closely. The cyclists then used the full width of the path and placed their front wheel next to the rear wheel of a predecessor, resulting in a compact queue.

The difference in wheel positioning could also explain the higher density than expected in the 3-2-3 configuration. Figure 6.9 shows two examples of observed queue configurations in configuration (d) and (e). When looking more closely at the wheel placement of queued-up cyclists, you see that the front wheels of consecutive cyclists are placed more forward in the 3-2-3 configuration, and further backwards in the 3-3-3 configuration (e). This indicates that when the lateral distance between adjacent cyclists is larger, the longitudinal distance

(a) queue in 3-2-3 configuration (d)   (b) queue in 3-3-3 configuration (e)
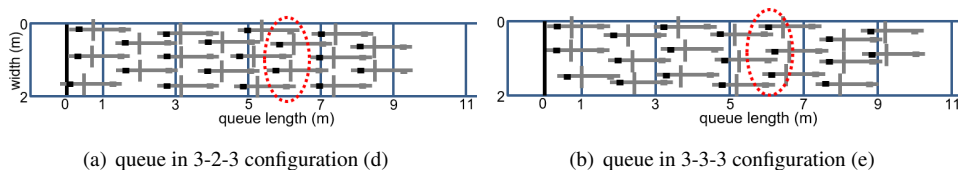
Figure 6.9: Observed queue configurations of run 18 (a) and 20 (b). Within the red mark-
ings is the difference in wheel placement, black is front wheel and gray dot is
rear wheel.

between consecutive cyclists can be smaller, which in the situation of the 3-2-3 configuration
leads to a higher density than the 3-3-3 configuration.

(a) queue - queue up closely   (b) discharge - queue up closely

(c) queue - no instructions   (d) discharge - no instructions
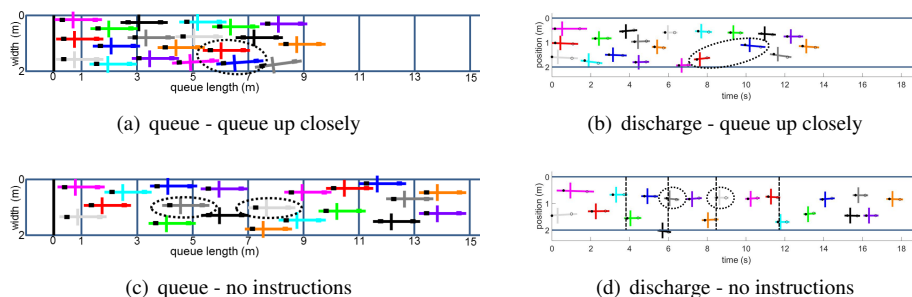
Figure 6.10: Observed queue and discharge configurations.

Based on the colored analyses of the discharge patterns the following observations are made:

- The cyclists more or less maintain their ranking, meaning that little overtaking actions
  take place and the queue position mostly determines the discharge sequence. An
  example of this is visualized in Figure 6.10a and b. Here, the blue cyclist indicated
  by the dashed circle, is queued up closely behind the red one, but it has a lower speed
  and uses 2.5 more seconds in the discharge process. The subsequent cyclists do not
  overtake but wait instead, thereby maintaining the same ranking.

- Some cyclists that are queued up in the middle merge towards the right-hand side of
  the path during the discharge process. This observation is highlighted by the dotted
  circles in Figure 6.10c and d.

- More cyclists cycled out of bounds when the jam density was high. This was partly
  caused by the fact that the starting position was already closer to the path edges, and
  partly because the average discharge speed was lower which led to more swaying
  behavior.

- Cyclists did not cycle side-by-side during discharge, but rather kept a distance to
  others in time and space. This behavior is illustrated by the dashed vertical lines in
  Figure 6.10d showing that the rear and front wheels pass the stop line simultaneously.

The full list of queue configurations and discharge patterns are presented in Appendix A at the end of this Chapter.

6.5 Practical Application

An example is given to illustrate how the findings regarding jam density and discharge rate can be applied in practice by updating the signal length. From the results of the experiment, we know that the efficiency of the queue discharge process can be improved by influencing the queue formation process to reach higher jam density. This means that the capacity of the intersection can be increased such that more cyclists can enter the intersection compared to the uninfluenced situation. The benefit of the increased capacity can be used to adjust the cycle length based on the new discharge rate for cyclists. As a result, the red times and associated delay reduce for all traffic participants. The remaining of this section discusses an example.

We will calculate the optimal cycle length for an intersection between cars and cyclists, based on two different discharge rates for cyclists; first the uninfluenced situation, then with queuing instructions. We use a simplified calculation for optimal cycle time (C). As input, we have the ratios between demand (D) and discharge rate (Q_{dis}) for each of the streams, and the clearance time (T_{clear}), i.e. the time the intersection cannot be used due to yellow time or safety bounds between directions. The fraction of green time required for each of the streams is D/Q. For a two-phase intersection, with cars and bicycles having one phase each, the time remaining for the clearance time is hence:

$$T_{\text{clear}} = C * \left(1 - \frac{D_{\text{car}}}{Q_{\text{dis,car}}} - \frac{D_{\text{bic}}}{Q_{\text{dis,bic}}} \right). \tag{6.5}$$

If the clearance time, the demands and the capacities are known, this equation can be reverted to find the cycle time:

$$C = T_{\text{clear}} \bigg/ \left(1 - \frac{D_{\text{bic}}}{Q_{\text{dis,bic}}} - \frac{D_{\text{car}}}{Q_{\text{dis,car}}} \right) \tag{6.6}$$

We will construct cumulative flow curves for cyclists and cars. These increase linearly with time if the flow is constant (inflow), and are constant for no outflow. The area between the curves is the delay. For more information on cumulative curves, we refer to Daganzo (2008). We construct the inflow and outflow curves for both directions separately.
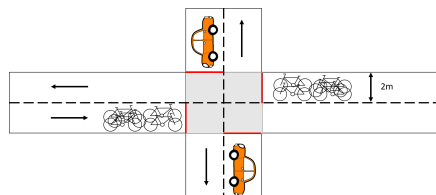

Figure 6.11: Sketch of bicycle–car intersection.

In the example, we consider an intersection with a two-phase traffic signal, in particular one where a stream of cyclists crosses a stream of car traffic, see Figure 6.11. The design is roughly based on the intersection between Catharijnesingel and Vredenburgviaduct in Utrecht, the Netherlands. It represents two-directional traffic for both cyclists and cars in a busy city center. The total width of the cycle path is 4 meter, so 2 meter per direction; the cars have one lane in each direction. During peak hours, the cyclist demand per direction is around 1300 cyclists per hour and for cars this is around 900 cars per hour per direction (Municipality Utrecht, 2020). We assume a queue discharge rate of 1800 veh/h. For this intersection, we consider a combined clearance time (T_{clear}) of 10 seconds, which includes all red and yellow times for both signal changes combined.

For the uninfluenced situation, we take a discharge rate of 0.56 bic/s/m (see Figure 6.7) which translates into an hourly rate of 4000 bic/h. Based on these numbers, a cycle length of 57 seconds is found optimal, with a green interval of 19 seconds for cyclists and 29 seconds for cars.

For the case with increased queuing density, these numbers change. The optimal cycle length decreases when the bicyclist discharge rate increases due to the influenced jam density. Now, we assume a queue discharge rate of 0.75 bic/s/m, based on the an average value obtained in a 3-2-3 configuration. The hourly discharge rate for cyclists is thus 5400 cyclists per hour. Entering the new numbers in Eq. 6.5–6.6, leads to an optimal signal length of 39 seconds, with a green interval of 9 seconds for cyclists and 19 seconds for cars. The higher discharge rate for cyclists thus results in a shorter cycle length.

The resulting cumulative flow curves are shown in Figure 6.12. Here, the inflow and outflow are depicted in time, showing a constant inflow based on the demand and zigzagging pattern for the outflow where the curve is horizontal during red interval and increases with the queue discharge rate during the green interval. The area between the inflow and outflow curves represents the waiting time for cyclists and cars. Comparing the total waiting time for the two situations shows that the changed signal reduces the waiting time for cyclists with 24% and 32% for cars.

The impact of reducing the cycle length is also illustrated in Figure 6.13, which shows the waiting time for individual cyclists. The maximum delay per cycle is 39 seconds in the uninfluenced situation, and this reduces to 29 seconds in the situation with a 3-2-3 queue configuration. The average waiting time per cyclist reduces with 4.6 seconds, and that per car with 4.7 seconds. When combining this for all traffic in a two hour peak period, the delay reduction adds up to 140 minutes for cars and 200 minutes for bicyclists.

6.6   Discussion and future research

A positive relation was found between jam density and queue discharge rate within the density range of 0.6 to 1.3 bic/m^2. The magnitude of the impact of increasing jam density is less in our study than reported in the literature for densities between 0.3 and 0.65 bic/m^2. Possibly, the specific characteristics of our sample play a role here, e.g. only single-speed
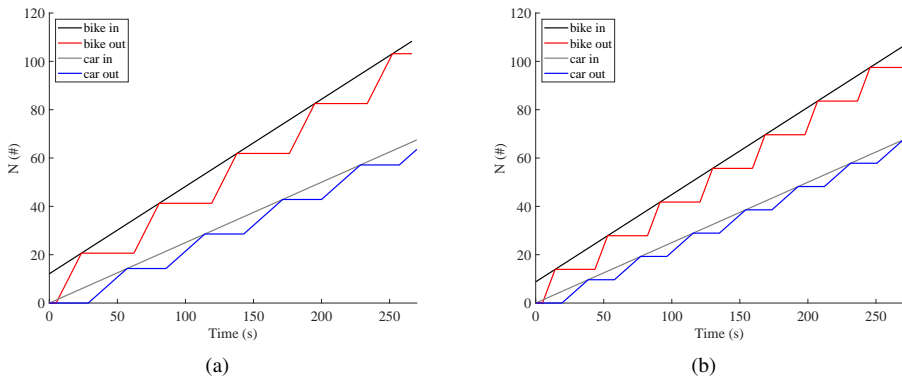
Figure 6.12: Cumulative flow curves for cars and cyclists for the situation of uninfluenced jam density (a) and increased jam density (b).
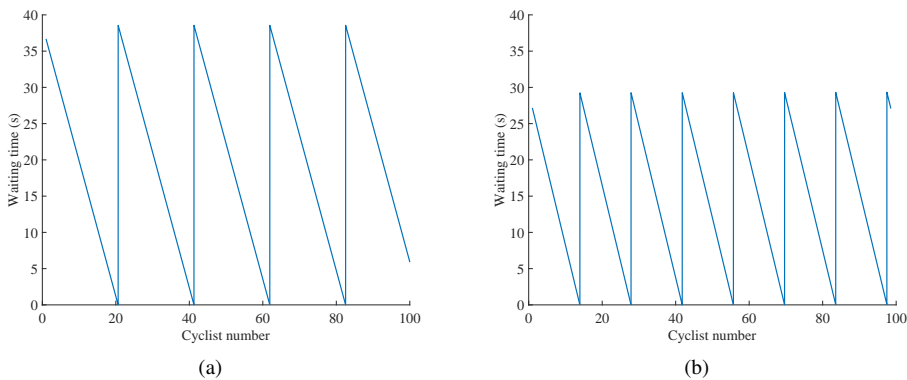
Figure 6.13: Waiting times per cyclist in the situation of uninfluenced jam density (a) and increased jam density (b).

bicycles, below-average cycling frequency in daily life, or absence of haste. Future research in a real-life setting covering the full range of jam densities could help to identify the nature of the positive relation between jam density and queue discharge flow.

The average speed during the queue discharge process decreased when the jam density increased, indicating that cyclists are hindered in their movements due to the proximity of other cyclists. It would be interesting to see if this effect leads to a stagnation or decrease in queue discharge rate for jam density values that exceed the highest value observed in this study.

The comparison of the queuing positions and discharge patterns resulted in the following observations: the discharge sequence is mostly determined by the queuing position, cyclists

keep a distance to each other in both time and space during the queue discharge phase, and more cyclists use the path edge or beyond when the jam density increases. The work of Goñi-Ros et al. (2018) reports on cyclists moving onto the road or the sidewalk during the discharge process but it does not specify under which density conditions this behavior occurs. It would be interesting to see of this enhanced 'out of bounds'-movement is also observed in real-life situations where side curbs and the presence of other traffic might prevent cyclists from moving out of bounds.

The quantitative analysis confirmed that increasing the jam density has a positive effect on the queue discharge rate, also for values of jam density that have not been observed before. The efficiency of the queue discharge process, measured in discharge rate, increased by 40% when comparing the situation with the highest jam density to an uninfluenced situation. Introducing control measures to increase the jam density is therefore a promising way to reduce congestion at intersections.

The delay at intersections can be reduced the most when cyclists are asked to queue up closely and when they use pre-assigned spots in a configuration of alternately in pairs and threes on a 2m-wide bicycle path. An interesting next step is to test this finding in daily traffic, and to study which measure is most effective in encouraging cyclists to queue up more closely. This could be done e.g. by placing visual signs asking cyclists to queue up closely, or adding a Formula-1-like starting grid on the path, indicating the cyclists to queue up alternately in pairs and threes.

Our findings are based on a homogeneous composition of the queue regarding bicycle type and social setting. The results may differ in practice when other means of transportation are also present on the bicycle path or when social groups stick together and do not queue up according to the optimal configuration. Examples are cargo bikes which have different dimensions, electrically driven bicycles which have atypical acceleration patterns or small children who stay next to their parents. Nevertheless, increasing the jam density is a promising way to reduce congestion at intersections.

6.7   Conclusion

A controlled experiment showed that giving queuing instructions to cyclists can increase the jam density. Jam densities between $1.1 - 1.3$ bic/m^2 can be achieved, which is approximately twice the density found in normal conditions. All queuing instructions have led to jam densities that exceed the values obtained in normal queuing conditions. The highest jam densities were observed when participants were asked to queue up closely and when they positioned themselves in a configuration that alternated in pairs and threes. The higher queue densities led to higher queue discharge rates for cyclists, up to 40% higher than in uncontrolled conditions. This paper explored the effect of intervening in the queue formation process in an experimental condition. Next step would be to verify the results in a field test. Once implemented, the signal control can be adapted to the higher queue discharge rate for cyclists, which will reduce the delay for all traffic participants.

APPENDIX A

(a) queue – run 1 – no instruction

(b) discharge – run 1

(c) queue – run 2 – no instruction

(d) discharge – run 2

(e) queue – run 3 – no instruction

(f) discharge – run 3

(g) queue – run 4 – no instruction

(h) discharge – run 4

(i) queue – run 5 – queue up closely

(j) discharge – run 5

(k) queue – run 6 – queue up closely

(l) discharge – run 6

(m) queue – run 7 – in pairs

(n) discharge – run 7

(o) queue – run 8 – in pairs

(p) discharge – run 8
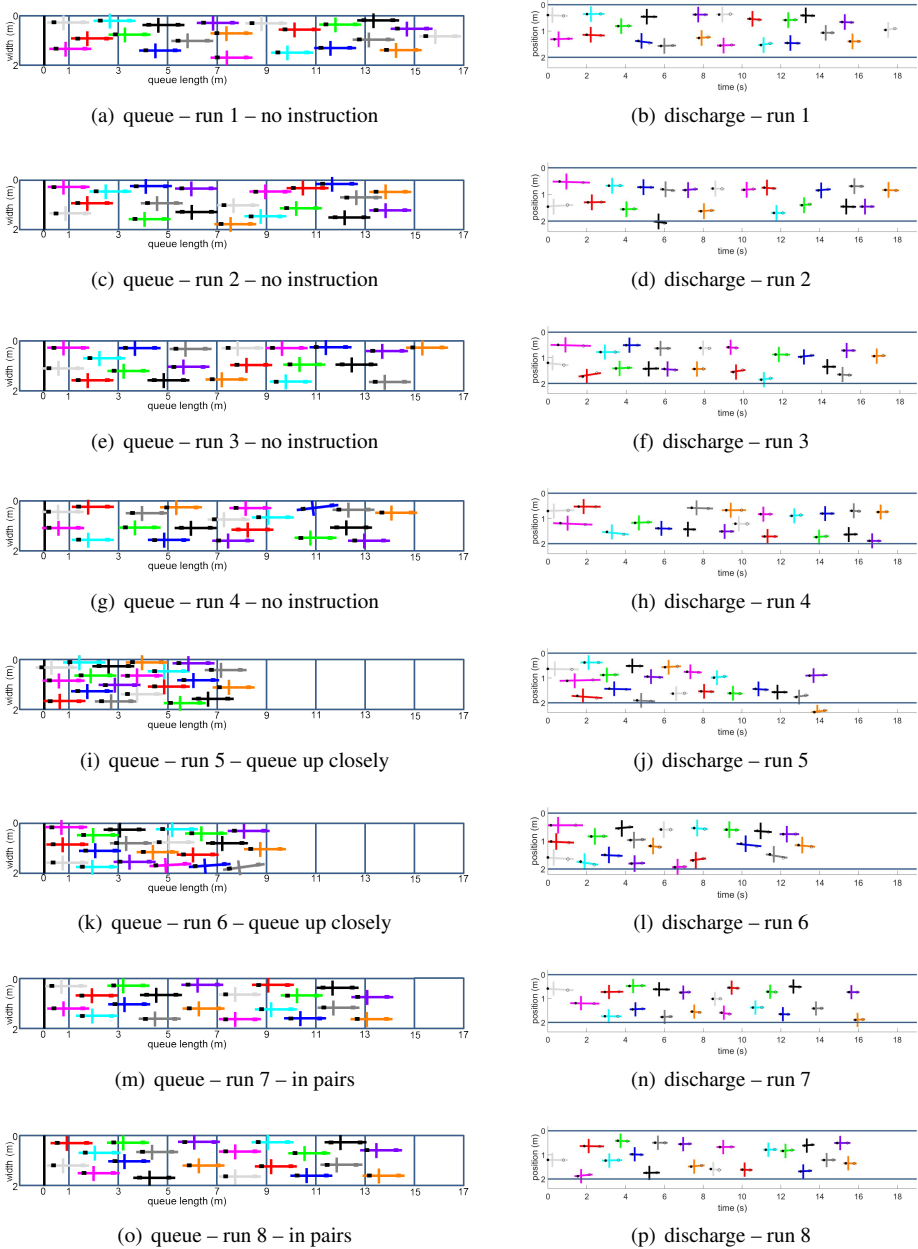
Figure 6.14: Observed queue configurations and discharge patterns of run 1-8.

(a) queue – run 9 – in pairs

(b) discharge – run 9

(c) queue – run 10 – in threes

(d) discharge – run 10

(e) queue – run 11 – in threes

(f) discharge – run 11

(g) queue – run 12 – in threes and v-shape

(h) discharge – run 12

(i) queue – run 13 – in threes and v-shape

(j) discharge – run 13

(k) queue – run 14 – in threes and v-shape

(l) discharge – run 14

(m) queue – run 15 – 3-2-3

(n) discharge – run 15

(o) queue – run 16 – 3-2-3

(p) discharge – run 16

(q) queue – run17 – 3-2-3

(r) discharge – run 17
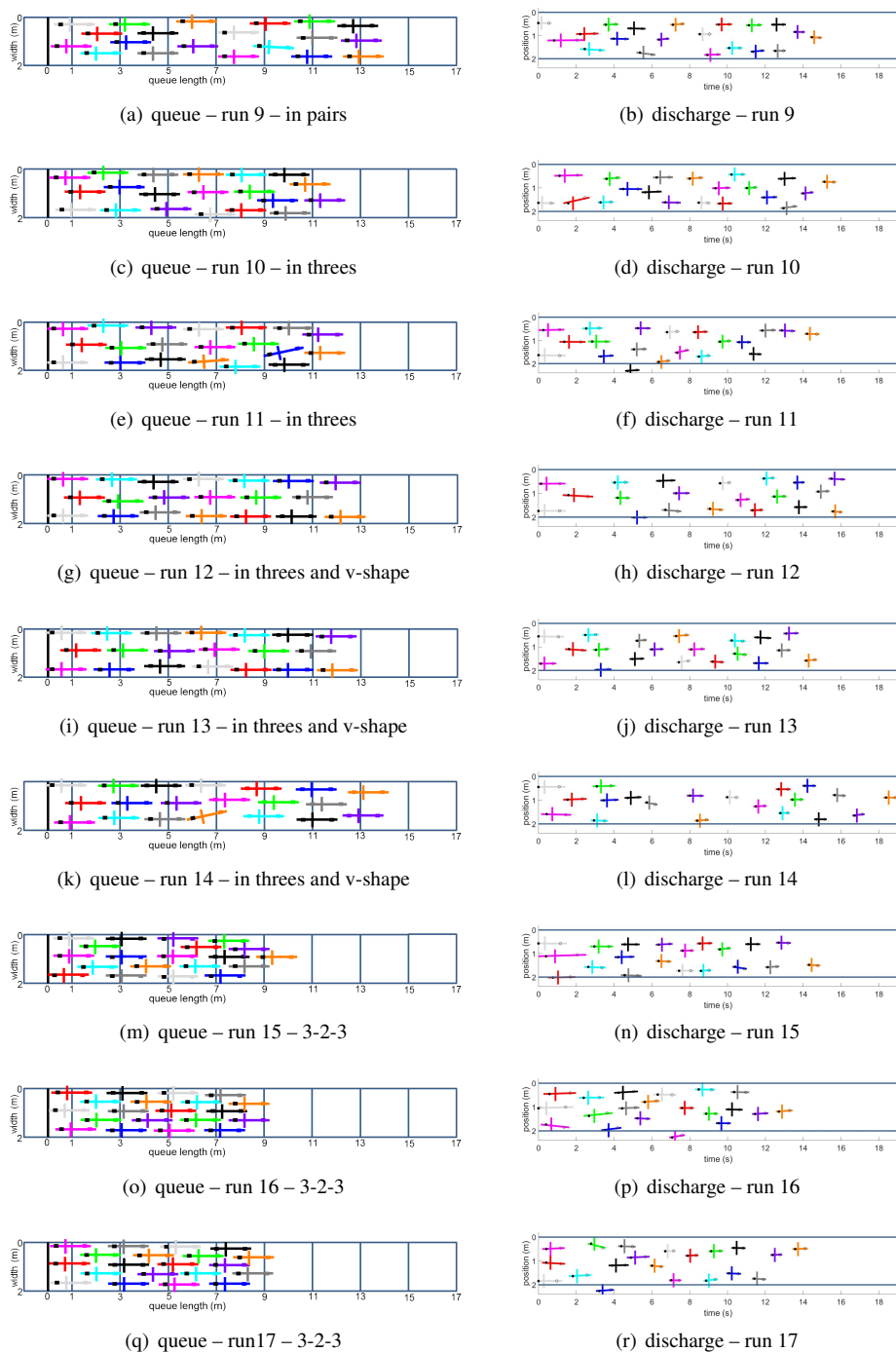
Figure 6.15: Observed queue configurations and discharge patterns of run 9-17.

(a) queue – run 18 – 3-2-3

(b) discharge – run 18

(c) queue – run 19 – in threes shift

(d) discharge – run 19

(e) queue – run 20 – in threes shift

(f) discharge – run 20

(g) queue – run 21 – in threes shift

(h) discharge – run 21

(i) queue – run 22 – normal

(j) discharge – run 22

(k) queue – run 23 – queue up closely

(l) discharge – run 23
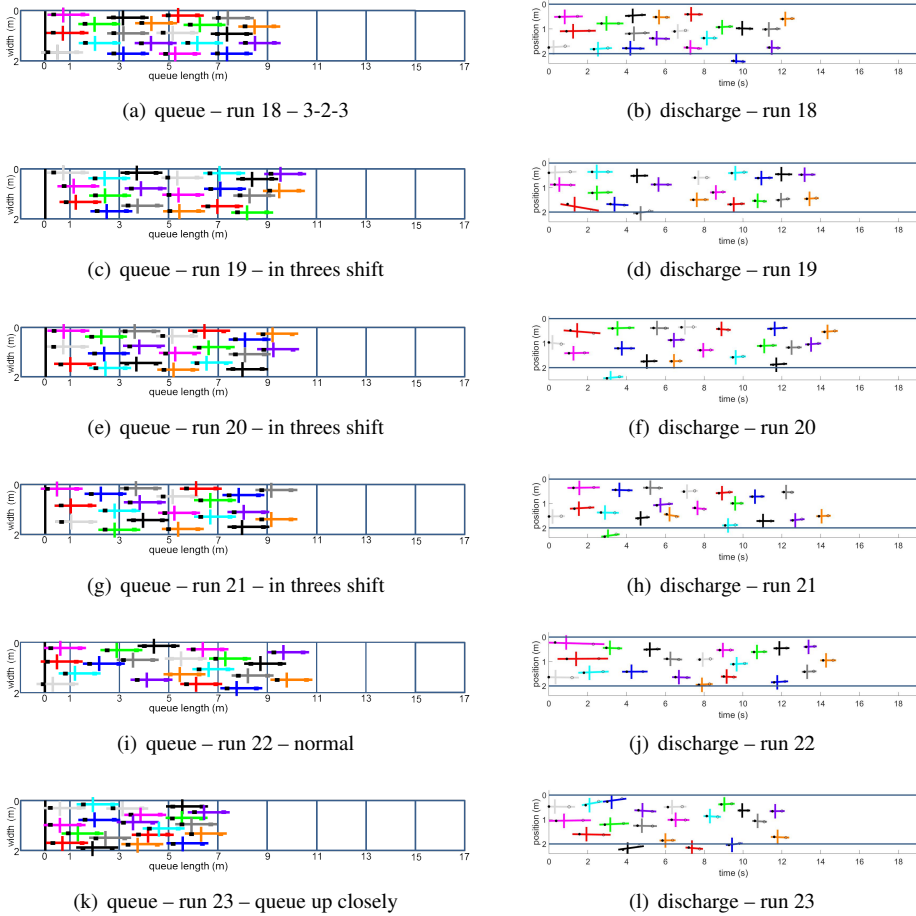
Figure 6.16: Observed queue configurations and discharge patterns of run 18-23.

Part III

Modeling bicycle flow

Chapter 7

A macroscopic flow model for mixed bicycle–car traffic

The focus of this dissertation now changes to simulating bicycle flow. Cyclists are rarely included in macroscopic traffic flow models, which makes it more difficult to design safe and congestion-free traffic situations. One reason for this absence is the scarcity of theory about bicycle traffic flow—a limitation that the previous chapters have addressed by collecting and analyzing empirical data. Another reason is that bicycle congestion is a relatively new problem, and the need to include cyclists has not been pressing enough in the past. Furthermore, it is unclear how to capture bicycle movements in a macroscopic model. Chapter 7 addresses this topic and thus tackles the final research question: *How can we describe and model bicycle flow in a mixed traffic situation?*

This chapter introduces class-specific speed functions based on two variables: space headway for cars and for cyclists. This enables the macroscopic modeling of mixed bicycle–car traffic. The multi-class macroscopic flow model is successfully tested for different traffic situations that arise on urban roads where cyclists and cars share the same infrastructure, for instance, cyclists overtaking a queue of cars and cars overtaking cyclists with reduced speed. The mixed bicycle–car flow model allows travel time estimation of both classes, which in turn can be used to evaluate the overall performance of a mixed-traffic road.

Abstract

Bicycles are gaining popularity as a mode of transport resulting in a mixed bicycle–car traffic situation on urban roads. Cyclists however, are hardly included in traffic flow models which complicates the design of safe and congestion-free traffic situations. This work introduces class-specific speed functions based on two variables, being space headway for both cars and cyclists. This enables the macroscopic modeling of mixed bicycle–car traffic. The multi-class macroscopic flow model is successfully tested for different traffic situations that occur on urban roads where cyclists and cars share the same infrastructure, e.g. cyclists overtaking a queue of cars and cars overtaking cyclists with reduced speed. The mixed bicycle–car flow model allows travel time estimation of both classes, which in turn can be used to evaluate the overall performance of a mixed traffic road.

7.1   Introduction

Traffic participants in urban environments often share the available infrastructure. In places with high cyclist volumes the roads are used simultaneously by cars and cyclists. This creates a mixed traffic situation in which both classes can be the fastest moving one depending on the traffic state. In low demand situations, cars have the opportunity to overtake cyclists, while in congested situations the cyclists can maneuver alongside a queue of cars and thus be the fastest moving class. An essential property of mixed traffic flow is this ability of cyclists to continue moving in congested traffic. Describing this feature is important for estimating the expected travel time loss, which is a common metric for road network performance. The travel time loss may differ for the multiple user types since the experienced delay depends on the traffic state and the specific class characteristics.

Macroscopic flow models are commonly used for travel time estimation. However, these models generally handle mixed traffic situations by selecting cars as the reference class and expressing the other classes in passenger car equivalents (pce) based on their impact to the traffic flow. The pce-concept was first introduced in the U.S. Highway Capacity Manual by (National Research Council, 1965) and has been used in many studies since then resulting in various methods to convert a mixed traffic stream into a uniform one, as summarized by Shalini and Kumar (2014). A consequence of using the pce-concept is that the speeds for both classes depend on one (pce-based) density, and cannot depend on the vehicle-bicycle composition leading to that density. Therefore, it does not fully represent the movements observed in mixed bicycle–car traffic. Our purpose here is to overcome this limiting model property by introducing an alternative approach that enables switching of the fastest moving class in congestion.

This work presents a multi-class macroscopic traffic flow model which uses class-specific speed functions that depend on the density of all classes as independent variables. The distinction into classes is based on mode of transportation only, so heterogeneity in e.g. driver type is not considered. A Lagrangian approach is used, following groups of traffic participants over time. Both group size and simulation time are discretized in the numerical implementation, while position is a continuum. The class-specific speed functions are

two-dimensional and take into account the space headway of both cars and cyclists. The successful working of the model is illustrated for different traffic situations that typically occur on urban roads. The proposed model allows for travel time estimation for multiple traffic modes by describing their joint traffic dynamics, which in turn can be used to evaluate the overall performance of a mixed traffic road.

The paper continues with a background on macroscopic traffic flow modeling in section 7.2, followed by an explanation of the modeling principles in section 7.3, the numerical implementation of the model in section 7.4 and the presentation of the class-specific speed functions in section 7.5. Afterwards, section 7.6 illustrates the successful working of the model and section 7.7 presents the discussion and conclusion.

7.2 Background on macroscopic modeling

This paper aims to describe mixed traffic flow in an urban setting where cars and cyclists share the infrastructure, using a macroscopic flow model. Macroscopic models describe the evolution of traffic movements over time and space at an aggregated scale using the quantities: density, average speed and flow. This differs to microscopic flow models, which describe the movements of individual traffic participants. The distinction between microscopic and macroscopic is therefore based on the level of detail. Macroscopic models often use an equilibrium relationship between speed and flow. This equilibrium relationship is commonly known as the fundamental diagram (Greenshields, 1935).

The earliest macroscopic model is the LWR model, which is a first-order kinematic wave model that was simultaneously introduced by Lighthill and Whitham (1955) and Richards (1956). It describes the flow based on the assumption that traffic is a continuum and obeys the physical law for mass conservation. Using the density k, flow q and average speed u at position x and time t, the continuity equation is given by:

$$\frac{\partial k(x,t)}{\partial t} + \frac{\partial q(x,t)}{\partial x} = 0, \tag{7.1}$$

with

$$q(x,t) = u(x,t)k(x,t) \tag{7.2}$$

and

$$u(x,t) = U(k(x,t)) \tag{7.3}$$

stating that velocity u is given by the fundamental diagram U.

The solution to the mentioned system of equations has two important properties: hyperbolicity and anisotropy. Hyperbolicity indicates that perturbations in the flow travel as waves through time and space, so they are not instantaneously felt in the whole domain. Anisotropy means that traffic flow is influenced by the traffic state in front and not from the back. For this, the wave speed of perturbations should never exceed the maximum velocity. Anisotropy requires the model to be weakly hyperbolic, which is the case if when the velocity function is nonincreasing (Zhang et al., 2006; van Wageningen-Kessels et al., 2013).

In simulation, the solution of the kinematic wave model is approximated using a numerical scheme. The LWR model is commonly solved using Godunov's method, which is a finite difference scheme (Godunov, 1959), but also other methods have been applied.

The LWR model is both loved and criticized for its simplicity. The main imperfection is that the model describes equilibrium states only, which implies that changes in traffic state result in instantaneous speed adjustments. In reality, traffic is often in non-equilibrium and a reaction time is observed for acceleration and deceleration. This deficiency has been partially addressed in higher-order models by replacing the fundamental diagram with a velocity function that includes acceleration behavior based on driver anticipation, relaxation and traffic inertia, e.g. Payne (1971). After critique that the higher-order model is not anisotropic and therefore unrealistic at traffic discontinuities (Daganzo, 1995), several adjustments are proposed to incorporate changes in e.g. density (Aw and Rascle, 2000), headway (Berg et al., 2000), velocity distribution (Zhang, 2002), speed gradient (Gupta and Katiyar, 2006) and driver physiological response (Khan et al., 2019). Despite these developments in second-order models, the first-order kinematic wave model remains an effective and popular method to describe traffic flow as long as traffic flow phenomena, e.g. capacity drop and stop-and-go waves, are not required.

The aforementioned models describe homogeneous traffic flow. The description of heterogeneous traffic has been addressed in the development of multi-class models by distinguishing traffic type using e.g. different velocities (Wong and Wong, 2002; Zhang et al., 2006), vehicle size (Chanut and Buisson, 2003; Logghe and Immers, 2008), and impact based on velocity using static (Ngoduy and Liu, 2007) and dynamic passenger car equivalent (pce) values (van Lint et al., 2008). Furthermore, developments have been made in describing traffic situations with multiple lanes, e.g. the "2-pipe regime" with slugs and rabbits (Daganzo, 2002), modified speed–density relation based on lane-changing (Jin, 2010) and utility-driven lane changes (Shiomi et al., 2015). The disordered traffic situation, in which lane discipline is lacking, has been captured in continuum models using e.g. available space (Benzoni-Gavage and Colombo, 2003; Nair et al., 2011; Fan and Work, 2015) and lateral distances (Gupta and Dhiman, 2014).

Heterogeneous models capture the characteristics of different traffic types and the effect of their interaction on the overall flow. Slow vehicles, such as buses (Lebacque et al., 1998) and lorries (Muñoz and Daganzo, 2002), are considered as moving bottlenecks for cars, whereas the impact of pedestrians on car traffic is addressed in Daganzo and Knoop (2016). The model of Fan and Work (2015) includes the characteristic trait of small vehicles, i.e. motor cyclists, to maneuver through congestion, maintaining a higher speed than cars. This interaction between cars and powered two-wheelers is further developed by Gashaw et al. (2018), whose model also takes into account that a higher share of two-wheelers results in a lower speed at similar road occupancy. To our knowledge, bicyclists have not been included yet in macroscopic models. However, there are examples of microscopic models that include bicycles, e.g. the individual-following model by Tang et al. (2010) and the cellular automata model by Luo et al. (2015).

All macroscopic flow models describe traffic using the relation between position, time and vehicle number. Three different representations of traffic arise by fixing one of the three variables (Laval and Leclercq, 2013). The most common one is the Eulerian coordinate system, which fixes the vehicle number and visualizes the number of vehicles that have passed a location at a certain time. Another well-known representation is the Lagrangian coordinate system in which time is fixed. Here, the time at which vehicles pass a certain location is simulated, resulting in trajectories. The third and least common representation fixes the position and describes the time at which vehicles cross a certain location.

Although the Eulerian method is most commonly used, the Lagrangian method has been successfully applied to numerically solve the kinematic wave model as well. This has been done for homogeneous traffic (Leclercq, 2007; Wu et al., 2014) as well as mixed traffic including trucks (van Wageningen-Kessels et al., 2011) and motor cyclists (Gashaw et al., 2018). Examples of the Lagrangian method applied to second-order flow models are Greenberg (2001, 2004); Zhang et al. (2012). In the macroscopic approach, the Lagrangian method calculates the traffic evolution for platoons consisting of multiple vehicles, whereas the microscopic approach gives the trajectories of individual traffic participants. The macroscopic model reduces to a microscopic car-following model when the platoon size is reduced to one vehicle only, as shown e.g. by (Aw et al., 2002) and Leclercq (2007). Information travels downstream only in the Lagrangian Godunov scheme, making it less prone for errors due to numerical diffusion. Using the Lagrangian methods therefore results in a more robust model compared to the Eulerian scheme where information travels both up and downstream.

Based on the above we have identified the gap in literature that bicycles are not yet represented in macroscopic traffic flow models, while they are an important part of daily traffic in countries such as The Netherlands and China. The common feature in the above-mentioned models is that a fastest class is assumed; one class, i.e. the passenger car, is assigned to have the highest speed irrespective of prevalent traffic conditions. This assumption is limiting when representing bicyclists, since they are able to switch into being the faster class when maneuvering forward in congestion. This occurs for instance in the situation where the road is wide enough for a car and cyclist to move alongside each other, and the cyclists can pass a queue of stopped cars. We include this phenomenon by introducing class-specific speed functions in the first-order macroscopic model, which depends on the density of all modes. We use the Lagrangian method because of its modeling accuracy.

7.3   Lagrangian model

The starting point of our model is the continuity equation in Eulerian coordinates, Eq. 7.1, which states that changes in density over time should match the change in flow over space, indicating that vehicles should not suddenly appear or disappear from the road. To rewrite into Lagrangian coordinates, we use the spacing s instead of the density k as the main variable. Spacing is equivalent to space headway and is defined as the average distance between travelers belonging to the same entity. Furthermore, the spacing is inversely proportional to the density,

$$s = \frac{1}{k}. \tag{7.4}$$

The spacing can also be expressed as the partial derivative of the position x to vehicle number n:

$$s = -\frac{\partial x}{\partial n}. \tag{7.5}$$

Here, the negative sign results from the choice in numbering of traffic units. These numbers are assigned when traffic units pass a certain position. When selecting a position further along the road (larger x), less vehicles will have passed it (lower n), resulting in a negative sign for the change in n.

When substituting Eq. 7.4 into the Eulerian continuity equation we get:

$$\frac{\partial}{\partial t}(1/s) + \frac{\partial}{\partial x}(v/s) = 0 \tag{7.6}$$

Now, using the quotient rule, Eq. 7.5 and the Lagrangian time derivative

$$\frac{D}{Dt} = \frac{\partial}{\partial t} + v\frac{\partial}{\partial x}, \tag{7.7}$$

we retrieve the continuity equation expressed in Lagrangian coordinates:

$$\frac{\partial s}{\partial t} - s\frac{\partial v}{\partial x} + v\frac{\partial s}{\partial x} = 0 \quad\Rightarrow\quad \frac{Ds}{Dt} + \frac{\partial v}{\partial n} = 0. \tag{7.8}$$

The Lagrangian continuity equation states that speed differences between traffic units coincide with changes in their spacing over time. In other words, when two following vehicles initially go at equal speed and the first one slows down, the distance between the two vehicle should decrease.

We now extend the model to describe multiple classes, similar to the multi-class LWR model expressed in Eulerian coordinates Wong and Wong (2002). The conservation equation holds separately for each class u and all variables are class-specific except for time:

$$\frac{Ds_u}{Dt} + \frac{\partial v_u}{\partial n_u} = 0. \tag{7.9}$$

The density of different classes are not combined into one effective density, but treats them independently instead. In practice, this implies that traffic participants of each class can move alongside each other as if they are using separate sections of the road. The interaction between classes is included in the model via the speed function, which will be elaborated on in section 7.5.

In the numerical implementation, both time and traffic units are discretized in finite steps, while space remains a continuum. Although more classes are possible, we continue with two only, being cars ($u = c$) and bicyclists ($u = b$). The traffic units within these classes are grouped into platoons of a certain size. More details are provided in the following section.

7.4   Numerical implementation

The Lagrangian continuity equation (7.9) is a hyperbolic equation which can be solved numerically using the Godunov scheme. We use an explicit time-stepping scheme to solve

the continuity equation, following the works of Leclercq (2007); van Wageningen-Kessels et al. (2011). This results in the following discretized equation:

$$s_{u_i}^{t+1} = s_{u_i}^t + \frac{\Delta t}{\Delta n}(v_{u_i-1}^t - v_{u_i}^t). \tag{7.10}$$

This equation states that the spacing s in platoon i of class u in the following time step $(t+1)$ can be retrieved by taking the spacing at time t and add it to the difference in speed (v) of subsequent platoons (i and $i-1$), corrected with the time step Δt divided by the number of traffic units in a platoon Δn. To ensure stability and convergence of (7.10), the CFL condition should be met, which limits the distance a platoon can travel downstream within one timestep (van Wageningen-Kessels, 2013). This condition is given by:

$$\frac{\Delta t}{\Delta n}\max|\frac{dv}{ds}| \leq 1. \tag{7.11}$$

The length of platoon i stretches between positions x_{u_i} and $x_{u_{i+1}}$ and the corresponding spacing within that platoon equals its length divided by its size:

$$s_{u_i} = \frac{x_{u_i} - x_{u_{i+1}}}{\Delta n_u}. \tag{7.12}$$

Using this discretization for spacing, we can express the discretized continuity equation (7.10) in position x_u which simplifies the simulation, resulting in Eq.7.13. The new position x of platoon i and class u is retrieved by adding up the previous position and the distance traveled within the time step Δt.

$$x_{u_i}^{t+1} = x_{u_i}^t + v_{u_i}^t \Delta t, \tag{7.13}$$

The change in position is based on the speed v, which in turn depends on the spacing of all classes in the previous time step. In our case, we use two classes, bicycles b and cars c:

$$v_u^{t+1} = V_u(s_b^t, s_c^t), \tag{7.14}$$

where V_u is the speed function specified by Eq. (7.18) and (7.19) in section 7.5.

The position and speed are given for the first car or cyclist of a platoon, which is defined here as a platoon of dn traffic participants. When the platoon size equals 1, the scheme is basically a microscopic car-following model. This equivalence has been demonstrated by Leclercq (2007) and Zhang et al. (2012). In the macroscopic approach, the platoon size exceeds 1 but it is not restricted to positive integers. Numerically, the platoon size consist of 1.43 or 15.43 traffic participants. However, using decimals would come at the cost of an intuitive physical interpretation of the modeling results. An example of the numbering of platoons, positions and spacings are visualized in Figure 7.1a. An additional position is added (x_{u_n}) to mark the end of the last platoon and to ensure that a spacing can be calculated for the area following the last platoon.

A choice is made on how the positions of the N platoons influence the spacing, which influences the speed. Since the speed of a car or cyclist in a platoon is influenced mostly by what happens in front of the platoon, we argue that the downstream spacing is mostly of

influence to the speed and to a lesser extent the spacing within the platoon. This way we ensure anisotropy in the numerical scheme. We use the downstream spacing for calculating the speed and the speed equation (7.14) is further specified to:

$$v_{u_i}^{t+1} = V_{u_i}(s_{b_{i-1}}^t, s_{c_{i-1}}^t).$$

(7.15)

This equation requires as input the spacing of both classes at the position of a platoon. For one of the classes, the spacing retrieved by Eq. (7.12) can directly be used. However, the spacing of the other class is unspecified yet because the values are known for different x-positions. Therefore, the spacings of the other class need to be determined which is done via linear interpolation. Giving the example of finding the car spacing at the position of a bicycle platoon, the linear interpolation is performed using the car spacing as base for the positions of the car platoons. Figure 7.1b presents a visualization of this process.

Using the spacing of the downstream area of the platoon comes with a challenge; the spacing in front of the first platoon cannot be determined using Eq. (7.12) without implementing additional boundary conditions. For this purpose, two additional x-positions are predefined which are similar for both classes: x_0 at a position very far away and x_{n+1} at $x = 0$, see Figure 7.1a. The first boundary condition ensures that the first platoon always experiences an empty road, while the second condition ensures an empty road after passing of the last platoon.

(a)   (b)
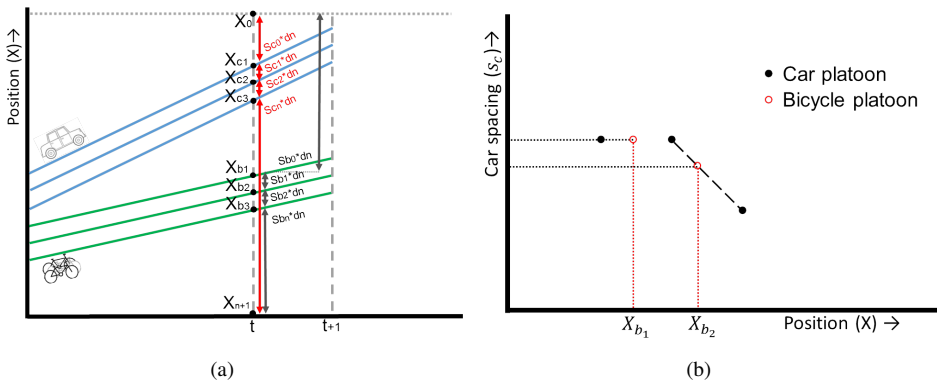
Figure 7.1: *Sketch showing the numbering of the position x and spacing s for two platoons of cars and cyclists (a) and the linear interpolation to retrieve the car spacing at the positions of the bicycle platoons (b).*

7.5 Class-specific speed functions

A main contribution of this work is that the model can handle class-specific speed functions which depend on densities of both classes. In a first-order macroscopic model, the speed function is typically provided by a fundamental diagram, describing the equilibrium relation between the aggregated variables spacing, speed and flow. The speed is typically given

by the function V that depends on density and in our case on spacing. In our multi-class situation, the class-dependent fundamental diagram is based on the spacing distribution of both cars and cyclists. Previous work in literature have tackled this multi-dependency by introducing a pce value for each class and calculating the speed based on the number of pce present, $v = V(s_{\text{pce}})$.

This study takes an alternative approach using two-dimensional speed functions. The main thought underlying this idea is that at a given generalized density, the speed of cars is fixed, while the speed of cyclists can vary depending on the traffic state, e.g. due to their ability to maneuver along a queue of cars. This feature of mixed traffic cannot be captured accurately by a model based on pce value, since this assumes the reference class to always be the fastest moving class. To model the characteristics of both classes correctly, this study introduces class-specific two-dimensional speed functions, which describes the speed of a class, based on the spacing of both cars and cyclists separately, so $v = V(s_c, s_b)$.

The framework presented here can handle various shapes of the fundamental diagram $V(s_c, s_b)$. The starting point for our two-dimensional speed functions is the triangular fundamental diagram in flow-density for single class traffic flow (Daganzo, 1994). In the speed-spacing format, this function is given by:

$$V_u(s_u) = \begin{cases} 0 & \text{if} & s_u = s_{u,\text{j}} & [1] \\ (s_c - s_{c,\text{j}})w_u & \text{if} & s_{u,\text{j}} < s_u \leq s_{u,\text{cr}} & [2] \\ v_{u,\text{f}} & \text{if} & s_u > s_{u,\text{cr}} & [3] \end{cases} \qquad (7.16)$$

with w the wave speed of traffic state characteristics, given by:

$$w_u = \frac{v_{u,\text{f}}}{s_{u,\text{cr}} - s_{u,\text{j}}}. \qquad (7.17)$$

Eq. (7.16) states that the traffic entities of class u are at stand still ($v = 0$) when the jam spacing ($s_{u,\text{jam}}$) is reached, their speed gradually increases with spacing until the desired speed ($v_{u,\text{f}}$) is reached at the critical spacing ($s_{u,\text{cr}}$), and continue to travel at the desired speed for larger spacings. The characteristic values for jam spacing, critical spacing and free flow speed used in this study are presented in Table 7.1. Figure 7.2 presents the resulting single-class speed-spacing diagram of cars and bicycles when no other class is present. To connect the two classes, additional cased are added to (7.16) while trying to maintain a linear expression where possible. This has resulted in the class-specific speed functions for bicycles (7.18) and cars (7.19).

For the speed of bicycles, a condition is introduced to reduce the speed to $v_{b,\text{red}}$ when cyclists are passing a queue of cars (7.18.4). Condition (7.18.5) is included to ensure that the cycling speed does not exceed the reduced speed when cars are slowed down in congestion but not standing still. Equation (7.18.6) is added to ensure a smooth transition at the boundaries between the reduced speed and the speed reduction caused by decreasing bicycle spacing (7.18.2). For cars, two additional rules are introduced. First, cars cannot overtake when there are too many cyclists on the road, and they have to adapt their speed to match the cyclist' speed (7.19.2). Second, when cyclists are sparsely present, i.e. $s_b > a$, sufficient space for cars is available to move in between and overtake at a reduced speed
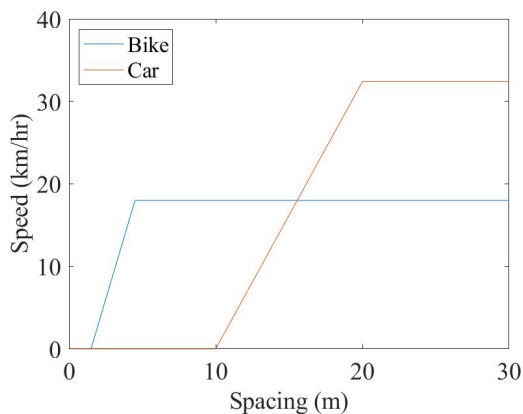
Figure 7.2: Single class speed functions for cars and bicyclists.
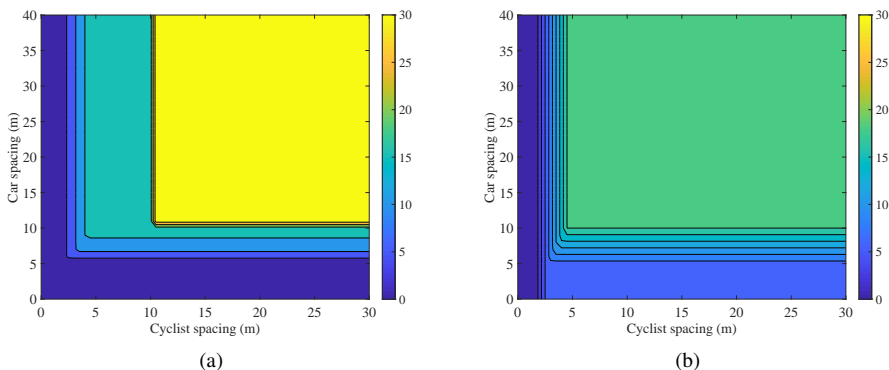
Figure 7.3: Two-dimensional speed functions for cars (a) and bicyclists (b).

(7.19.4). We assume this sufficient spacing to be 10m ($a = 10$m). The parameter w_{bc} is the tangent of the connecting line between the reduced and free flow speed of bicycles, given by Eq. (7.20). A contour plot of the two-dimensional speed functions are shown in Figure 7.3.

The class-specific speed functions presented here are non-decreasing with spacing ($\frac{\partial v}{\partial s} \geq 0$), which according to van Wageningen-Kessels (2013) should ensure the model to be weakly hyperbolic and therefore able to show anisotropic behavior. Further investigation of the hyperbolicity of the model is not performed.

$$V_b(s_b, s_c) = \begin{cases} 0 & \text{if} & s_b = s_{b,j}, & s_c > s_{c,j} & [1] \\ (s_b - s_{b,j})w_b & \text{if} & s_{b,j} < s_b \leq s_{b,cr}, & s_c > s_{c,j} & [2] \\ v_{b,f} & \text{if} & s_b > s_{b,cr}, & s_c > s_{c,j} & [3] \\ v_{b,red} & \text{if} & s_b > s_{b,cr}, & s_c = s_{c,j} & [4] \\ \min(v_{b,red}, (s_b - s_{b,j})w_b) & \text{if} & s_{b,j} < s_b \leq s_{b,cr}, & s_c \leq s_{c,j} & [5] \\ \min\Big((s_b - s_{b,j})w_b, & & & & \\ \quad v_{b,red} + w_{bc}(s_c - s_{c,cr})\Big) & \text{if} & s_{b,j} < s_b \leq s_{b,cr}, & s_{c,j} < s_c \leq s_{c,cr} & [6] \end{cases}$$
$$(7.18)$$

$$V_c(s_b, s_c) = \begin{cases} 0 & \text{if} & s_c = s_{c,j} & s_b > s_{b,j} & [1] \\ \min(V_b, (s_c - s_{c,j})w_c) & \text{if} & s_{c,j} < s_c \leq s_{c,cr} & s_b > s_{b,j} & [2] \\ v_{c,f} & \text{if} & s_c > s_{c,cr} & s_b > a & [3] \\ \min(v_{c,f}, V_b) & \text{if} & s_c > s_{c,cr} & s_b \leq a & [4] \end{cases}$$
$$(7.19)$$

$$w_{bc} = \frac{v_{b,f} - v_{b,red}}{s_{c,cr} - s_{c,j}} \tag{7.20}$$

7.6 Case study

To illustrate the working of the model, we consider several situations which occur on unidirectional urban streets with mixed bicycle–car traffic. A specific example is a so called 'cycling street' which is gaining popularity in The Netherlands. The traffic behavior has specific characteristics resulting from the property that bicyclists are prioritized over car drivers. No uniform design of a cycling street exists but it is typically wide enough for cars to overtake cyclists. However, cars are considered as guests on the road and have to slow down when cyclists are present. Furthermore, cars cannot overtake when the cyclist density exceeds a certain threshold and as a result, the cars have to match the cyclists' speed. When cars are moving slowly in a queue there is enough space for cyclists to carefully pass the queue and create their own queue closer to an intersection. The speed limit on this cycling street is 30 km/hr.

In the following three cases we follow several platoons of five traffic units in space and time ($\Delta n = 5$) and the simulations are performed with time steps of two seconds ($\Delta t = 2$ s). The speed is given by equations 7.18 and 7.19 and the characteristic values in the speed functions are presented in table 7.1.

Table 7.1: *Characteristic values used in the speed functions: jam spacing s_j, critical spacing (s_{cr}), free flow speed (v_f) and reduced speed (v_{red}).*

	s_j[m]	s_{cr}[m]	v_f[m/s]	v_{red}[m/s]
cyclists	1.5	4.5	5.0	2.0
cars	5.0	10	9.0	-

7.6.1   Little to no interaction

We consider a situation with low demand for the purpose of face-validation. All traffic participants can move at their maximum allowed speed and the spacing is large. As a result, the two classes have sufficient space to maneuver freely and are unhindered by each others presence. This is the case when we set the initial spacing of both classes to 20 m, which results in a total platoon length of 100 m.

Two cases can occur depending on the starting positions, displayed in Figure 7.4; either the cars have a head start over the bicycles (a) or the other way around (b). In both cases there are two platoons of cars and three platoons of cyclists. In the primary case, the cars are given a head start of 350 m. As a result, no interaction between the two classes takes place since the desired speed of cars is higher than that of cyclists causing a rapid divergence of the two classes. Interaction does occur in the second case where the starting positions are switched and the cyclists have a 350 m head start over the cars. Since cars have a higher desired speed, the first platoon of cars catches up with the final platoon of cyclists. Figure 7.4b shows that this happens after approximately 40 s in the simulation. The spacing of the cyclists however is sufficiently large and cars can overtake without having to reduce their speed. Note that the speed limit on the bicycle road is 30 km/hr, which is considered a safe speed to overtake and no further speed reduction is required. In our simulation it takes about 170 s before all cars have passed the cyclists and the two classes start to diverge.

7.6.2   Interaction and adjustment by cars

Interaction takes place when more cyclists are occupying the road and their space headway is decreased. For visualization purposes, we only consider two car and three bicycle platoons but the model will work for any number of platoons. The initial spacing for cars remains 20m, while the bicycle spacing is decreased, resulting in a more compact platoon length.

Different interactions take place depending on the exact initial spacing. This is best visualized when the initial bicycle spacing is set close to the threshold for interaction, which is $a = 10$ m according to Eq. 7.19. The initial spacing is set to 10.2 m in Figure 7.5a and 10 m in Figure 7.5b. As a result, the cars overtake the bicycles with reduced speed in the first case and have to match the cycling speed in the latter case. The speed reduction is visualized by the magenta colored cells which intensifies when the reduction increases. In both cases, the cyclists start with a 350 m head start over the cars, and they can move unhindered and at their desired speed throughout the simulation.

The magenta coloring in Figure 7.5a and b illustrates that the speed adaptation sets in before the complete platoon has reached the cyclists. Also, in Figure 7.5a can be seen that the speed increases already before all cyclists are overtaken. This results from our choice in the numerical implementation to determine the speed based on the spacing in front (Eq. 7.15), which can be interpreted as anticipation behavior. As a result, the car spacing after overtaking the cyclists is larger than before the cars reached the cyclists.

7.6.3   Queuing situations

Both cyclists and cars have to adjust their speed in congested situations where the spacing reduces to values below the critical density. This is included in the simulation by introducing a temporary obstruction; the first platoon is enforced to stop in the first time step causing queue formation behind it. Again, two cases can occur based on the starting positions of the two classes. When the cyclists have a head start over the cars, the first platoon of cyclists is stopped creating a growing queue of first cyclists and then cars, see Figure 7.6a. The speed reduction of the cars and cyclists is visualized by the colors magenta en cyan respectively; no color is shown when speed coincides with the desired speed. In total, three car and four platoons are followed in time and space. The first cyclists have a 450 m head start over the first cars. After some time in the simulation, the first cars catch up with the last cyclists and the cars have to reduce speed until they come to a complete stop. The bottleneck is removed after 200 s after which the cyclists restart moving and the queue is gradually cleared. The cyclists quickly move at their desired speed again, but the spacing is too small for the cars to overtake.

A different situation occurs when the starting positions are switched around and the first car platoon is stopped instead. The cyclists can pass the queue of cars but have to do so at a reduced speed. The cars have a head start of 300 m over the cyclists and it takes some time for the first cyclists to catch up with the last cars. When looking closely at the coloring, the cyclists are reducing speed well before they reach the actual position of the queue, and they are increasing in speed before the queue is actually passed. This results from the assumption that the speed is influenced most by the spacing in front of the traffic participants instead of the spacing at their current position. When the cars start moving again after the obstruction is removed, the cars can first move at their maximum allowed speed until they catch up with the cyclists and reduce their speed to gradually overtake them.

(a)   (b)
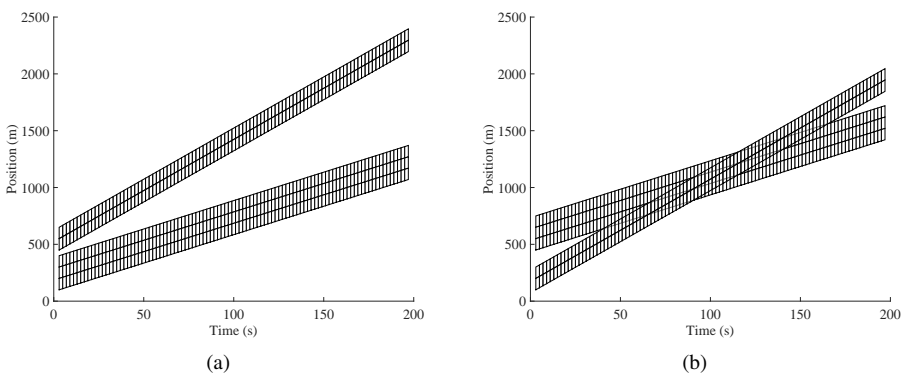
Figure 7.4: Simulation results for low demand situation ($s_b(t_0) = s_c(t_0) = 20m$), showing no speed adjustments when cars have a head start over cyclists (a) and cyclists have a head start over cars (b).
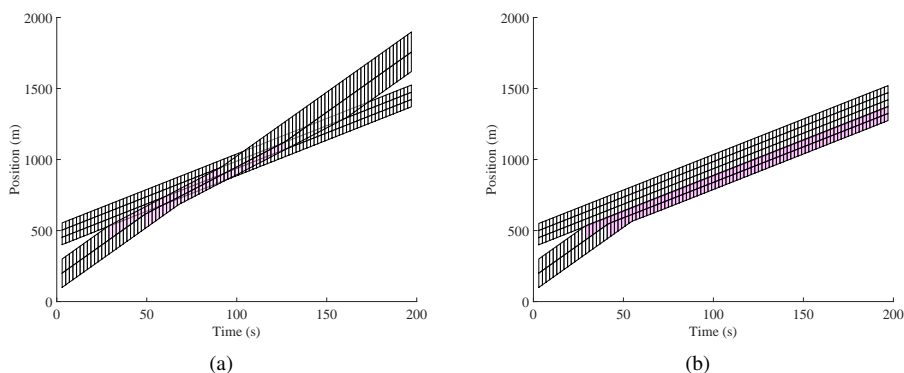
Figure 7.5: Simulation results for different demand situations. When initial spacings are $s_b(t_0) = 10.2m$ and $s_c(t_0) = 20m$, cars can still overtake cyclists but at a reduced speed (a) and when initial spacings are $s_b(t_0) = 10m$ and $s_c(t_0) = 20m$ cars have to match the speed of cyclists (b). The magenta coloring appears when the speed is reduced and is more intense for lower speeds.
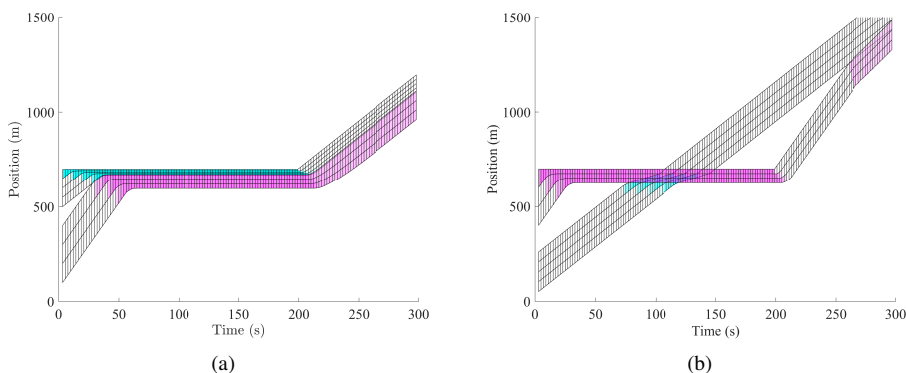
Figure 7.6: Simulation results for queuing situations. In (a) $s_b(t_0) = 10.2m$ and $s_c(t_0) = 20m$ and the cyclist have a head start of 450m. In (b) $s_b(t_0) = 10.4m$ and $s_c(t_0) = 20m$ and the cars have a head start of 300m. The cyan and magenta coloring appear when the speed is reduced for respectively cyclists and cars.

7.6.4   Discussion

The face-validation of the three cases show that the model can accurately handle various conditions that occur in mixed traffic situations where bicycles and cars share the same infrastructure. The main feature is that both classes can be the fastest moving one, depending on the traffic state. Furthermore, the model includes anisotropy by considering only the spacing of all classes in front of the current position to adjust the speed. This modeling approach leads to plausible results including anticipation; traffic participants slow down be-

fore reaching a queue and accelerate when a queue is about to dissolve.

When comparing our modeling outcome to available research on mixed bicycle-car traffic, we have two observations. Our model includes a two-way interaction between cars and cyclists; the speed of cars is influenced by the presence of bicycles and vice versa. This property is an improvement compared to the individual-following model by Tang et al. (2010), which includes one-way interaction only. However, the bicycle-car interaction in our model is based on space headway only and does not take the lateral spacing into account, which is the case in the cellular automata model by Luo et al. (2015). To include the interaction due to lateral distance, future development of our model could include a fundamental diagram based on an area density.

The presented model is tested solely to qualitative criteria and has not yet been validated with observational data. The model is tested for the Dutch 'cycling street' scene but could also be applied in other mixed traffic situation, e.g. where lane discipline is lacking. However, this would require an adjustment to the speed functions. The development of a more general description of the speed function will be beneficial for the applicability of the presented macroscopic flow model.

7.7 Conclusion

A first-order multi-class macroscopic flow model is presented to describe mixed bicycle-car traffic. The model uses class-specific speed functions, enabling each class to be the fastest moving one depending on density. This trait facilitates the modeling of e.g. congested situations where cyclists can maneuver along a queue of cars. The presented model is specifically relevant for shared street situations, which typically occur in urban environments. Three test cases show the ability of the model to handle various traffic flow conditions that occur in mixed traffic situations where bicycles and cars share the infrastructure. The model shows anisotropic behavior by considering the spacing of all classes in front to adjust the speed. This modeling approach leads to plausible results including anticipation; traffic participants slow down before reaching a queue and start accelerating when a queue is about to dissolve.

The working of the model has been successfully tested based on qualitative criteria, showing the expected behavior of mixed bicycle-car traffic. The next step would be to perform a validation of the model to quantitatively test it against observational data. This data however, is not yet available. Furthermore, the mathematical properties of the model could be further investigated, e.g. hyperbolicity. In this study, mixed traffic consisting of bicycles and cars are considered but the model is equally applicable to other configurations of mixed traffic. However, this would require adjustments to the speed functions. Possible applications of the model are estimation of e.g. class-specific travel time and road capacity in a mixed traffic situations, which is all relevant input data to network-wide traffic models and route choice models.

Chapter 8

Conclusions and future research

This final chapter concludes the dissertation by presenting the answers to the research questions (section 8.1) and reflecting on the main objective (section 8.2). Then, several implications of the findings for practice are addressed (section 8.3) and new ideas for future research are proposed by stating matters that are still open to question (section 8.4).

8.1 Answers to research questions

The main objective of this study was to unravel the macroscopic quantities of uni-directional bicycle traffic such that bicycle flow could be integrated in a macroscopic flow model. To this end, six research questions were drawn up which treated three different aspects of bicycle traffic: i.e., motion properties on single paths, flow characteristics at controlled intersections, and modeling bicycle traffic. The answers to the associated questions are given below.

Research question 1: How to design a cycling experiment that can capture the key flow characteristics of bicycle traffic? (Chapter 2)

The motivation for this question was the need for empirical data on bicycle flow dynamics. A large-scale cycling experiment could fulfill this need if thoroughly organized and implemented. It was established that the experiment needed to be designed in such a way that a wide range of cycling behavior could be observed, both on the individual and aggregated level. Further considerations were made regarding location, track design, number of participants, bicycle type and more. In the final design, a track was created that could mimic different infrastructural settings, i.e. crossing, merging, narrowing, bi-directional situation. An indoor location was selected to minimize weather influences and to enable a top-down observation with cameras. This angle was optimal for two reasons: first, it resulted in a high quality of trajectory data, and second, the privacy of participants was easily guaranteed since faces were not recorded. During the execution of the large-scale experiment, some

imperfections were encountered in the design. Two conclusions on how not to design an experiment were: one, the lighting conditions of an indoor location can compromise the quality of the images. In our case, the resolution decreased in such a way that individual markings could not be recognized. Two, aiming for participants with a specific bike type can result in shortage. In our case, we were unable to recruit cyclists with cargo bikes. Despite these setbacks, the experiment resulted in an abundant data set of cycling movements, which was used in further study.

Research question 2: How do density, speed and flow relate to each other for uni-direc-tional bicycle flow, and how are these affected by path width and anticipation behavior? (Chapter 3)

The cycling characteristics were studied based on the trajectory data that was gathered with the large-scale experiment. It was found that an increase in density coincided with a lower average speed and a higher flow. In other words, cyclists went slower when they cycled closer together, but at the same time more cyclists moved along the path per unit of time. Moreover, the flow continued to increase in congested conditions, which indicated that cyclists can maintain moving even when cycling close to others. The movements ceased when speed dropped below 5 km/h, indicating that this is the minimum cycling speed. A change from free-flow to congested conditions was observed around 0.15 cyclists/m^2.

When looking at the quantities separately, it was found that narrowing the path decreased the speed and flow, while it increased the density. This result is in line with the intuitive reasoning that fewer cyclists fit on a smaller path and that a narrow opening restricts the personal space and requires more caution to pass. Less intuitive is that the connection between the path width and the macroscopic quantities was not linear and thus depends on other factors as well. In this research, path usage was identified as an influencing factor.

The path width was found to affect the possible configurations that cyclists could move in, which consequently influenced the density and cycling speed. Depending on the width, cyclists displayed overtaking, staggered, and strictly-following movements. Overtaking was observed on 2-meter and 1.25-meter paths, and facilitated most that cyclists moved at their desired speed. In staggered formation, cyclists kept distance both in lateral and longitudinal direction. Here, cyclists already had to adapt their speed to maintain the formation. Paths of one meter and smaller only facilitated following behavior, meaning that cyclists moved along the same lane.

Anticipation to downstream traffic conditions was observed in two ways: Either cyclists reduced speed when they saw congestion ahead, or they sped up to fill gaps that appeared by the slowing down of other cyclists. Furthermore, some cyclists temporarily accepted cycling close together when more space was available downstream. As a result, more connections of low density and low speed, and high density and high speed were observed. Consequently, the density–speed relation showed a more gradual speed decline with increasing density and the clear boundary between free-flow and congested conditions disappeared.

Research question 3: How does path width influence the maximum flow on a uni–directional bike path? (Chapter 4)

The maximum sustained flow, also called capacity, is the highest number of cyclists per unit of time that can be maintained on a certain bicycle facility. Knowing this figure is important in designing urban infrastructure that can cope with growing bicycle demand. We determined the capacity of different path widths by changing the size of a narrowing during a bottleneck experiment. The path width was varied in steps of 25 centimeter between 0.5 and 1.5 meter.

It was found in chapter 4 that the maximum flow showed a positive and linear increase with path width. This means that widening the path resulted in a higher capacity and that this growth occurred at a constant rate. In other words, a 50-centimeter path accommodated around 3700 cyclists per hour, and every additional 25 centimeter increased the capacity with 1000 cyclists per hour. Furthermore, the maximum flow was found to be influenced by the traffic state. The highest values were obtained just before the onset of congestion, and showed a drop afterwards. This phenomenon, known as the capacity drop in motorized traffic, had not been observed in bicycle flow before, and indicated that the underlying behavior was similar for drivers and cyclists, regardless of relaxing the restriction to keep lanes. The magnitude of the drop was about 1300 cyclists per hour, meaning that the maximum flow on a one-meter path dropped from 5700 to 4400 cyclists per hour after the onset of congestion. Also in the congested situation, the path width showed a positive and linear relation to the flow. The drop in observed maximum flow is most likely connected to the reaction time during the process of accelerating. After the onset of congestion, cyclists brake and re-accelerate. Due to reaction time, the moment of speeding up is delayed, resulting in a larger headway and thus lower capacity.

Research question 4: What is the influence of jam density and merging cyclists on the queue discharge rate at a controlled intersection? (Chapter 5)

With this question, the focus shifted from bicycle flow operations at bike paths to those at intersections. The dynamics of bicycle congestion was studied by analyzing the queue discharge process at a controlled intersection. More specifically, the proximity of cyclists in the queuing phase (jam density) was connected to the cycling movements while leaving the queue. This involved the rate at which cyclists entered the intersection (discharge rate) and how many cyclists crawled forward by merging into the cyclists' stream before the queue was cleared (merging cyclists). Results showed that higher discharge rates were obtained when cyclists stood closer to each other while waiting in the queue. In other words, a positive relation was obtained between jam density and queue discharge rate. Furthermore, cyclists who crawled forward during the discharge phase where found to affect the discharge rate differently depending on the merging angle. On the one hand, cyclists that overtook the queue from behind had a positive influence since they filled up available spots without hindering others. On the other hand, people that merged from the side held up cyclists in the original queue and thereby negatively influenced the overall discharge process.

Research question 5: Can the jam density of bicycle queues be influenced by managing the queue build-up and if so, does the relation between jam density and discharge rate hold for higher jam density values? (Chapter 6)

A controlled experiment was conducted to test whether guiding cyclists in positioning themselves in a queue would result in higher jam density and a more rapid discharge process. Cyclists were asked to queue up according to multiple predetermined grids and by merely instructing them to queue up closely together. It was found that the jam density indeed increased when cyclists were provided with queuing instructions. The vocal-only instruction to queue up closely and the vocal-plus-visual command to create a three-two-three pattern, led to the highest jam density. Furthermore, it was found that the higher jam density coincided with a higher queue discharge rate. Moreover, the positive relation between jam density and discharge rate was confirmed to exist also for the higher density range. This implies that the efficiency of the queue discharge process at an intersection can be improved, and the intersection throughput increased, by instructing cyclists to queue up in close proximity to others. By close, one must think of roughly 0.80 meters in lateral direction and a bit over one meter in longitudinal direction, resulting in a personal waiting area of approximately 0.90 m^2.

Research question 6: How can we describe and model bicycle flow in a mixed traffic situation? (Chapter 7)

With this question, the research focus changed from understanding bicycle flow dynamics to incorporating cycling behavior in a traffic flow model. More specifically, we aimed to describe the mixed bicycle-car traffic on a uni-directional bicycle street. Such streets usually have a high volume of bicyclists and are therefore suitable for a macroscopic approach. The starting point for the modeling exercise was a first order macroscopic flow model for car traffic, which was extended to also include bicycle flow. This model assumed an equilibrium relation between density, speed and flow, and therefore did not include reaction time or anticipation behavior. However, a form of anticipation behavior was included in the model by allocating speed based on the density of cyclists and cars further downstream. As a result, traffic participants slowed down when approaching a queue and sped up when exiting a congested area. The modeling approach was found effective in describing mixed bicycle–car traffic and showed the ability of cyclist to move faster than cars in congestion. This result was obtained by prescribing separate density–speed functions for cars and cyclists in the model.

8.2   Conclusions

In this section, the insights of the individual chapters are connected, thereby focusing on the macroscopic cycling characteristics and the underlying behavior of cyclists.

Highest bicycle flow is reached in congested conditions
The flow variables were found to vary widely, both in motion and at standstill. While moving along a one-way path, cyclists were observed to move at their desired speed as long as

there was enough available space to overtake others. When overtaking was no longer possible, the bicycle stream became congested, resulting in a lower average speed and higher density. Initially, the speed decrease resulted from a more synchronized flow, meaning that faster cyclists had to adapt their speed to the slower ones, while the slower cyclists still moved at their desired speed. The combination of high density and low speed, led to a higher flow than at the transition between free and congested flow, indicating that capacity was reached in congested conditions. At the same time, a capacity drop was observed after the onset of congestion. Combining these findings shows that, most likely, the highest flow is obtained as long as the synchronized flow is stable, and drops as soon as the first cyclist brakes in response to a local density change.

Cycling speed depends on local and downstream space availability
The average cycling speed was found to decrease in response to a reduction in maneuvering space. This available space was influenced by the proximity of other cyclists (higher density) and by the infrastructural setting, meaning that a more narrow path led to a slower cycling pace. Remarkably, the minimum average speed was observed within a narrow bottleneck and not in the highest density conditions. On the contrary, cyclists were still capable of moving while cycling close to others. Most likely, this was connected to the visual confirmation that cyclists further downstream were moving as well. Vice versa, cyclists were observed to slow down in low density conditions when congestion was present downstream. In doing so, the flow at medium density was reduced but at the same time, the flow was increased at higher density because cyclists were able to keep moving, thereby preventing a complete standstill. This anticipation behavior affects the flow in such a way that incorporating it in a model is vital to reproduce realistic bicycle flow. A possible way to do so is by assigning the cycling speed based on both local and downstream conditions of density.

Cyclists organize themselves in patterns
Cyclists were found to move in different configurations, meaning that they formed a certain pattern while optimizing the available space. The patterns were connected to the overlap in effective sublanes. More specifically, cyclists were observed to hold a larger longitudinal distance when the lateral distance was smaller and vice versa. When visualizing the change in cycling configuration from a two-meter-wide path to smaller, the consecutive formations showed close resemblance to that in a merging process. Configuration was also found important at a standstill, although cyclists did not appear to intrinsically optimize the available space. Rather, they created a queue with a chaotic build-up while waiting at an intersection. Some people kept a large person-to-person distance, were others chose to keep a minimum space, resulting in a wide variation in average jam density. This queue compactness was found to affect the discharge process, with a higher jam density resulting in a higher discharge rate. As a result, the capacity of an intersection was found to increase if cyclists were to stand close to each other. During the queue discharge, cyclists show similar patterns again such as maintaining an equal distance to each other in time and space. This is best illustrated by front and rear wheels moving at similar height.

Anticipation behavior of cyclists affects the relation between density, speed and flow
The relation between the macroscopic quantities was found to be affected by anticipation to downstream conditions. In the absence of upcoming obstacles, such as congestion, cyclists

reacted predominantly to their direct surrounding. In the density–flow relation, this means that flow increased with density and that a clear transition occurred between free-flow and congested conditions. In the density–speed relation, a constant average speed was observed in free flow and a speed decrease in congested conditions. Unlike the density–flow relation in following bicycle traffic, the transition point was not linked to a capacity point, but rather marked a change in relation strength. For higher density, the flow in bicycle traffic did not drop as it does for cyclists in following motion, but it remained high when density further increased. This research did not identify at which density level the flow breaks down, resulting in a standstill. The wide variation in observed jam density suggests that this breakdown point can vary depending on the preferred personal space of cyclists.

Using class-specific speed functions to model mixed bicycle–car traffic
Typical cycling behavior was captured in a macroscopic model for mixed bicycle–car traffic by implementing a density–speed relation for cars and bicyclists separately. Furthermore, the downstream spacing of both traffic modes was taken into account, leading to a representation of mixed traffic flow that also included anticipation. However, the proposed speed functions were based on single-file bicycle movement and should be updated based on the insights regarding multi-channel bicycle flow presented in this dissertation.

8.3   Implications for practice

The new insights into bicycle traffic flow can be applied in a practical manner. The implications are categorized into the design of infrastructure and the modeling of bicycle traffic.

8.3.1   Infrastructure design

Findings regarding capacity values and knowledge on anticipation behavior, can be applied in practice, in particular for the design of new, or adaptation of existing, bicycle facilities. The findings and their applications are addressed below.

Capacity of bike paths
Knowing the maximum flow possible on bike paths is crucial for the design of infrastructure that is suitable to accommodate many cyclists. This dissertation has determined capacity values for separated bike lanes of 0.75, 1.00, 1.25, 1.50 and 2.00 meters wide. However, these values are not directly applicable in design manuals because they represent the peak flow that a path can handle, and is not comfortable to cycle in. It therefore differs greatly from the numbers mentioned in the Dutch design manual for bicycle traffic (CROW, 2017a), which are based on average demand during peak hour and take into account cycling comfort. This guide advises a path width of 2.00m for a peak flow below 150 cyclists per hour, and a 4.00m-wide path in case of a peak demand exceeding 750 cyclists per hour. Our obtained maximum values vary between 3500 (0.75m) and 8000 (2.00m) cyclists per hour. Despite the large differences, the obtained capacity values can be used, for instance, to establish whether a bicycle path is able to cope with a peak demand downstream of a busy intersection. Also, implementing the capacity values in traffic demand models may help to identify crowded locations or bottlenecks on the network level.

Capacity of intersections

During peak hours, the bicycle demand often exceeds capacity, resulting in congestion and delays. This dissertation has shown that managing the queue build-up can lead to a more efficient throughput at intersections by increasing the jam density. Two ways of managing the queue build-up were found most effective. The first is by vocally asking cyclists to queue up closely together, and the second is by asking cyclists to line up according to 3-2-3 pattern which was visualized on the two-meter wide pavement. However, these findings do not include cyclists moving in groups or pairs who want to stay together, which may influence the jam density in practice. On the one hand, acquaintances might be more willing to queue up closely, while on the other hand, it can lead to open spots in the predefined grid. This latter situation does not have to harm the discharge efficiency when the gaps are filled by cyclists merging from behind. It was found that cyclists merging from the side had a disturbing effect on the queue discharge process, while cyclists joining in from the back were found to increase the discharge flow. This means that facilitating a merging angle that is more aligned with the main stream can enhance the queue outflow. Although the methods need to be further tested in practice, managing the queuing process offers great potential to optimize bicycle flow at intersections in the future.

Anticipation behavior

Cyclists were found to adapt their speed based on both local and downstream conditions. By anticipating upon downstream conditions, cyclists affect the flow both positively and negatively. In this process, visual information during cycling is key. Although a clear field of vision was already important for safety, it now appears that it can contribute to a smooth traffic flow. Therefore, a bike path needs to be designed in such a way that for instance, obstacles, curves and other cyclists are clearly visible.

COVID-19

At the time of writing this conclusion, the world is heavily impacted by a worldwide pandemic. Although vaccines against the disease are starting to get available, the time-line of returning back to normal is yet unclear. Until that time, some of the findings in this dissertation should be addressed with care since they involve decreasing the inter-personal distance and with it, increase the risk of virus spreading. Findings regarding increasing the jam density, optimizing the cycling configuration, and the relation between density, speed and flow density for higher density values should therefore only be applied in practice when the situation allows for it. At the same time, the findings in this thesis can be used to adjust the cycling infrastructure in such a way that it matches the prevailing insights regarding a safe personal distance. For instance, by increasing path width to facilitate safe cycling conditions, or by marking configurations on the pavement that visualizes this safe distance both at standstill and in motion, assuming a certain cycling speed. For similar demand and infrastructure situation as before COVID-19, the increased inter-personal distance will negatively affect the maximum flow at bike paths and intersections. Therefore, cyclists are expected to experience more delay during their trip. To prevent long queues, the green-signal time could be lengthened according to the lower capacity, in such a way that the same throughput can be reached as in normal conditions. However, this will negatively affect the capacity for other traffic modes.

8.3.2   Model development

A number of findings can be applied as a starting point for model development. Three of them are listed below.

Density–speed and density–flow relations
This dissertation has addressed the relation between density, speed and flow on uni-directional bike paths. It showed that the density–speed and density–flow relations have different shapes when cyclists are free to overtake than when only following movement is allowed. Especially when the bicycle stream becomes congested, the differences in cycling speed reduce while a high flow can be maintained. An exact function has not been presented, but the insights gained on this topic are vital to implemented in future bicycle models in order to represent bicycle flow in a realistic manner.

Cyclists configuration
In crowded situations, cyclists were found to move in different configurations, thereby making effective use of the available space. Logically, the highest flow is reached with the most effective pattern. However, this is not necessarily connected to a unique path width. For example, it was found that a path width of 1.00m and 1.25m accommodated the same formation, leading to an equal flow. This implies that simply widening the path does not always help the overall bicycle flow. Rather, it would be wise to choose a path width based on the optimal configuration that fits with the demand on that location. It could even indicate that creating two smaller paths might be more effective than having one wider path. By including the configuration in a bicycle model, the optimal path width can be determined.

Modeling mixed traffic
The speed functions for mixed car and bicycle traffic were found effective to describe mixed bicycle–car traffic. Similar concepts can be used to describe other forms of mixed traffic as well, such as bicycle–pedestrian, pedestrian–car, or even extending to traffic situations with three or more modes.

8.4   Future research directions

This research has made an important step in the comprehension of bicycle traffic flow and the modeling thereof. However, the understanding is far from complete and many questions remain. This section selects a number of issues that are yet unaddressed and are worth investigating in future research. Furthermore, the work underlying this dissertation offers opportunities for other research directions.

Further exploring the obtained bicycle trajectory data set
First of all, the data set that was gathered during the large-scale cycling experiment was only partially used in this research, and permits to study other aspects of bicycle flow as well. The recordings captured cycling movements at two crossings, a merging, a diversion and a stretch with bi-directional movement, all of which would be interesting to analyze both on the microscopic and macroscopic level. On the one hand, the trajectories can be used as starting point for developing new theory, and on the other hand, the data can be used to

verify the accuracy of newly developed modeling results. The trajectory data set is expected to become available in the future. Until that time, please contact the Active Mode Lab at Delft University of Technology.

Transformation from movement to standstill
Regarding the macroscopic characteristics of bicycle flow, the transition from movement to a standstill is not addressed in this thesis. It is yet unclear at which density a multi-channel bicycle stream becomes unstable, resulting in stop-and-go waves. Furthermore, it would be interesting to investigate whether the density at standstill varies as much as it does for jam density at intersections, and what role anticipation has in this process.

Impact of anticipation to the density–speed relation
This thesis showed that cyclists reacting to downstream conditions leads to an early slowing down while cyclists approach a high density area. This behavior leads to the dispersion of cyclists, resulting in lower density. As a result, traffic breakdown in the form of stop-and-go waves might occur less frequently in the situation where cyclists have sight on downstream conditions than when they do not have this visual information. However, it is an open question whether this is indeed the case and if so, how far ahead cyclists look and adapt their cycling speed accordingly. Also the role of (anticipation to) height differences is worth exploring further to increase the research relevance to places with a more distinct vertical topography than the Netherlands. Understanding the relation between density and speed, and the impact of anticipation, is key to further develop bicycle flow models that can represent all facets of aggregated bicycle movements.

Flow characteristics at (uncontrolled) intersections
Other open questions remain regarding the bicycle flow at intersections. This research has focused on analyzing the flow at controlled situations, while also uncontrolled crossings exist. The capacity at such intersections and its relation to the interaction between crossing streams, such as the gap acceptance, typical headway and differences in speed, are interesting topics to explore. This could, for instance, be investigated using the data obtained from the large-scale experiment. Regarding controlled intersections, it was found that increasing the jam density leads to a more efficient discharge process and thus a higher intersection capacity. However, it is yet unclear how cyclists are best motivated to queue up closer together in practice. Further research in collaboration with a behavioral scientist could be an interesting next step.

Effect queuing area and bicycle type to discharge process
Furthermore, it would be worthwhile to investigate the jam density and discharge rates for situations where the queuing areas have an irregular shape in such a way that the available space can be used most optimal. Also, it is unclear what effect increasing the jam density has on the occurrence of cyclists merging during the discharge phase. If this reduces, the efficiency of the main stream may be optimized, but the delay in the secondary stream might be increased. Furthermore, it is likely that a heterogeneous composition regarding bicycle types has impact on the jam density and capacity. Electrically driven bicycles are known to accelerate faster than a traditional bike, while a (non-electric) cargo bike or young child can act as a moving bottleneck. For the optimal calculation of green signal time at a specific

location, it would be useful to develop a modeling tool that can provide the optimal signal time based on e.g., demand, jam density, and typical composition of the bicycle flow. This adaptation could be based on static data, but potentially also on dynamic data collected via a mobile sensing system, such as AMSense (Vial et al., 2020), which uses visual sensors in connected vehicles to locate cyclists. When the share of connected vehicles increases in the future, this system might be used to, for instance, estimate the bicycle demand and composition and send this information to intelligent intersection control systems.

Modeling bicycle traffic flow
Finally, this dissertation has proposed a macroscopic model that showed typical cycling behavior on a bicycle street. However, the results were only face-validated and should be tested more thoroughly. Furthermore, other numerical schemes can be examined to test the working of the model. Our choice to take into account the downstream density for determining the speed, resulted in the early slowing down of cyclists in case of upcoming congestion and accelerating in response to seeing the queue resolve. However, this anticipation to downstream conditions could possibly be introduced more directly via the density–speed relation. Exploring ways to describe anticipation behavior in bicycle traffic would be an interesting research direction to pursue. A possible option to explore could be the higher-order macroscopic flow model developed by Payne (1971), which incorporates a reaction time to determine the speed of cars. Possibly, this reaction time is able capture also the anticipation behavior of cyclists.

Alternatively, the mode-specific speed functions that were proposed could be used in other types of modeling as well, such as network wide models. A research spin-off has already resulted in the development of a multi-modal macroscopic fundamental diagram (MFD) for urban traffic (i.e., Loder et al. (2019)). Continuing this research direction could lead to a more complete representation of urban traffic and with it, an optimal distribution of urban travelers over different traffic modes.

Bibliography

Allen, D., N. Rouphail, J. Hummer, and J. Milazzo (1998). Operational Analysis of Uninterrupted Bicycle Facilities. *Transportation Research Record 1636*(1), 29–36.

Andresen, E., M. Chraibi, A. Seyfried, and F. Huber (2014). Basic Driving Dynamics of Cyclists. In M. Behrisch (Ed.), *SUMO 2013*, Volume 1, pp. 18–32. Springer-Verlag Berlin Heidelberg.

Aw, A., A. Klar, M. Rascle, and T. Materne (2002). Derivation of Continuum Traffic Flow Models from Microscopic Follow-the-Leader Models. *SIAM Journal on Applied Mathematics 63*(1), 259–278.

Aw, A. and M. Rascle (2000). Resurrection of "Second Order" Models of Traffic Flow. *SIAM Journal on Applied Mathematics 60*(3), 916–938.

Benzoni-Gavage, S. and R. M. Colombo (2003). An n-Populations Model for Traffic Tlow. *European Journal of Applied Mathematics 14*(5), 587–612.

Berg, P., A. Mason, and A. Woods (2000). Continuum Approach to Car-Following Models. *Physical Review E - Statistical Physics, Plasmas, Fluids, and Related Interdisciplinary Topics 61*(2), 1056–1066.

Botma, H. and H. Papendrecht (1991). Traffic Operation of Bicycle Traffic. *Transportation Research Record: Journal of the Transportation Research Board 1320*(1), 65–72.

Cao, J., R. Liu, and B. Li (2011). Research on the Bicycle Flow in Signalized Intersections with Video-based Detection Technologies. In *ICTIS 2011*, pp. 629–635.

Cao, N. Y. and K. Sano (2012). Estimating Capacity and Motorcycle Equivalent Units on Urban Roads in Hanoi, Vietnam. *Journal of Transportation Engineering 138*(6), 776–785.

Cassidy, M. J. and R. L. Bertini (1999). Some Traffic Features at Freeway Bottlenecks. *Transportation Research Part B 33*, 25–42.

Chanut, S. and C. Buisson (2003). Macroscopic Model and Its Numerical Solution for Two-Flow Mixed Traffic with Different Speeds and Lengths. *Transportation Research Record: Journal of the Transportation Research Board 1852*, 209–219.

Chen, X., K. An, and L. Li (2014). Study on the Influencing Factors of Bicycle Lane Capacity. In *Transportation Research Board*, Washington D.C. Transportation Research Board.

Chen, X., H. Han, and B. Lin (2012). Developing Bicycle Equivalents for Mopeds in Shanghai, China. *Transportation Research Record: Journal of the Transportation Research Board 2317*, 60–67.

Chen, X., H. Han, J. Ye, S. Ma, and Y. Xu (2011). Normalized Volume Measurement for Nonmotorized Traffic Flow Mixed with Mopeds. *Transportation Research Record: Journal of the Transportation Research Board 2239*, 9–15.

Chen, X., B. Lin, H. Han, and T. R. Board (2013). Characteristics of Mixed Non-motorized Traffic Flow: A Comparative Analysis with Motorized and Pedestrian Traffic Flow. In *Transportation Research Board 92nd Annual Meeting Compendium of Papers*, pp. 16p.

Christian, K., S.-h. Cho, S.-y. Kho, and D.-k. Kim (2019). Bayesian models with spatial autocorrelation for bike sharing ridership variability based on revealed preference GPS trajectory data. *IET Intelligent Transport Systems 13*(11), 1658–1667.

CROW (2017a). Dutch design manual bicycle traffic (in Dutch). Technical report.

CROW (2017b). Over drukte valt te twisten (in Dutch).

Daamen, W. and S. P. Hoogendoorn (2003). Experimental Research of Pedestrian Walking Behavior. *Transportation Research Record* (1828), 20–30.

Daganzo, C. F. (1994). The Cell Transmission Model: A Dynamic Representation of Highway Traffic Consistent with the Hydrodynamic Theory. *Transportation Research Part B 28*(4), 269–287.

Daganzo, C. F. (1995). Requiem for Second-Order Fluid Approximations of Traffic Flow. *Transportation Research Part B 29*(4), 277–286.

Daganzo, C. F. (2002). A Behavioral Theory of Multi-Lane Traffic Flow. Part I: Long Homogeneous Freeway Sections. *Transportation Research Part B: Methodological 36*, 131–158.

Daganzo, C. F. (2008). Cumulative plots. In *Fundamentals of Transportation and Traffic Operations*, Chapter 2, pp. 25–46. Emerald Group Publishing Limited.

Daganzo, C. F. and V. L. Knoop (2016). Traffic Flow on Pedestrianized Streets. *Transportation Research Part B: Methodological 86*, 211–222.

De Haas, M. and M. Hamersma (2020). Cycling facts: new insights. pp. 1–34.

De Winter, F. (2020). *Druktebeleving op Utrechtse fietspaden*. In dutch, Utrecht University and Arcadis.

Deng, H. and H. M. Zhang (2015). On traffic relaxation, anticipation, and hysteresis. *Transportation Research Record 2491*, 90–97.

Deng, X. H. and J. Xu (2014). Study on Bicycle Flow Characteristics at Intersections. In Mohammadian, Goulias, Cicek, Wang, and Maraveas (Eds.), *Civil Engineering and Urban Planning III*, London, pp. 393–399. Taylor & Francis Group.

Duives, D., W. Daamen, and S. Hoogendoorn (2014). Anticipation behavior upstream of a Bottleneck. *Transportation Research Procedia 2*(2009), 43–50.

Duives, D. C., W. Daamen, and S. P. Hoogendoorn (2015). Quantification of the level of crowdedness for pedestrian movements. *Physica A: Statistical Mechanics and its Applications 427*, 162–180.

Fan, S. and D. B. Work (2015). A Hetergeneous Multiclass Traffic Flow Model With Creeping. *SIAM Journal on Applied Mathematics 75*(2), 813–835.

Forsyth, A. and J. M. Oakes (2015). Cycling, the Built Environment, and Health: Results of a Midwestern Study. *International Journal of Sustainable Transportation 9*, 49–58.

Gashaw, S., P. Goatin, and J. Härri (2018). Modeling and Analysis of Mixed Flow of Cars and Powered Two Wheelers. *Transportation Research Part C: Emerging Technologies 89*, 148–167.

Gashaw, S., J. Harri, and P. Goatin (2018). Lagrangian Formulation for Mixed Traffic Flow Including Two-Wheelers. In *21st IEEE Conference on Intelligent Transportation Systems*, pp. 1956–1961.

Gavriilidou, A., W. Daamen, Y. Yuan, and S. P. Hoogendoorn (2019). Modelling Cyclist Queue Formation Using a Two-Layer Framework for Operational Cycling Behaviour. *Transportation Research Part C: Emerging Technologies 105*, 468–484.

Gavriilidou, A., M. J. Wierbos, W. Daamen, Y. Yuan, V. L. Knoop, and S. P. Hoogendoorn (2019, may). Large-Scale Bicycle Flow Experiment: Setup and Implementation. *Transportation Research Record: Journal of the Transportation Research Board 2673*(5), 709–719.

Ghahramani, M., M. Zhou, and G. Wang (2020). Urban Sensing Based on Mobile Phone Data : Approaches , Applications , and Challenges. *IET Intelligent Transport Systems 7*(3), 627–637.

Godunov, S. (1959). Finite difference method for numerical computation of discontinuous solutions of the equations of fluid dynamics. *Matematicheskii Sbornik 47(89)*(3), 271–306.

Goñi-Ros, B., Y. Yuan, W. Daamen, and S. P. Hoogendoorn (2018). Empirical Analysis of the Macroscopic Characteristics of Bicycle Flow during the Queue Discharge Process at a Signalized Intersection. *Transportation Research Record 2672*(36), 51–62.

Greenberg, J. M. (2001). Extensions and Amplifications of a Traffic Model of Aw and Rascle. *SIAM Journal on Applied Mathematics 62*(3), 729–745.

Greenberg, J. M. (2004). Congestion Redux. *SIAM Journal on Applied Mathematics 64*(4), 1175–1185.

Greenshields, B. (1935). A Study of Traffic Capacity. In *Highway Research Board Proceedings*, Volume 14, pp. 448–477.

Greibe, P. and T. S. Buch (2016). Capacity and Behaviour on One-way Cycle Tracks of Different Widths. *Transportation Research Procedia 15*, 122–136.

Gulhare, S., A. P M, and A. Verma (2020). Pedestrian Flow Characteristics at Upstream and Downstream of Bottleneck for Unidirectional Flow under Normal Conditions. *Collective Dynamics 5*, 10–16.

Guo, N., R. Jiang, S. C. Wong, Q.-y. Hao, S.-q. Xue, and M.-b. Hu (2019). Bicycle Flow Dynamics on Wide Roads: Experiment and Modeling. *arXiv:1904.06084*.

Gupta, A. K. and I. Dhiman (2014). Analyses of a Continuum Traffic Flow Model for a Nonlane-based System. *International Journal of Modern Physics C 25*(10).

Gupta, A. K. and V. K. Katiyar (2006). A New Anisotropic Continuum Model for Traffic Flow. *Physica A: Statistical Mechanics and its Applications 368*, 551–559.

Harms, L., L. Bertolini, and M. T. Brömmelstroet (2016). Performance of Municipal Cycling Policies in Medium-Sized Cities in the Netherlands since 2000. *Transport Reviews 36*(1), 134–162.

Harms, L. and M. Kansen (2018). Cycling Facts. Technical report.

Heinen, E., B. van Wee, and K. Maat (2010). Commuting by Bicycle: An Overview of the Literature. *Transport Reviews 30*(1), 59–96.

Hoogendoorn, S. (2014). ERC Advanced Grant proposal Allegro.

Hoogendoorn, S. and W. Daamen (2016, jan). Bicycle Headway Modeling and Its Applications. *Transportation Research Record: Journal of the Transportation Research Board 2587*(1), 34–40.

Hoogendoorn, S. P. and W. Daamen (2005). Pedestrian Behavior at Bottlenecks. *Transportation Science 39*(2), 147–159.

Jia, B., X. G. Li, R. Jiang, and Z. Y. Gao (2007). Multi-value cellular automata model for mixed bicycle flow. *European Physical Journal B 56*(3), 247–252.

Jiang, H., T. Wen, P. Jiang, and H. Han (2013). Research on Cyclists Microscopic Behavior Models at Signalized Intersection. In *16th Road Safety on Four Continents Conference*, Number May.

Jiang, R., M.-b. Hu, Q.-s. Wu, and W.-g. Song (2016). Traffic Dynamics of Bicycle Flow: Experiment and Modeling. *Transportation Science 51*(3), 998–1008.

Jin, S., M. Liu, L. Shen, and D. Ma (2017a). Modelling speed – flow relationships for bicycle traffic flow. *Proceedings of the Institution of Civil Engineers - Transport 170*(4), 194–204.

Jin, S., M. Liu, L. Shen, and D. Ma (2017b). Modelling speed – flow relationships for bicycle traffic flow. In *Proceedings of the Institution of Civil Engineers - Transport*, Volume 170, pp. 194–204.

Jin, S., X. Qu, C. Xu, D. Ma, and D. Wang (2015). An improved multi-value cellular automata model for heterogeneous bicycle traffic flow. *Physics Letters, Section A: General, Atomic and Solid State Physics 379*(39), 2409–2416.

Jin, S., X. Qu, D. Zhou, C. Xu, D. Ma, and D. Wang (2015). Estimating Cycleway Capacity and Bicycle Equivalent Unit for Electric Bicycles. *Transportation Research Part A: Policy and Practice 77*, 225–248.

Jin, W. L. (2010). A kinematic wave theory of lane-changing traffic flow. *Transportation Research Part B: Methodological 44*(8-9), 1001–1021.

Khan, Z. H., T. A. Gulliver, H. Nasir, A. Rehman, and K. Shahzada (2019). A Macroscopic Traffic Model Based on Driver Physiological Response. *Journal of Engineering Mathematics 115*(1), 21–41.

KiM (2019). Mobiliteitsbeeld 2019. Technical report, Netherlands Institute for Transport Policy Analysis.

Kim, D. (2020). Pedestrian and Bicycle Volume Data Collection Using Drone Technology. *Journal of Urban Technology 27*(2), 45–60.

Kneidl, A. (2016). How Do People Queue? A Study of Different Queuing Models. In V. L. Knoop and W. Daamen (Eds.), *Traffic and Granular Flow '15*, pp. 201–208. Springer International Publishing.

Knoop, V. L., F. S. Hanseler, M. J. Wierbos, W. Daamen, and S. P. Hoogendoorn (2020). Voronoi densities for bicylists : adaptation for finite object size and speed. In I. Zuriguel, A. Garcimartin, and R. Cruz (Eds.), *Proceedings of Traffic and Granular Flow 2019*, pp. 515–521. Springer International Publishing.

Knoop, V. L., S. P. Hoogendoorn, and H. J. van Zuylen (2009, jan). Processing Traffic Data Collected by Remote Sensing. *Transportation Research Record: Journal of the Transportation Research Board 2129*(1), 55–61.

Kucharski, R., A. Drabicki, K. Żyłka, and A. Szarata (2019). Multichannel Queuing Behaviour in Urban Bicycle Traffic. *European Journal of Transport and Infrastructure Research 19*(2), 116–141.

Laval, J. A. (2011). Hysteresis in traffic flow revisited: An improved measurement method. *Transportation Research Part B: Methodological 45*(2), 385–391.

Laval, J. A. and L. Leclercq (2013). The Hamilton – Jacobi Partial Differential Equation and the Three Representations of Traffic Flow. *Transportation Research Part B 52*, 17–30.

Lebacque, J., J. Lesort, and F. Giorgi (1998). Introducing Buses into First-Order Macroscopic Traffic Flow Models. *Transportation Research Record 1644*, 70–79.

Leclercq, L. (2007). Hybrid Approaches to the Solutions of the "Lighthill-Whitham-Richards" Model. *Transportation Research Part B: Methodological 41*(7), 701–709.

Li, Z., M. Ye, Z. Li, and M. Du (2015). Some Operational Features in Bicycle Traffic Flow. *Transportation Research Record: Journal of the Transportation Research Board 2520*, 18–24.

Lighthill, M. J. and G. B. Whitham (1955). On Kinematic Waves. II. A Theory of Traffic Flow on Long Crowded Roads. In *Proceedings of the Royal Society A: Mathematical, Physical and Engineering Sciences*, Volume 229, pp. 317–345.

Loder, A., L. Bressan, M. J. Wierbos, H. Becker, A. Emmonds, M. Obee, V. L. Knoop, M. Menendez, and K. W. Axhausen (2019). A general framework for multi-modal macroscopic fundamental diagrams (MFD) (under review).

Logghe, S. and L. Immers (2008). Multi-Class Kinematic Wave Theory of Traffic Flow. *Transportation Research Part B: Methodological 42*(6), 523–541.

Lü, Y.-X., Z.-X. Wu, and J.-Y. Guan (2020). Pedestrian dynamics with mechanisms of anticipation and attraction. *Physical Review Research 2*(4), 43250.

Luo, Y., B. Jia, J. Liu, W. H. K. Lam, X. Li, and Z. Gao (2015). Modeling the Interactions Between Car and Bicycle in Heterogeneous Traffic. *Journal of Advanced Transportation 49*, 29–47.

Ma, X. and D. Luo (2016). Modeling cyclist acceleration process for bicycle traffic simulation using naturalistic data. *Transportation Research Part F: Traffic Psychology and Behaviour 40*, 130–144.

Mai, X., W. Lv, X. Wei, W. Song, and R. Jiang (2013). Analyzing the Characteristics of Unidirectional Bicycle Movement Around a Track Based on Digital Image Processing. *Procedia Engineering 62*, 519–524.

Municipality Utrecht (2020). Traffic Counts Utrecht. *http://mobiliteitsdata-utrecht.nl/tellingen/*, accessed September 25, 2020.

Muñoz, J. C. and C. F. Daganzo (2002). Moving Bottlenecks: A Theory Grounded on Experimental Observation. In *Transportation and Traffic Theory in the 21 st Century*, pp. 441–461. Emerald Group Publishing Limited.

Nair, R., H. S. Mahmassani, and E. Miller-Hooks (2011). A Porous Flow Approach to Modeling Heterogeneous Traffic in Disordered Systems. *Transportation Research Part B: Methodological 45* '(9), 1331–1345.

National Research Council (1965). *Highway Capacity Manual*. Washington DC: The Board.

Navin, F. P. D. (1994). Bicycle Traffic Flow Characteristics: Experimental Results and Comparisons. *ITE Journal 64*(3), 31–37.

Ngoduy, D. and R. Liu (2007). Multiclass First-Order Simulation Model to Explain Non-linear Traffic Phenomena. *Physica A: Statistical Mechanics and its Applications 385*(2), 667–682.

Nikolić, M. and M. Bierlaire (2018). Data-driven spatio-temporal discretization for pedestrian flow characterization. *Transportation Research Part C: Emerging Technologies 94*, 185–202.

Opiela, K. S., S. Khasnabis, and T. K. Datta (1980). Determination of the Characteristics of Bicycle Traffic at Urban Intersections. *Transportation Research Record 743*, 30–38.

Paulsen, M. and K. Nagel (2019). Large-Scale Assignment of Congested Bicycle Traffic Using Speed Heterogeneous Agents. *Procedia Computer Science 151*, 820–825.

Payne, H. (1971). Model of Freeway Traffic and Control. In *Simulation Council Proceedings*, pp. 51–61.

Prati, G., F. Fraboni, M. De Angelis, L. Pietrantoni, D. Johnson, and J. Shires (2019). Gender Differences in Cycling Patterns and Attitudes Towards Cycling in a Sample of European Regular Cyclists. *Journal of Transport Geography 78*, 1–7.

Pucher, J. and R. Buehler (2008). Cycling for Everyone: Lessons from Europe. *Transportation Research Record: Journal of the Transportation Research Board 2074*, 58–65.

Raksuntorn, W. and S. I. Khan (2003, jan). Saturation Flow Rate, Start-Up Lost Time, and Capacity for Bicycles at Signalized Intersections. *Transportation Research Record: Journal of the Transportation Research Board 1852*(1), 105–113.

Richards, P. I. (1956). Shock Waves on the Highway. *Operations Research 4*(1), 42–51.

Richardson, M. and B. Caulfield (2015). Investigating traffic light violations by cyclists in Dublin City Centre. *Accident Analysis and Prevention 84*, 65–73.

Roess, R. . P. and E. . S. Prassas (2014). *The Highway Capacity Manual: A Conceptual and Research History*, Volume 5 of *Springer Tracts on Transportation and Traffic*. Springer.

Saifuzzaman, M., Z. Zheng, M. M. Haque, and S. Washington (2017). Understanding the mechanism of traffic hysteresis and traffic oscillations through the change in task difficulty level. *Transportation Research Part B: Methodological 105*, 523–538.

Schleinitz, K. (2016). *Cyclists ' Road Safety - Do Bicycle Type , Age and Infrastructure*. Ph. D. thesis, Technische Universitt Chemnitz, Chemnitz, Germany.

Seriani, S., R. Fernandez, and E. Hermosilla (2015). Experimental Study for Estimating Capacity of Cycle Lanes. *Transportation Research Procedia 8*, 192–203.

Shalini, K. and B. Kumar (2014). Estimation of the Passenger Car Equivalent: A Review. *International Journal of Emerging Technology and Advanced Engineering 4*(6), 97–102.

Shepherd, R. (1994). Road and Path Quality for Cyclists. In *Proc. 17th ARRB Conference, Gold Coast, Queensland, Australia, Vol. 17*.

Shiomi, Y., T. Taniguchi, N. Uno, H. Shimamoto, and T. Nakamura (2015). Multilane First-Order Traffic Flow Model with Endogenous Representation of Lane-Flow Equilibrium. *Transportation Research Part C 59*, 198–215.

Steffen, B. and A. Seyfried (2010). Methods for measuring pedestrian density, flow, speed and direction with minimal scatter. *Physica A: Statistical Mechanics and its Applications 389*(9), 1902–1910.

Tang, T., H. Huang, and H. Shang (2010). A Dynamic Model for the Heterogeneous Traffic Flow Consisting of Car, Bicycle and Pedestrian. *International Journal of Modern Physics C 21*(02), 159–176.

Ton, D., D. C. Duives, O. Cats, S. Hoogendoorn-Lanser, and S. P. Hoogendoorn (2019). Cycling or walking? Determinants of mode choice in the Netherlands. *Transportation Research Part A: Policy and Practice 123*(August 2018), 7–23.

Transportation Research Board (2000). *Highway Capacity Manual*. Washington, DC.: National Research Council.

Treiterer, J. and J. Myers (1974). The hysteresis phenomenon in traffic flow. *Transportation and traffic theory 6*, 13–38.

Twaddle, H. and G. Grigoropoulos (2016). Modeling the speed, acceleration, and deceleration of bicyclists for microscopic traffic simulation. *Transportation Research Record 2587*(1), 8–16.

United Nations, Department of Economic and Social Affairs (2018). World Urbanization Prospects: The 2018 Revision. *Online Edition*.

van Lint, J. W. C., S. P. Hoogendoorn, and M. Schreuder (2008). Fastlane: A New Multiclas First-Order Traffic Flow Model. *Transportation Research Record: Journal of the Transportation Research Board 2088*, 177–187.

van Wageningen-Kessels, F. L. M. (2013). *Multi-Class Continuum Traffic Flow Models : Analysis and Simulation Methods*. Ph. D. thesis, Delft University of Technology.

van Wageningen-Kessels, F. L. M., H. van Lint, S. P. Hoogendoorn, and K. Vuik (2011). Lagrangian Formulation of Multiclass Kinematic Wave Model. *Transportation Research Record: Journal of the Transportation Research Board 2188*, 29–36.

van Wageningen-Kessels, F. L. M., B. van't Hof, S. P. Hoogendoorn, H. van Lint, and K. Vuik (2013). Anisotropy in Generic Multi-Class Traffic Flow Models. *Transportmetrica A: Transport Science 9*(5), 451–472.

Vansteenkiste, P., G. Cardon, E. D'Hondt, R. Philippaerts, and M. Lenoir (2013). The visual control of bicycle steering: The effects of speed and path width. *Accident Analysis and Prevention 51*, 222–227.

Vial, A., W. Daamen, A. Y. Ding, B. van Arem, and S. Hoogendoorn (2020). AMSense: How Mobile Sensing Platforms Capture Pedestrian/Cyclist Spatiotemporal Properties in Cities. *IEEE Intelligent Transportation Systems Magazine*.

Wang, D., D. Zhou, S. Jin, and D. Ma (2015). Characteristics of Mixed Bicycle Traffic Flow on the Conventional Bicycle Path. *TRB 94th Annual Meeting Compendium of Papers* (86), 14p.

Wang, J. and H. Wei (1993). Traffic Segregation on Spatial and Temporal Bases: The Experience of Bicycle Traffic Operations in China. *Transportation Research Record: Journal of the Transportation Research Board 1396*, 11–17.

Wang, Y. G., G. Wei, X. Zhu, and Y. L. Pei (2011). Capacity of Bicycle Platoon Flow at Two-Phase Signalized Intersection: A Case Analysis of Xi'an City. *Promet - Traffic & Transportation 23*(3), 177–186.

Wierbos, M. J., V. L. Knoop, R. L. Bertini, and S. P. Hoogendoorn (2021). Influencing the queue configuration to increase bicycle jam density and discharge rate : An experimental study on a single path. *Transportation Research Part C 122*(102884), 1–15.

Wierbos, M. J., V. L. Knoop, B. Goñi-Ros, and S. P. Hoogendoorn (2020). The Influence of Jam Density and Merging Cyclists on the Queue Discharge Rate. *Journal of Advanced Transportation 2020*, 1–10.

Wierbos, M. J., V. L. Knoop, F. S. Hänseler, and S. P. Hoogendoorn (2019). Capacity, Capacity Drop, and Relation of Capacity to the Path Width in Bicycle Traffic. *Transportation Research Record 2673*(5), 693–702.

Wierbos, M. J., V. L. Knoop, F. S. Hänseler, and S. P. Hoogendoorn (2020). A macroscopic flow model for mixed bicycle–car traffic. *Transportmetrica A: Transport Science 9935*.

Winters, M., R. Buehler, and T. Götschi (2017). Policies to Promote Active Travel: Evidence from Reviews of the Literature. *Current environmental health reports 4*(3), 278–285.

Wong, G. C. K. and S. C. Wong (2002). A Multi-Class Traffic Flow Model – an Extension of LWR Model with Heterogeneous Drivers. *Transportation Research Part A: Policy and Practice 36*(9), 827–841.

Wu, C. X., P. Zhang, S. C. Wong, and K. Choi (2014). Steady-State Traffic Flow on a Ring Road with Up- and Down-Slopes. *Physica A: Statistical Mechanics and its Applications 403*, 85–93.

Yuan, K., V. L. Knoop, and S. P. Hoogendoorn (2017). A Microscopic Investigation Into the Capacity Drop: Impacts of Longitudinal Behavior on the Queue Discharge Rate. *Transportation Science 53*(3), 852–862.

Yuan, Y., W. Daamen, B. Goñi-Ros, and S. Hoogendoorn (2018). Investigating cyclist interaction behavior through a controlled laboratory experiment. *Journal of Transport and Land Use 11*(1), 833–847.

Yuan, Y., B. Goñi-Ros, M. Poppe, W. Daamen, and S. P. Hoogendoorn (2019, jun). Analysis of Bicycle Headway Distribution, Saturation Flow and Capacity at a Signalized Intersection using Empirical Trajectory Data. *Transportation Research Record: Journal of the Transportation Research Board 2673*(6), 10–21.

Zeegers, T. (2004). Width of Bicycle Paths. Technical report.

Zhang, H. (1999, feb). A mathematical theory of traffic hysteresis. *Transportation Research Part B: Methodological 33*(1), 1–23.

Zhang, H. M. (2002). A Non-Equilibrium Traffic Model Devoid of Gas-Like Behavior. *Transportation Research Part B: Methodological 36*, 275–290.

Zhang, J., W. Mehner, E. Andresen, S. Holl, M. Boltes, A. Schadschneider, and A. Seyfried (2013, dec). Comparative Analysis of Pedestrian, Bicycle and Car Traffic Moving in Circuits. *Procedia - Social and Behavioral Sciences 104*, 1130–1138.

Zhang, J., W. Mehner, S. Holl, M. Boltes, E. Andresen, A. Schadschneider, and A. Seyfried (2014). Universal flow-density relation of single-file bicycle, pedestrian and car motion. *Physics Letters, Section A: General, Atomic and Solid State Physics 378*(44), 3274–3277.

Zhang, P., R. X. Liu, S. C. Wong, and S. Q. Dai (2006). Hyperbolicity and Kinematic Waves of a Class of Multi-Population Partial Differential Equations. *European Journal of Applied Mathematics 17*(2), 171–200.

Zhang, P., C. X. Wu, and S. C. Wong (2012). A Semi-Discrete Model and its Approach to a Solution for a Wide Moving Jam in Traffic Flow. *Physica A: Statistical Mechanics and its Applications 391*(3), 456–463.

Zhao, Y. and H. Zhang (2017, nov). A Unified Follow-the-Leader Model for Vehicle, Bicycle and Pedestrian Traffic. *Transportation Research Part B: Methodological 105*, 315–327.

Zhou, D., C. Xu, D.-H. Wang, and J. Sheng (2015). Estimating Capacity of Bicycle Path on Urban Roads in Hangzhou, China. In *TRB 94th Annual Meeting Compendium of Papers*.

Samenvatting

Het gebruik van de fiets als vervoersmiddel wordt toegejuicht omdat het een duurzame en gezonde manier van reizen is. Maar het groeiende aantal fietsers in Nederlandse steden zorgt steeds vaker voor overvolle fietspaden en lange wachtrijen bij verkeerslichten. Deze drukte is problematisch, omdat het fietscomfort hierdoor afneemt en de fietsveiligheid in het gedrang komt. Om een goede doorstroming van het fietsverkeer te faciliteren, zoeken gemeentes naar manieren om de infrastructuur aan te passen aan het grotere aantal fietsers. Dit vereist een beter begrip van fietsverkeer dan er tot nu toe is. Het onderzoek in dit proefschrift geeft inzicht in kenmerkende eigenschappen van fietsbewegingen waardoor fietsverkeer beter kan worden beschreven in verkeersmodellen.

Dit proefschrift beschrijft fietsverkeer op het macroscopische niveau. Hierbij zijn drie grootheden belangrijk, te weten dichtheid, snelheid en intensiteit. De dichtheid wordt beschreven als het aantal fietsers per vierkante meter, de snelheid is de gemiddelde snelheid van fietsers in km/u en de intensiteit is het aantal fietsers wat per tijdseenheid (bijvoorbeeld seconde of uur) langs een bepaald punt op de weg beweegt. De fietsbewegingen worden dus op een hoger niveau beschreven dan wanneer alleen gekeken wordt naar individuele bewegingen. Deze geaggregeerde manier van beschrijven maakt dat patronen en verbanden in fietsverkeer inzichtelijk worden.

Een belangrijke vraag in dit proefschrift is hoe de drie grootheden dichtheid, snelheid en intensiteit met elkaar samenhangen. Het verband tussen deze drie grootheden staat in de verkeerskunde bekend als het fundamentele diagram en is nog nauwelijks onderzocht voor fietsverkeer. Om dit te kunnen bestuderen is data cruciaal, maar bruikbare datasets zijn schaars. Daarom zijn er in dit proefschrift meerdere experimenten uitgevoerd waarvan de data vervolgens is geanalyseerd. Hierbij is gekeken naar bewegingen op rechte paden en naar fietsverkeer bij kruisingen. De omstandigheden worden tijdens het onderzoek zo simpel mogelijk gehouden om het fietsgedrag zo min mogelijk te verstoren door interacties met tegenliggers of andere weggebruikers. Dit wordt bewerkstelligd door te kijken naar eenrichtingsbewegingen op fietspaden zonder ander verkeer, dus vrijliggende fietspaden en kruispunten die worden geregeld met verkeerslichten. Verder worden voornamelijk de drukke momenten onderzocht om inzicht te krijgen in hoe fietsers de ruimte op het fietspad benutten. Dit is interessant omdat er tot nu toe vooral onderzoek is gedaan naar "volgend" fietsverkeer, waarbij men elkaar niet mag inhalen. In de praktijk bewegen fietsers ook naast elkaar en halen ze in, dus het loslaten van deze volginstructie geeft een betere representatie van het dagelijkse fietsverkeer.

Om meer data te verkrijgen, is er een grootschalig experiment gehouden waarbij de bewegingen van ongeveer 200 fietsers zijn vastgelegd terwijl ze rondjes over een indoor-parcours reden. Hierbij zijn er verschillende verkeerssituaties nagebootst, zoals een kruising, T-splitsing en een versmalling. Het resultaat is een rijke dataset aan trajectoriën, oftewel plaats- en tijdsbepalingen van fietsers, die gebruikt kan worden voor onderzoek naar zowel individuele fietsbewegingen als collectieve patronen.

Een selectie van de verzamelde dataset is gebruikt om de relatie tussen dichtheid, snelheid en intensiteit op rechte fietspaden te onderzoeken. Het gevonden resultaat is dat net als bij autoverkeer, ook bij fietsverkeer de snelheid afneemt als het drukker wordt, terwijl de intensiteit toeneemt met de drukte. Er is echter geen capaciteitspunt gevonden waarbij de intensiteit piekt en afneemt bij hogere dichtheden, zoals bij autoverkeer het geval is. In fietsverkeer bereikt de intensiteit een plateau waarbij de doorstroming hoog blijft bij toenemende drukte. Hierbij speelt anticipatiegedrag op veranderende omstandigheden een grote rol. De snelheid blijkt niet alleen beïnvloed te worden door de individuele dichtheid, dus de hoeveelheid ruimte die een fietser daadwerkelijk om zich heen heeft, maar ook door de stroomafwaartse verkeerssituatie. De gemiddelde snelheid neemt af als de weg verderop smaller wordt of als er filevorming zichtbaar is. Bij een smallere weg fietsen mensen voorzichtiger, en dus langzamer, en bij een dreigende opstopping stopt een deel van de mensen al met trappen, terwijl anderen hun snelheid behouden en al inhalend de gaten opvullen die de langzaamrijdenden hebben laten vallen. Hierdoor neemt de gemiddelde snelheid af, maar blijft de intensiteit hoog.

In een ander experiment is de relatie tussen capaciteit en wegbreedte onderzocht. Hierbij is gekeken naar de maximale hoeveelheid fietsers die per seconde door een vernauwing fietsen op het moment voor en na het optreden van file. Het blijkt dat, ongeacht de padbreedte, de maximale wegcapaciteit lager is na optreden van congestie dan wanneer er nog geen rembewegingen zijn geweest. Deze capaciteitsval bij filevorming is een bekend fenomeen in gemotoriseerd wegverkeer, maar was nog niet eerder gezien in fietsverkeer. Verder is er gekeken naar de positionering van fietsers op het pad terwijl ze door de vernauwing fietsen. Er blijkt een patroon te zitten in de onderlinge afstand die fietsers tot elkaar houden. Dit patroon is te vergelijken met een momentopname van een invoegbeweging. Hiermee wordt bedoeld dat men daar waar mogelijk naast elkaar fietst, en dat dit geleidelijk verandert naar een volgbeweging bij smallere paden. Tijdens dit proces wordt de tussenafstand in de rijrichting groter naarmate de padbreedte, en daarmee de zijdelingse afstand tussen fietsers, kleiner wordt.

Soortgelijke patronen in fietsposities zijn ook van belang in stilstaand fietsverkeer, zoals bij verkeerslichten. Dit proefschrift laat zien dat de stoppositie van fietsers de uiteindelijke dichtheid van de wachtrij beïnvloedt, wat op zijn beurt weer invloed heeft op de afrijcapaciteit. Dus hoe dichter mensen bij elkaar stilstaan tijdens het rode licht, hoe meer fietsers er per seconde de stopstreep passeren tijdens het groene licht. Het wegrijproces bij groen licht wordt ook beïnvloed door invoegende bewegingen. Wachtrijen met lage dichtheid hebben gaten die door invoegende fietsers opgevuld kunnen worden. Dit invoeggedrag verhoogt

de afrijcapaciteit als het gebeurt door een achteropkomende fietser die met een inhalende beweging het gat opvult. Het wegrijproces wordt echter verstoord als er wordt ingevoegd vanuit een zijweg, met als gevolg dat de afrijcapaciteit afneemt.

De connectie tussen wachtrijdichtheid en afrijcapaciteit doet vermoeden dat de capaciteit van een kruising kan worden verhoogd door de onderlinge afstand van fietsers in de wachtrij verder te verkleinen. Dit verband is verder onderzocht in een experiment waarin fietsers verschillende instructies kregen over hoe ze de wachtrij moesten opbouwen. Het doel hiermee was om hogere wachtrijdichtheden te creëren dan normaal gesproken in het dagelijkse verkeer te zien zijn. Het blijkt inderdaad dat er flink meer fietsers door groen licht kunnen fietsen als de dichtheid van de wachtrij verder wordt verhoogd. Dit effect is het grootst bij twee manieren van wachtrijmanipulatie, namelijk door fietsers vocaal aan te moedigen om dichtbij elkaar te stoppen, en door mensen te vragen om hun voorwielen te plaatsen op een op de straat uitgetekend patroon. Deze beïnvloeding van de wachtrijdichtheid kan worden gebruikt om de capaciteit van kruispunten te verhogen. Hiermee verbetert niet alleen de verkeerssituatie voor fietsers, maar kan de algehele verkeersdoorstroming in de stad verbeteren.

In dit proefschrift wordt een manier geïntroduceerd om fietsverkeer te beschrijven in een macroscopisch verkeersstroommodel. Hiervoor is een bestaand model voor autoverkeer uitgebreid zodat een gemengde verkeerssituatie zoals voorkomt op een fietsstraat, gemodelleerd kan worden. De vernieuwing zit hierbij in een uitgebreidere beschrijving van de snelheidsfuncties. Voor auto's en fietsers wordt namelijk een aparte snelheidsfunctie beschreven die zowel afhangt van de onderlinge afstand tussen auto's als die tussen fietsers. Dit maakt het mogelijk om twee specifieke verkeerssituaties te simuleren, namelijk een lagere autosnelheid tijdens het inhalen van fietsers, en het voorbijfietsen van langzamere auto's tijdens file. Het model kan onder andere gebruikt worden om de doorstroming te simuleren voor verschillende (toekomstige) scenario's met betrekking tot de verkeersdrukte.

De bevindingen in dit proefschrift hebben een aantal praktische implicaties. Zo zijn er capaciteitswaardes gevonden van fietspaden tussen 0.75 en 2.00 meter breed. Hoewel het oncomfortabel is om langere tijd in deze drukte te fietsen, geven de capaciteitswaardes wel aan hoe breed een fietspad moet zijn om een bepaalde piekintensiteit op te kunnen vangen. Dit is bijvoorbeeld van belang op het fietspad na een druk verkeerslicht. Verder kan het gevonden verband tussen de wachtrijdichtheid en afrijcapaciteit gebruikt worden om de capaciteit van een kruispunt te verhogen. Hierbij moet gedacht worden aan het faciliteren van invoegbewegingen die vanuit achteren komen in plaats van opzij, en aan het verhogen van de wachtrijdichtheid. Dit laatste kan gedaan worden door bijvoorbeeld de ideale opstelconfiguratie aan te geven op het fietspad.

Dit proefschrift geeft ook handvatten voor de verdere ontwikkeling van verkeersmodellen voor fietsers. Zo kunnen de verkregen inzichten in de relatie tussen dichtheid, snelheid en intensiteit gebruikt worden als input voor verkeersstroommodellen. Vooral het inzicht dat fietsverkeer een capaciteitsplateau kent in plaats van een capaciteitspunt, is van belang om fietsverkeer op een realistische manier te modelleren. Verder kan de methode om gemengd auto- en fietsverkeer te beschrijven via de snelheidsfunctie ook uitgewerkt worden om andere vormen van gemengd verkeer te beschrijven.

Summary

Using the bicycle as a means of transport is encouraged because it is a sustainable and healthy way of traveling. But the growing number of cyclists in Dutch cities is increasingly causing overcrowded situations at bike paths and long queues at traffic lights. This crowding is problematic because it reduces the comfort and safety of cyclists. To facilitate the flow of bicycle traffic, municipalities are looking for ways to adapt their infrastructure to the larger number of cyclists. This requires a better knowledge of bicycle traffic than is currently available. The research in this dissertation provides insight into characteristic properties of bicycle movements, which allows for a better representation of bicyclists in traffic flow models.

This dissertation describes bicycle traffic at the macroscopic level. Three parameters are important in this, being density, speed and flow. The density is described as the number of cyclists per square meter, the speed is the average speed of cyclists in km/h and the flow is the number of cyclists that move along a certain point on the road per unit of time (e.g., second or hour). The bicycle movements are therefore described at a higher level than when considering only individual movements. This aggregated description is better suited to reveal patterns and connections in bicycle traffic.

The main question in this dissertation is how the quantities density, speed and flow are related. The relationship between these three variables is known as the fundamental diagram and is widely studied for motorized traffic, but has hardly been researched for bicyclists. Data is crucial to study this but useful data sets are scarce. To this end, several experiments are performed in this dissertation, which focus on capturing cycling movements on straight paths and at intersections. Along the way, the cycling conditions are kept as simple as possible to minimize the influence of interactions with oncoming traffic or other road users. This is done by looking at one-way movements on cycle paths without other traffic, i.e. cycle paths that are segregated from car traffic and intersections that are controlled by traffic lights. Furthermore, mainly the busy moments are investigated to gain insight into the space usage by cyclists on the path. This is of interest because so far research has primarily focused on one-dimensional bicycle traffic, where people are not allowed to overtake each other. In practice, cyclists also move alongside and overtake each other, so letting go of the instruction to follow gives a better representation of daily bicycle traffic.

To obtain more data, a large-scale experiment was conducted in which the movements of about 200 cyclists were recorded as they circled an indoor track. Various traffic situations

have been mimicked, such as a crossing, T-junction and a narrowing. The result is a rich data set of trajectories, i.e. position and time information of cyclists, that can be used for research into individual cycling movements as well as collective patterns.

A selection of the collected data set was used to investigate the relationship between density, speed and flow on straight cycle paths. The obtained result is that, similar to car traffic, the cycling speed decreases when density increases, and that the flow increases with growing crowdedness. However, a clear capacity point was not obtained, as is the case for car traffic. Instead, the bicycle flow was found to reach a plateau where it remained high with increasing density. Anticipating behavior on changing circumstances was found to play a major role in this. Speed was found to be influenced not only by individual density, i.e. the amount of space a cyclist has available around him/her, but also by the downstream traffic situation. The average speed decreased when the road ahead narrowed or when an upcoming traffic jam was visible. This is explained by the observation that people cycle more carefully on a narrower path, and therefore move more slowly. In case of an impending traffic jam, some people already stop pedaling and thus slow down, while others maintain at speed and, while overtaking, fill the gaps that the slow-moving people have created. This combination causes the average speed to decrease, while the flow remains high.

Another experiment revealed the relationship between capacity and road width. Here, the maximum number of cyclists per second who cycle through a narrowing at the time before and after the onset of congestion was examined. It turns out that, irrespective of the path width, the road capacity is lower after congestion occurs than when braking has not yet taken place. This capacity drop in congestion is a well-known phenomenon in motorized road traffic, but had not been seen before in bicycle traffic. Furthermore, the positioning of cyclists on the path while cycling through the narrowing was examined. There appears to be a pattern in the inter-personal distance that cyclists keep from each other. This pattern can be compared to a snapshot of a merging move. This means that people cycle side by side where possible, and that this gradually changes to a following movement on narrower paths. During this process, the inter-personal distance in the direction of travel increases as the path width, and thus the lateral distance between cyclists, decreases.

Similar patterns in cycling positions are also important at standstill, such as at traffic lights. This dissertation shows that the stopping position of cyclists influences the final density of the queue, which in turn influences the queue discharge rate. So the closer people queue up during the red signal, the more cyclists per second can pass the stop line during the green signal. The discharge process is also affected by merging movements. Low-density queues have gaps that can be filled by merging cyclists. It turns out that the discharge rate increases when a cyclist fills the gap by coming in from behind. However, the discharge process is disrupted by a cyclist merging from a side road, resulting in a lower discharge rate.

The connection between queue density and discharge rate suggests that the capacity of an intersection can be increased by further reducing the inter-personal distance of cyclists in the queue. This relationship was further explored by an experiment in which cyclists were given different instructions on how to build up the queue. The aim was to create higher queue densities than would normally be seen in daily traffic. Indeed, it appears that con-

siderably more cyclists can catch the green signal if the queue density is further increased. This effect is greatest with two types of queue manipulation, namely by vocally encouraging cyclists to stop close to each other, and by asking people to place their front wheels on a pattern that is indicated on the street. This queue-formation manipulation can be used to increase the capacity of intersections. This not only improves the traffic situation for cyclists, but can improve the overall traffic flow in a city.

This dissertation describes a method to include bicycle traffic in a macroscopic traffic flow model. For this, an existing model for car traffic has been extended so that a mixed traffic situation, such as occurs on a bicycle street, can be modeled. The contribution lies in a more extensive description of the speed functions, which depend both on the inter-personal distance of cars and that of cyclists. This enables the modeling of two specific traffic situations, namely a lower car speed when overtaking cyclists, and cyclists passing slower cars during traffic jams. The model can be used, e.g., to simulate the traffic flow for different (future) scenarios with regard to traffic density.

The findings in this dissertation have a number of practical implications. Capacity values were found for cycle paths between 0.75 and 2.00 meters wide. Although it is uncomfortable to cycle for a long duration in this crowded situation, the capacity values do indicate how wide a bicycle path should be to be able to handle a certain peak flow. This is important, for example, on the cycle path downstream of a busy traffic light. Furthermore, the relationship between queue density and discharge rate can be used to increase the capacity of an intersection. This includes facilitating merging movements that are aligned with the discharge direction, and increasing queue density. The latter can be done, for example, by indicating the ideal setup configuration on the bicycle path.

Finally, this dissertation suggests ideas for the further development of traffic models for cyclists. For example, the obtained insights into the relationship between density, speed and flow can be used as input for traffic flow models. The insight that bicycle traffic has a capacity plateau instead of a capacity point is especially important for modeling bicycle traffic in a realistic manner. Furthermore, the method to describe mixed traffic on a bicycle street via the speed function can also be elaborated to describe other forms of mixed traffic, such as cyclists and pedestrians in a city center.

About the author

Maria Jentina (Marie-Jette) Wierbos was born in Zuidwolde, the Netherlands on August 28th, 1986. She received the gymnasium diploma at the Roelof van Echten College in Hoogeveen in 2004, and moved to the city of Utrecht afterwards. There, she studied Earth Sciences at the Utrecht University and complemented this bachelor study with courses in Physics and Mathematics. During the academic year of 2007/2008, she was a full-time board member of the study association A-Eskwadraat, which represents the majority of students at the Faculty of Science at Utrecht University. After this one-year break, she continued her studies by pursuing a master's degree in Physics and Climate Science. She obtained the MSc degree in 2011.

For almost five years, she worked as an operational meteorologist and team manager in an international organization. In this role, she traveled around the world to manage offshore weather forecasting activities. Despite the challenging character of the job, she was drawn back to the scientific community by her drive to extend her knowledge in societal topics. When the opportunity presented itself to dive into the working of active mode traffic, she was keen to join the Delft University of Technology and use her background in physics and weather modeling to better understand urban traffic flow.

She started the PhD project in November 2016 at the department of Transport and Planning, within the Faculty of Civil Engineering and Geosciences. While pursuing the degree, she extended her knowledge into Transport and Traffic by following courses at the TRAIL Research School, attending national and international conferences, and organizing monthly meetings to discuss ongoing studies on active mode research.

Over the years, Marie-Jette expanded her knowledge in a wide range of topics related to the physical side of natural sciences. It is unclear where her career path will lead next, but it will likely be somewhere with high societal relevance.

List of publications

During the PhD project, several studies were shared at conferences and published in scientific journals. All contributions are listed below.

Published journal articles

- **Wierbos, M.J.**, Knoop, V.L., Hänseler, F.S., Hoogendoorn, S.P. (2019), Capacity, Capacity Drop, and Relation of Capacity to the Path Width in Bicycle Traffic. *Transportation Research Record: Journal of the Transportation Research Board* 2673, 5, 693-702, DOI: 10.1177/0361198119840347.

- Gavriilidou, A., **Wierbos, M.J.**, Daamen, W., Yuan, Y., Knoop, V.L., Hoogendoorn, S.P. (2019), Large-Scale Bicycle Flow Experiment: Setup and Implementation. *Transportation Research Record: Journal of the Transportation Research Board* 2673, 5, 709-719, DOI: 10.1177/0361198119839974.

- **Wierbos, M.J.**, Knoop, V.L., Hänseler, F.S., Hoogendoorn, S.P. (2020), A Macroscopic Flow Model for Mixed Bicycle–Car Traffic. *Transportmetrica A: Transport Science*, 9935, DOI: 10.1080/23249935.2019.1708512.

- **Wierbos, M.J.**, Knoop, V.L., Goñi-Ros, B., Hoogendoorn, S.P. (2020), The Influence of Jam Density and Merging Cyclists on the Queue Discharge Rate. *Journal of Advanced Transportation,* 1-10, DOI: 10.1155/2020/9272845.

- **Wierbos, M.J.**, Knoop, V.L., Bertini, R.L., Hoogendoorn, S.P. (2021), Influencing the Queue Configuration to Increase Bicycle Jam Density and Discharge Rate: An Experimental Study on a Single Path. *Transportation Research Part C: Emerging Technologies*. 122, p.1-15, DOI: 10.1016/j.trc.2020.102884.

- Loder, A., Bressan, L., **Wierbos, M.J.**, Becker, H., Emmonds, A., Obee, M., Knoop, V.L., Menendez, M., Axhausen, K.W. (2021), How Many Cars in the City Are Too Many? Towards Finding the Optimal Modal Split for a Multi-Modal Urban Road Network. *Frontiers in Future Transportation*. 2:665006, DOI: 10.3389/ffutr.2021.665006.

- Knoop, V.L., **Wierbos, M.J.**, Van Boggelen, O. (2021), Capacity Gains of Splitting Cross Traffic into Multiple Sub-Streams. *Transportation Research Record: Journal of the Transportation Research Board*. DOI:10.1177/03611981211036683

Manuscripts under review

- **Wierbos, M.J.**, Knoop, V.L., Hoogendoorn, S.P. (submitted), Macroscopic properties of a cyclist stream and the effect of anticipation

- Navabi Niaki, M., Gavriilidou, A., **Wierbos, M.J.**, Daamen, W., Hoogendoorn, S.P., Knoop, V.L., Van Nes, N. (submitted), Effects of Lane Marking Nudges on Cyclist Behavior and Safety

Conference contributions

- **Wierbos, M.J.**, Knoop, V.L., Goñi-Ros, B., Hoogendoorn, S.P., Bicycle Queue Dynamics: Influence of Queue Density and Merging Cyclists on Discharge Rate at an Intersection, in proceedings of the *97th Annual Meeting of the Transportation Research Board (TRB 2018)*, Washington D.C., USA.

- **Wierbos, M.J.**, Hänseler, F.S., Knoop, V.L., Hoogendoorn, S.P., Auto te gast, wat is het effect op de verkeersdoorstroming?, presented at *PLATOS 2018*, Utrecht, The Netherlands.

- **Wierbos, M.J.**, Knoop, V.L., Hoogendoorn, S.P., Empirical Data Analysis: Travel Times of Bicyclists in a Mixed Traffic Situation, presented at *Cycling Research Board (CRB) 2018*, Amsterdam, The Netherlands.

- **Wierbos, M.J.**, Knoop, V.L., Hänseler, F.S., Hoogendoorn, S.P., A Macroscopic Flow Model for Mixed Bicycle–Car Traffic, presented at *hEART 2018*, Athens, Greece.

- **Wierbos, M.J.**, Hänseler, F.S., Knoop, V.L., Hoogendoorn, S.P., A Macroscopic Flow Model For Mixed Traffic Using Two-Dimensional Speed Functions, presented at *Mathematics Applied in Transport and Traffic Systems (MATTS) 2018*, Delft, The Netherlands.

- Loder, A., Bressan, L., **Wierbos, M.J.**, Becker, H., Emmonds, A., Obee, M., Knoop, V.L., Menendez, M., Axhausen, K.W., A multimodal network interaction model for the macroscopic fundamental diagram (MFD), presented at *hEART 2019*, Budapest, Hungary.

- Zomer, L., Vial, A., Reggiani, G., Ton, D., **Wierbos, M.J.**, Gong, X., Schneider, F., Feng, Y., Sparnaaij, M., Gavriilidou, A., Van Oijen, T., Duives, D.C., Yuan, Y., Cats, O., Knoop, V.L., Daamen, W., Hoogendoorn, S.P., The Impact of Cycling Research: Connecting Science and Practice, presented at *Cycling Research Board (CRB) 2019*, Delft, The Netherlands.

- Knoop, V.L., Hänseler, F.S., **Wierbos, M.J.**, Gavriilidou, A., Daamen, W., Hoogendoorn, S.P. (2020) Voronoi Densities for Bicylists: Adaptation for Finite Object Size and Speed. In *Traffic and Granular Flow (TGF) 2019* (pp 515-521). Springer, Cham.

TRAIL Thesis Series

The following list contains the most recent dissertations in the TRAIL Thesis Series. Visit the TRAIL website (http://rstrail.nl/) for the complete overview of approximately 300 titles.

The TRAIL Thesis Series is a series of the Netherlands TRAIL Research School on transport, infrastructure and logistics.

Wierbos, M.J., *Macroscopic Characteristics of Bicycle Traffic Flow: a bird's-eye view of cycling*, T2021/24, September 2021, TRAIL Thesis Series, the Netherlands

Qu, W., *Synchronization Control of Perturbed Passenger and Freight Operations*, T2021/23, July 2021, TRAIL Thesis Series, the Netherlands

Nguyen, T.T., *Highway Traffic Congestion Patterns: Feature Extraction and Pattern Retrieval*, T2021/22, July 2021, TRAIL Thesis Series, the Netherlands

Pudāne, B., *Time Use and Travel Behaviour with Automated Vehicles*, T2021/21, July 2021, TRAIL Thesis Series, the Netherlands

Gent, P. van, *Your Car Knows Best*, T2021/20, July 2021, TRAIL Thesis Series, the Netherlands

Wang, Y., *Modeling Human Spatial Behavior through Big Mobility Data*, T2021/19, June 2021, TRAIL Thesis Series, the Netherlands

Coevering, P. van de, *The Interplay between Land Use, Travel Behaviour and Attitudes: a quest for causality*, T2021/18, June 2021, TRAIL Thesis Series, the Netherlands

Landman, R., *Operational Control Solutions for Traffic Management on a Network Level*, T2021/17, June 2021, TRAIL Thesis Series, the Netherlands

Zomer, L.-B., *Unravelling Urban Wayfinding: Studies on the development of spatial knowledge, activity patterns, and route dynamics of cyclists*, T2021/16, May 2021, TRAIL Thesis Series, the Netherlands

Núñez Velasco, J.P., *Should I Stop or Should I Cross? Interactions between vulnerable road users and automated vehicles*, T2021/15, May 2021, TRAIL Thesis Series, the Netherlands

Duivenvoorden, K., *Speed Up to Safe Interactions: The effects of intersection design and road users' behaviour on the interaction between cyclists and car drivers*, T2021/14, April 2021, TRAIL Thesis Series, the Netherlands

Nagalur Subraveti, H.H.S., *Lane-Specific Traffic Flow Control*, T2021/13, March 2021, TRAIL Thesis Series, the Netherlands

Beirigo, B.A., *Dynamic Fleet Management for Autonomous Vehicles: Learning- and optimization-based strategies*, T2021/12, March 2021, TRAIL Thesis Series, the Netherlands

Zhang, B., *Taking Back the Wheel: Transition of control from automated cars and trucks to manual driving*, T2021/11, February 2021, TRAIL Thesis Series, the Netherlands

Boelhouwer, A., *Exploring, Developing and Evaluating In-Car HMI to Support Appropriate use of Automated Cars*, T2021/10, January 2021, TRAIL Thesis Series, the Netherlands

Li, X., *Development of an Integrity Analytical Model to Predict the Wet Collapse Pressure of Flexible Risers*, T2021/9, February 2021, TRAIL Thesis Series, the Netherlands

Li, Z., *Surface Crack Growth in Metallic Pipes Reinforced with Composite Repair System*, T2021/8, January 2021, TRAIL Thesis Series, the Netherlands

Gavriilidou, A., *Cyclists in Motion: From data collection to behavioural models*, T2021/7, February 2021, TRAIL Thesis Series, the Netherlands

Methorst, R., *Exploring the Pedestrians Realm: An overview of insights needed for developing a generative system approach to walkability*, T2021/6, February 2021, TRAIL Thesis Series, the Netherlands

Walker, F., *To Trust or Not to Trust? Assessment and calibration of driver trust in automated vehicles*, T2021/5, February 2021, TRAIL Thesis Series, the Netherlands

Schneider, F., *Spatial Activity-travel Patterns of Cyclists*, T2021/4, February 2021, TRAIL Thesis Series, the Netherlands

Madadi, B., *Design and Optimization of Road Networks for Automated Vehicles*, T2021/3, January 2021, TRAIL Thesis Series, the Netherlands

Krabbenborg, L.D.M., *Tradable Credits for Congestion Management: support/reject?*, T2021/2, January 2021, TRAIL Thesis Series, the Netherlands

Castelein, B., *Accommodating Cold Logistics Chains in Seaport Clusters: The development of the reefer container market and its implications for logistics and policy*, T2021/1, January 2021, TRAIL Thesis Series, the Netherlands

Huang, B., *The Influence of Positive Interventions on Cycling*, T2020/20, December 2020, TRAIL Thesis Series, the Netherlands

Xiao, L., *Cooperative Adaptive Cruise Control Vehicles on Highways: Modelling and Traffic Flow Characteristics*, T2020/19, December 2020, TRAIL Thesis Series, the Netherlands

Polinder, G.J., *New Models and Applications for Railway Timetabling*, T2020/18, December 2020, TRAIL Thesis Series, the Netherlands

Scharpff, J.C.D., *Collective Decision Making trough Self-regulation*, T2020/17, November 2020, TRAIL Thesis Series, the Netherlands

Guo, W. *Optimization of Synchromodal Matching Platforms under Uncertainties*, T2020/16, November 2020, TRAIL Thesis Series, the Netherlands